HOST GENES ASSOCIATED WITH BK POLYOMAVIRUS ENTRY AND

INTRACELLULAR TRAFFICKING

By

Linbo Zhao

A dissertation submitted in partial fulfillment
of the requirements for the degree of
Doctor of Philosophy
(Cancer Biology)
in the University of Michigan
2016

Doctoral Committee:

      Professor Michael J. Imperiale, Chair
      Professor David G. Beer
      Professor Colin S. Duckett
      Professor Katherine R. Spindler
      Associate Professor Christiane E. Wobus

ACKNOWLEDGEMENTS

I would like to thank my Ph.D. mentor, Dr. Mike Imperiale. This dissertation would never come to exist without the opportunity he offered me six years ago. My gratitude for the opportunity to learn from him is simply beyond words.

I would like to thank the members of my thesis committee: Dr. David Beer, Dr. Colin Duckett, Dr. Katherine Spindler, and Dr. Christiane Wobus, for inspiring me, challenging me, and advising me throughout my Ph.D. program. I would like to thank Dr. Billy Tsai for his critical review of my BKPyV endocytosis manuscript. I also owe my gratitude to my first mentor, Dr. Shengfang Ge, who kindly took me in as an undergraduate research assistant and inspired me to go into this field.

I would like to thank my fellow labmates, especially Mengxi Jiang, Shauna Bennett, and Heather Manza. They offered selfless help and valuable advice on my projects. It is my honor to work with them and join them in this scientific adventure.

To the Center for Chemical Genomics, I would like to thank Martha Larsen, Steven Swaney, Nicholas Santoro, Renju Jacob, Tom McQuade, and Steve Roest for their help during the whole genome siRNA screen. They reserved all the best equipment for my project. Without their help, it would have been impossible for me to finish the whole genome screen in three months.

TABLE OF CONTENTS

LIST OF FIGURES

LIST OF TABLES

ABSTRACT

BK polyomavirus (BKPyV) is a small DNA icosahedral virus measuring about 45nm in diameter, and it was first isolated in 1971. BKPyV infection is ubiquitous and usually asymptomatic; however, BKPyV reactivates in immunosuppressed transplant patients and causes two diseases, polyomavirus associated nephropathy (PVAN) and hemorrhagic cystitis (HC). Due to a lack of specific antiviral drugs, the first-line treatment for BKPyV reactivation is to reduce immunosuppression in PVAN patient or to target host DNA synthesis machinery in HC patient. None of the current treatments is optimal; therefore, elucidating details of the BKPyV life cycle will potentially benefit therapy development and uncover interesting viral and cell biology.

Despite being isolated more than 40 year ago, details of the BKPyV life cycle require further elucidation. BKPyV has been considered to infect host cells via a caveolin-mediated pathway. In order to study viral entry in greater detail, caveolin 1, caveolin 2, and clathrin heavy chain were silenced with siRNA in renal proximal tubule epithelial (RPTE) cells. Our experiments showed that caveolin 1, caveolin 2, and clathrin heavy chain knockdown did not block BKPyV infection. However, knocking down UDP-glucose ceramide glucosyltransferase (UGCG), an enzyme required for ganglioside synthesis, decreased BKPyV infection. This suggests that there is a caveolin- and clathrin-independent pathway during BKPyV entry in RPTE cells, and BKPyV does require gangliosides for efficient infection.

To further identify host factors associated with BKPyV entry and intracellular trafficking, a whole genome siRNA screen was performed on BKPyV in RPTE cells. The DnaJ heat shock protein family, which has previously been implicated in BKPyV entry, was our top hit. The other hits we identified have not been previously reported; however, many of them are involved in vesicular transport. After validating our top interesting hits, a protein complex was identified to be essential for BKPyV infection. Considering that all of these proteins localize to the ER membrane and participate in the Golgi to ER trafficking, the Golgi to ER trafficking pathway may play an important role in BKPyV infection.

CHAPTER I

Introduction

Polyomaviridae

Polyomaviruses are a group of non-enveloped icosahedral DNA viruses about 45 nm in diameter. Initially, both polyomaviruses and papillomaviruses were classified as two genera in the *Papovaviridae* family [1]. Eventually in 2001 the family was divided into *Polyomaviridae* and *Papillomaviridae* [2]. The first member of the *Polyomaviridae* family is murine polyomavirus (MPyV), which was identified as a filterable agent that causes salivary gland carcinomas in mice, and it was named with the Greek roots of multiple (poly-) tumors (-oma) [3]. Polyomaviruses have a broad range of host tropism, having been demonstrated as mainly capable of infecting mammals and birds. After the discovery of the first two human polyomaviruses BKPyV [4] and JCPyV [5], an additional 11 human polyomaviruses were identified with the help of sequencing techniques, including KIPyV [6], WUPyV [7], MCPyV [8], HPyV6, HPyV7 [9], TSPyV [10], HPyV9 [11], HPyV10 [12], MWPyV [13], MXPyV [14] and STLPyV [15]. Although polyomaviruses have demonstrated their abilities to induce tumors in mice, a majority of polyomaviruses do not directly cause human cancer. MCPyV is the only polyomavirus that causes a human cancer, Merkel cell carcinoma. In addition to MCPyV, BKPyV, JCPyV, and TSPyV are also associated

with various human diseases [16], while more research is required in order to reveal the links between other polyomaviruses and human diseases.

BK Polyomavirus

BK Polyomavirus (BKPyV) was first isolated from a kidney transplant patient (with the initials B.K) who was hospitalized for ureteric obstruction in 1971 [4]. Subsequent serology studies revealed a crucial fact, that BKPyV infection is ubiquitous regardless of geographic location, with over 80% of adults worldwide testing seropositive [17]. Seroconversion for BKPyV usually occurs during early childhood [18], and the transmission route of BKPyV is not yet fully understood. It has been speculated that BKPyV is transmitted via a respiratory route, based on sporadic reports that BKPyV can be detected from the respiratory tract [19-21]. After the initial exposure, BKPyV establishes a persistent infection in uroepithelium cells, with periodic urinary shedding of viruses. Despite the fact that BKPyV infection is ubiquitous, BKPyV rarely causes any symptoms in most immunocompetent individuals, even though BKPyV can be periodically detected in the urine. However, in immunosuppressed patients, BKPyV occasionally reactivates and directly causes two major human diseases: polyomavirus associated nephropathy (PVAN) and hemorrhagic cystitis (HC) [22]. PVAN is one of the major causes of graft failure after kidney transplant. Up to 10% of renal transplant recipients suffer from PVAN, and up to 80% of PVAN patients experience allograft loss [23]. In a recent study, 16.6% of the allogeneic hematopoietic cell transplant patients suffered from HC, and BKPyV viruria was detected in 90% of the HC patients [24]. Taking into account that roughly 70,000 kidney and 50,000 bone marrow transplants occur annually according to WHO reports, and that the only treatment is to reduce immunosuppression in PVAN patients, thereby increasing the likelihood of graft rejection, understanding the life

cycle of BKPyV and establishing a detailed virus infection model will undeniably benefit future research and help to reveal potential drug targets.

Similar to the other polyomaviruses, BKPyV is a small virus with a relatively simple structure. The BKPyV capsid is composed of three capsid proteins: the major capsid protein VP1 and two minor capsid proteins, VP2 and VP3. Based on studies of the other polyomaviruses, 360 copies of the VP1 protein first form 72 pentamers with intrapentameric disulfide bonds [25,26]. Each VP1 pentamer binds one copy of one of the minor capsid proteins. The minor capsid proteins are buried in the center of the pentamers and anchored by hydrophobic interactions [25,27]. The 72 subunits finally assemble into the shell of BKPyV in a T=7 manner with interpentameric disulfide bonds and calcium interactions [28-30].

Inside the capsid of BKPyV, a 5.2 kb double stranded circular DNA genome is associated with host histones in the same way as SV40 [31], and the DNA forms a pearl necklace-like structure called a minichromosome [32,33]. The circular DNA genome can be arbitrarily divided into three regions (Figure 1.1): early, late, and non-coding control region (NCCR). The early region encodes three proteins, including large tumor antigen (TAg), small tumor antigen (tAg), and truncated tumor antigen (truncTAg) [34]. The late region encodes all the capsid proteins and agnoprotein. The NCCR is equipped with all the necessary promoters for viral transcription. Recombination in the NCCR is fairly common between BKPyV strains.

Other than capsid proteins, BKPyV only encodes another four viral proteins. TAg is one of the most studied viral proteins. TAg functions as a helicase/ATPase that binds to the replication origin located in the NCCR in the form of hexamers and initiates viral genome replication. In addition, TAg also interacts with and inactivates tumor suppressors p53 [35] and pRB [36]. By inactivating p53 and pRb, BKPyV manages to subvert cell cycle control and trigger
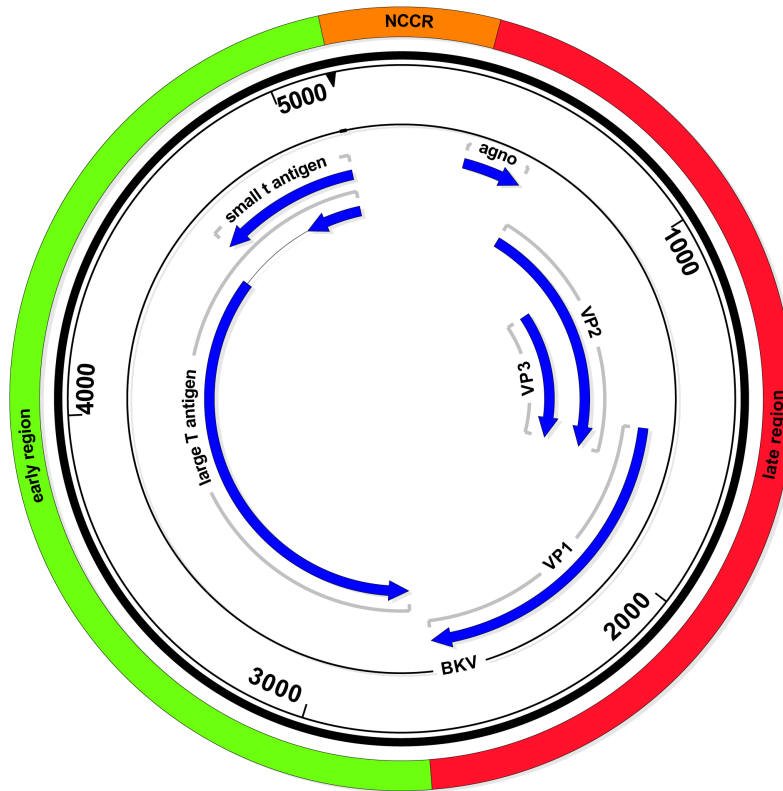
Figure 1.1: A schematic view of the genome of BKPyV.
The double stranded circular DNA genome of BKPyV can be arbitrarily divided into three regions: early (Green), late (Red), and non-coding control region (NCCR, Orange). Protein coding regions are illustrated with blue arrows which correspond to the direction of transcription.

cell proliferation [37]. Compared to TAg, the function of tAg is much less clear, and most

polyomavirus tAg studies were performed on SV40 [38]. Owing to the similarities between SV40

and BKPyV, BKPyV tAg is predicted to promote S phase entry by interacting with PP2A via a

CxxxPxC motif [39]. In addition to TAg and tAg, our lab also discovered a truncated form of TAg

expressed from an alternatively spliced mRNA [34]. The function of this protein has not yet been

determined. The agnoprotein regulates viral egress by interacting with α-SNAP, and

agnoprotein-deficient BKPyV mutant is about 50% less infective compared to wild type virus

[40,41]. More studies are necessary to further reveal the detailed functions of tAg, truncTAg, and

agnoprotein.

Current model of entry and intracellular trafficking

Polyomaviruses bind to various gangliosides, and some of the polyomaviruses take

advantage of gangliosides as receptors [42]: SV40 attaches to ganglioside receptor GM1 [43]; MPyV

binds ganglioside receptors GD1a and GT1b [44]; virus-like particles of JCPyV bind gangliosides

GM3, GD2, GD3, GD1b, GT1b, and GQ1b [45]; TSPyV binds to GM1 [46]; and BKPyV binds to its

ganglioside receptors GT1b and GD1b (Figure 1.2A) [47]. The pentameric VP1 structures of many

polyomaviruses have been solved, including SV40 [29,48], MPyV [49], JCPyV [50], MCPyV [51], KIPyV

and WUPyV [52], LPyV [53], HPyV6 and HPyV7 [54]. Based on the capsid structure analysis, HPyV9,

BKPyV, SV40, MCPyV, LPyV, JCPyV, and MPyV are predicted to interact with sialic acids

with similar binding pockets located between two VP1 monomers [46]. On the other hand, the

canonical sialic acid interacting pockets of HPyV6 and 7 are obstructed from interacting with

sialic acid [54], indicating that polyomaviruses may also use receptors other than gangliosides.

Subsequent studies on TSPyV show that there is a novel sialic acid-interacting pocket about 18

angstroms away from the canonical pocket [46]; therefore, HPyV6 and HPyV7 may also interact with sialic acid with a novel pocket similar to the majority of polyomaviruses.

Whether polyomaviruses require co-receptors is still unclear. Several glycoproteins have been reported as co-receptors, however, the functions of these glycoproteins with respect to infection are still controversial. Major histocompatibility complex I was initially considered as a receptor for SV40 [55], but subsequent experiments rebutted this idea [56,57]. Moreover, integrin was identified as a co-receptor for MPyV [58], and it also coordinates endocytic signal transduction for SV40 [59]. In addition, JCPyV relies on the glycosylated serotonin receptor 5TH2A to establish efficient infection [60]. On the other hand, digesting membrane proteins with proteinase K did not block MPyV infection; on the contrary, proteinase K treatment increased MPyV infection. Moreover, MPyV enters non-productive pathway without proper ganglioside receptors [61]. Both of these experiments suggest that glycoproteins serve as traps instead of co-receptors for polyomavirus. More studies are required to reveal the real function of glycoproteins during polyomavirus infection.

After initial attachment, different polyomaviruses have been reported to follow different endocytic pathways. SV40, MPyV, and BKPyV have been considered to use a caveolin-mediated pathway for internalization [55,62,63]. However, subsequent experiments showed that SV40 and MPyV infect cells via a caveolin- and clathrin-independent pathway [64-66]. In addition, JCPyV was considered to use the clathrin-mediated pathway for infection [67]. Upon endocytosis, particles were found immobilized in plasma membrane invaginations [63,64,66]. Several experiments showed that cell signaling may also play a role during viral endocytosis: a tyrosine kinase inhibitor, genistein, blocks polyomaviruses infection [43,64,68]; SV40 activates AKT via PI3K [59]; and JCPyV activates ERK1 and ERK2, which is required for its infection [69]. Actin filaments are

5

important for many endocytic processes; however, disassembly of actin filaments does not impact the endocytic process of MPyV or BKPyV [70,71], suggesting that actin filaments are dispensable for vesicle formation. Dynamin proteins are important for the scission of newly formed vesicles from the cell membrane during caveolin- and clathrin-dependent endocytosis [72]; however, expressing dominant negative dynamin does not block MPyV infection [73,74]; therefore, the fission step of polyomavirus entry is still not understood.

Internalized polyomaviruses are packaged in tight-fitting vesicles [64,75-77], and then they enter the endosome (Figure 1.2B) [66,78-80]. It has been reported that there is an intermediate compartment called the caveosome before polyomavirus enters the ER [81,82]; however, subsequent studies demonstrate that the caveosome is more likely to be an artifact. The acidification of the endosome is essential for polyomaviruses infection [66,80,83]. Acidification and maturation of late endosome/lysosome activate a ganglioside sorting machinery that involves Rab 5, Rab 7, Rab 9, and Rab 11 proteins [66,80,84]. After sorting through the late endosome/lysosome, vesicles that contains polyomaviruses traffic along microtubules and fuse to the ER at 8-12 hours post infection (Figure 1.2C) [71,83,85,86].

ER lumen proteins are important for polyomavirus disassembly and egress from the ER (Figure 1.2D) [83,87-89]. Protein disulfide isomerases induce capsid conformational changes and minor capsid protein exposure [62,83,90-94]. These exposed minor proteins insert into the ER membrane [95,96], and partially disassembled polyomaviruses penetrate the ER membrane and enter cytosol through the endoplasmic reticulum associated degradation (ERAD) pathway [87,88,97-99]. In the cytosol, the nuclear localization signal of minor capsid protein guides polyomaviruses into nuclei via the importin α/β pathway (Figure 1.2E) [100-102].
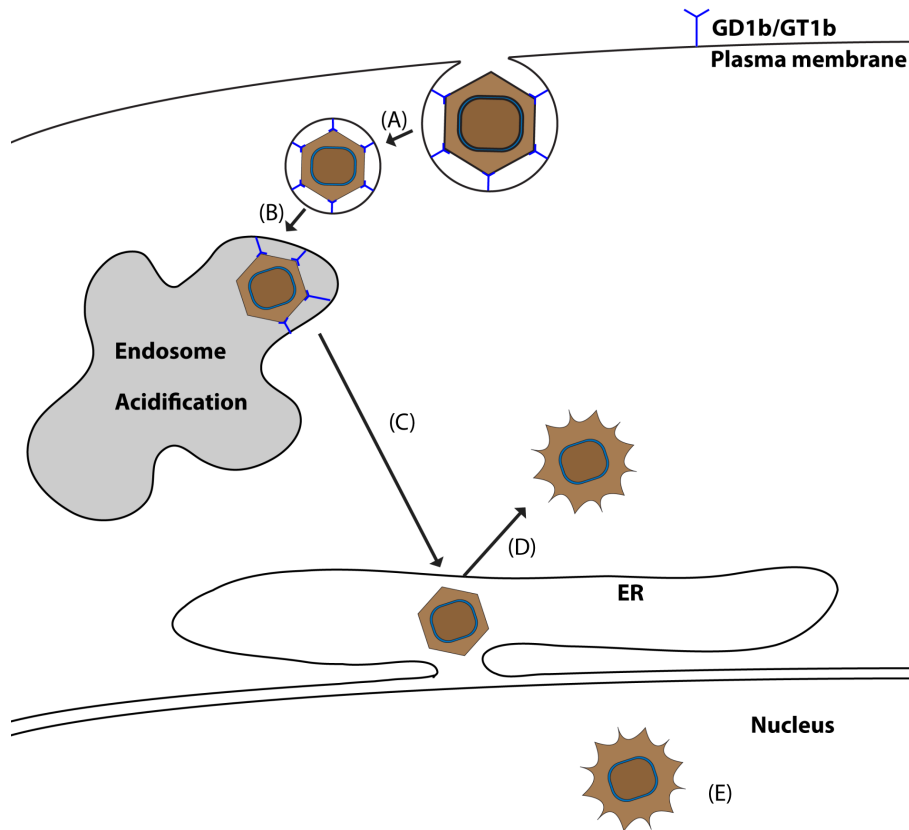
Figure 1.2: The current model of BKPyV entry and intracellular trafficking.
(A) BKPyV attaches to its receptor, ganglioside GD1b or GT1b, on the cell membrane and gets internalized by a caveolin-mediated endocytosis pathway. (B) Internalized BKPyV traffics to the endosome. (C) BKPyV traffics to the ER along microtubules after the acidification of the endosome. (D) BKPyV partially disassembles in the ER and translocates into the cytosol. (E) Partially disassembled virus enters the nucleus by importin α/β pathway.

RNA interference screening

BKPyV does not encode any DNA polymerase; thus the host DNA replication machinery is indispensable for viral replication [103,104]. In order to fully access the DNA replication machinery, BKPyV must traffic from outside the host cell and deliver its viral genome to the cell nucleus. Because of the nature of BKPyV replication, the most practical strategy to block viral infection would be to block the pathways that BKPyV uses during entry. Therefore, elucidating the trafficking pathway that BKPyV undergoes is not only important for understanding viral biology but also potentially important for identifying drug targets.

Our laboratory has demonstrated that the polyomavirus SV40 traffics differently in monkey kidney CV-1 cells than it does in primary human renal proximal tubule epithelial (RPTE) cells, which are the natural host cells for BKPyV replication [97]. Because much of the current model of BKPyV entry and trafficking is built on research using African green monkey kidney cells, our findings with SV40 drew our attention to the possibility that BKPyV may traffic differently in RPTE cells. To determine whether more such differences exist, in chapter 2, I re-examined the BKPyV entry process in RPTE cells. Interestingly, BKPyV did not follow the same entry pathway as it does in monkey cells [105]. Our results show that BKPyV entry is dependent on gangliosides (GT1b/GD1b), but independent of caveolin and clathrin. Moreover, most of the details of BKPyV trafficking are not yet revealed in the current models, nor have host factors assisting BKPyV infection been identified. In order to identify more host factors associated with BKPyV infection and to enrich the details of the BKPyV life cycle model, in chapter 3, I performed a whole genome siRNA screen on BKPyV.

Numerous assays have been developed for identifying host factors associated with viral infections, including one of the widely used assays in viral research: the genome-wide siRNA

screen. RNA interference (RNAi) is a post transcriptional regulation mechanism that is generally conserved in eukaryotic cells [106]. It was first reported in plant cells in 1986 [107]. RNAi had not been applied to biological research until 1998 when siRNA, a short (~22-nucleotide) double stranded RNA, was introduced as a tool [108]. Barely two years after the introduction of siRNA methods, genomic siRNA screens were performed in *C. elegans* [109]. After the completion of the human genome project in 2006, whole genome siRNA screening in human cells became possible. Silencing every human gene with an siRNA library and assessing the effects of the knockdown on BKPyV infection allows the dissection of the functions of individual host proteins during the viral life cycle. siRNA screens have been extensively applied to viral studies, such as HIV [110], West Nile virus [111], HPV [112], VSV [113], and another polyomavirus, SV40 [114], and hundreds of host factors associated with these virus have been identified. However, no genome-wide siRNA screening has been reported for BKPyV.

Due to our previous finding that polyomavirus infection is cell type- and species-specific [97], we wished to identify host factors in the natural host cells of BKPyV, human primary RPTE cells. Existing strategies for siRNA screens could not be directly adapted to the study of BKPyV study. Therefore, a novel strategy based on cell cycle arrest was developed, and a whole genome siRNA screen was performed on BKPyV in RPTE cells. With the help of whole genome siRNA screening, we identified a series of potential host factors that may be involved in BKPyV infection. By further validating our primary results, we found that the off-target effect of siRNA severely limited the efficiency of the siRNA screen. After validating our primary screen results, we identified RAB18, STX18, and the NRZ complex as our top hits, which may work together in capturing, docking, and fusing BKPyV-containing vesicles to the ER.

References

1.   Fenner F, Maurin J. The classification and nomenclature of viruses. *Arch Virol*. 1976;51(1-2):141-149. doi:10.1007/BF01317843.

2.   Fauquet CM, Mayo MA. The 7 th ICTV Report. *Arch Virol*. 2001;146(1):189-194. doi:10.1007/s007050170203.

3.   Gross L. A filterable agent, recovered from Ak leukemic extracts, causing salivary gland carcinomas in C3H Mice. *Experimental Biology and Medicine*. 1953;83(2):414-421. doi:10.3181/00379727-83-20376.

4.   Gardner SD, Field AM, Coleman DV, Hulme B. New human papovavirus (B.K.) isolated from urine after renal transplantation. *The Lancet*. 1971;1(7712):1253-1257. doi:10.1016/s0140-6736(71)91776-4.

5.   Padgett BL, Walker DL, ZuRhein GM, Eckroade RJ, Dessel BH. Cultivation of papova-like virus from human brain with progressive multifocal leucoencephalopathy. *The Lancet*. 1971;1(7712):1257-1260.

6.   Allander T, Andreasson K, Gupta S, et al. Identification of a third human polyomavirus. *J Virol*. 2007;81(8):4130-4136. doi:10.1128/JVI.00028-07.

7.   Gaynor AM, Nissen MD, Whiley DM, et al. Identification of a novel polyomavirus from patients with acute respiratory tract infections. *PLoS Pathog*. 2007;3(5):e64. doi:10.1371/journal.ppat.0030064.

8.   Feng H, Shuda M, Chang Y, Moore PS. Clonal integration of a polyomavirus in human Merkel cell carcinoma. *Science*. 2008;319(5866):1096-1100. doi:10.1126/science.1152586.

9.   Schowalter RM, Pastrana DV, Pumphrey KA, Moyer AL, Buck CB. Merkel cell polyomavirus and two previously unknown polyomaviruses are chronically shed from human skin. *Cell Host Microbe*. 2010;7(6):509-515. doi:10.1016/j.chom.2010.05.006.

10.   van der Meijden E, Janssens RWA, Lauber C, Bouwes Bavinck JN, Gorbalenya AE, Feltkamp MCW. Discovery of a new human polyomavirus associated with trichodysplasia spinulosa in an immunocompromized patient. *PLoS Pathog*. 2010;6(7):e1001024. doi:10.1371/journal.ppat.1001024.

11.   Scuda N, Hofmann J, Calvignac-Spencer S, et al. A novel human polyomavirus closely related to the african green monkey-derived lymphotropic polyomavirus. *J Virol*. 2011;85(9):4586-4590. doi:10.1128/JVI.02602-10.

12.   Buck CB, Phan GQ, Raiji MT, Murphy PM, McDermott DH, McBride AA. Complete genome sequence of a tenth human polyomavirus. *J Virol*. 2012;86(19):10887-10887. doi:10.1128/JVI.01690-12.

13.   Siebrasse EA, Reyes A, Lim ES, et al. Identification of MW polyomavirus, a novel polyomavirus in human stool. *J Virol*. 2012;86(19):10321-10326. doi:10.1128/JVI.01210-12.

14.   Yu G, Greninger AL, Isa P, et al. Discovery of a novel polyomavirus in acute diarrheal samples from children. *PLoS ONE*. 2012;7(11):e49449–. doi:10.1371/journal.pone.0049449.

15.   Lim ES, Reyes A, Antonio M, et al. Discovery of STL polyomavirus, a polyomavirus of ancestral recombinant origin that encodes a unique T antigen by alternative splicing. *Virology*. 2013;436(2):295-303. doi:10.1016/j.virol.2012.12.005.

16.   Dalianis T, Hirsch HH. Human polyomaviruses in disease and cancer. *Virology*. 2013;437(2):63-72. doi:10.1016/j.virol.2012.12.015.

17.   Egli A, Infanti L, Dumoulin A, et al. Prevalence of polyomavirus BK and JC infection and replication in 400 healthy blood donors. *J Infect Dis*. 2009;199(6):837-846. doi:10.1086/597126.

18.   Gardner SD. Prevalence in England of antibody to human polyomavirus (B.K.). *BMJ*. 1973;1(5845):77-78. doi:10.1136/bmj.1.5845.77.

19.   Goudsmit J, Wertheim-van Dillen P, van Strien A, van der Noordaa J. The role of BK virus in acute respiratory tract disease and the presence of BKV DNA in tonsils. *J Med Virol*. 1982;10(2):91-99.

20.   Sundsfjord A, Spein AR, Lucht E, Flaegstad T, Seternes OM, Traavik T. Detection of BK virus DNA in nasopharyngeal aspirates from children with respiratory infections but not in saliva from immunodeficient and immunocompetent adult patients. *J Clin Microbiol*. 1994;32(5):1390-1394.

21.   Sandler ES, Aquino VM, Goss-Shohet E, Hinrichs S, Krisher K. BK papova virus pneumonia following hematopoietic stem cell transplantation. *Bone Marrow Transplant*. 1997;20(2):163-165. doi:10.1038/sj.bmt.1700849.

22.   Jiang M, Abend JR, Johnson SF, Imperiale MJ. The role of polyomaviruses in human disease. *Virology*. 2009;384(2):266-273. doi:10.1016/j.virol.2008.09.027.

23.   Brennan DC, Drachenberg CB, Ginevri F, et al. Polyomavirus-associated nephropathy in renal transplantation: interdisciplinary analyses and recommendations. *Transplantation*. 2005;79(10):1277-1286. doi:10.1097/01.TP.0000156165.83160.09.

24.   Lunde LE, Dasaraju S, Cao Q, et al. Hemorrhagic cystitis after allogeneic hematopoietic cell transplantation: risk factors, graft source and survival. *Bone Marrow Transplant*. 2015;50(11):1432-1437. doi:10.1038/bmt.2015.162.

25.   Salunke DM, Caspar DLD, Garcea RL. Self-assembly of purified polyomavirus capsid

protein VP1. *Cell*. 1986;46(6):895-904. doi:10.1016/0092-8674(86)90071-1.

26.   Li PP, Nakanishi A, Clark SW, Kasamatsu H. Formation of transitory intrachain and interchain disulfide bonds accompanies the folding and oligomerization of simian virus 40 Vp1 in the cytoplasm. In: Vol 99. 2002:1353-1358. doi:10.1073/pnas.032668699.

27.   Chen XS, Stehle T, Harrison SC. Interaction of polyomavirus internal protein VP2 with the major capsid protein VP1 and implications for participation of VP2 in viral entry. *EMBO J*. 1998;17(12):3233-3240. doi:10.1093/emboj/17.12.3233.

28.   Li TC, Takeda N, Kato K, et al. Characterization of self-assembled virus-like particles of human polyomavirus BK generated by recombinant baculoviruses. *Virology*. 2003;311(1):115-124.

29.   Liddington RC, Yan Y, Moulai J, Sahli R, Benjamin TL, Harrison SC. Structure of simian virus 40 at 3.8-A resolution. *Nature*. 1991;354(6351):278-284. doi:10.1038/354278a0.

30.   Ishizu KI, Watanabe H, Han SI, et al. Roles of disulfide linkage and calcium ion-mediated interactions in assembly and disassembly of virus-like particles composed of simian virus 40 VP1 capsid protein. *J Virol*. 2001;75(1):61-72. doi:10.1128/JVI.75.1.61-72.2001.

31.   Varshavsky AJ, Bakayev VV, Chumackov PM, Georgiev GP. Minichromosome of simian virus 40: presence of histone HI. *Nucl Acids Res*. 1976;3(8):2101-2114. doi:10.1093/nar/3.8.2101.

32.   Griffith JD. Chromatin structure: deduced from a minichromosome. *Science*. 1975;187(4182):1202-1203. doi:10.1126/science.187.4182.1202.

33.   Meneguzzi G, Pignatti PF, Barbanti-Brodano G, Milanesi G. Minichromosome from BK virus as a template for transcription in vitro. *PNAS*. 1978;75(3):1126-1130. doi:10.1073/pnas.75.3.1126.

34.   Abend JR, Joseph AE, Das D, Campbell-Cecen DB, Imperiale MJ. A truncated T antigen expressed from an alternatively spliced BK virus early mRNA. *J Gen Virol*. 2009;90(Pt 5):1238-1245. doi:10.1099/vir.0.009159-0.

35.   Shivakumar CV, Das GC. Interaction of human polyomavirus BK with the tumor-suppressor protein p53. *Oncogene*. 1996;13(2):323-332.

36.   Harris KF, Christensen JB, Imperiale MJ. BK virus large T antigen: interactions with the retinoblastoma family of tumor suppressor proteins and effects on cellular growth control. *J Virol*. 1996;70(4):2378-2386.

37.   Topalis D, Andrei G, Snoeck R. The large tumor antigen: a "Swiss Army knife" protein possessing the functions required for the polyomavirus life cycle. *Antiviral Res*.

2013;97(2):122-136. doi:10.1016/j.antiviral.2012.11.007.

38. Khalili K, Sariyer IK, Safak M. Small tumor antigen of polyomaviruses: role in viral life cycle and cell transformation. *J Cell Physiol*. 2008;215(2):309-319. doi:10.1002/jcp.21326.

39. Mungre S, Enderle K, Turk B, et al. Mutations which affect the inhibition of protein phosphatase 2A by simian virus 40 small-t antigen in vitro decrease viral transformation. *J Virol*. 1994;68(3):1675-1681.

40. Johannessen M, Myhre MR, Dragset M, Tümmler C, Moens U. Phosphorylation of human polyomavirus BK agnoprotein at Ser-11 is mediated by PKC and has an important regulative function. *Virology*. 2008;379(1):97-109. doi:10.1016/j.virol.2008.06.007.

41. Johannessen M, Walquist M, Gerits N, Dragset M, Spang A, Moens U. BKV agnoprotein interacts with α-soluble N-ethylmaleimide-sensitive fusion attachment protein, and negatively influences transport of VSVG-EGFP. *PLoS ONE*. 2011;6(9):e24489–. doi:10.1371/journal.pone.0024489.

42. O'Hara SD, Stehle T, Garcea R. Glycan receptors of the Polyomaviridae: structure, function, and pathogenesis. *Curr Opin Virol*. 2014;7:73-78. doi:10.1016/j.coviro.2014.05.004.

43. Campanero-Rhodes MA, Smith A, Chai W, et al. N-glycolyl GM1 ganglioside as a receptor for simian virus 40. *J Virol*. 2007;81(23):12846-12858. doi:10.1128/JVI.01311-07.

44. Tsai B, Gilbert JM, Stehle T, Lencer W, Benjamin TL, Rapoport TA. Gangliosides are receptors for murine polyoma virus and SV40. *EMBO J*. 2003;22(17):4346-4355. doi:10.1093/emboj/cdg439.

45. Komagome R, Sawa H, Suzuki T, et al. Oligosaccharides as receptors for JC virus. *J Virol*. 2002;76(24):12992-13000. doi:10.1128/JVI.76.24.12992-13000.2002.

46. Ströh LJ, Gee GV, Blaum BS, et al. Trichodysplasia spinulosa-associated polyomavirus uses a displaced binding site on VP1 to engage sialylated glycolipids. *PLoS Pathog*. 2015;11(8):e1005112. doi:10.1371/journal.ppat.1005112.

47. Low JA, Magnuson B, Tsai B, Imperiale MJ. Identification of gangliosides GD1b and GT1b as receptors for BK virus. *J Virol*. 2006;80(3):1361-1366. doi:10.1128/JVI.80.3.1361-1366.2006.

48. Stehle T, Gamblin SJ, Yan Y, Harrison SC. The structure of simian virus 40 refined at 3.1 A resolution. *Structure*. 1996;4(2):165-182.

49. Stehle T, Yan Y, Benjamin TL, Harrison SC. Structure of murine polyomavirus

complexed with an oligosaccharide receptor fragment. *Nature*. 1994;369(6):160-163. doi:10.1038/369160a0.

50. Neu U, Maginnis MS, Palma AS, et al. Structure-function analysis of the human JC polyomavirus establishes the LSTc pentasaccharide as a functional receptor motif. *Cell Host Microbe*. 2010;8(4):309-319. doi:10.1016/j.chom.2010.09.004.

51. Neu U, Hengel H, Blaum BS, et al. Structures of Merkel cell polyomavirus VP1 complexes define a sialic acid binding site required for infection. Imperiale M, ed. *PLoS Pathog*. 2012;8(7):e1002738. doi:10.1371/journal.ppat.1002738.

52. Neu U, Wang J, Macejak D, Garcea RL, Stehle T. Structures of the major capsid proteins of the human Karolinska Institutet and Washington University polyomaviruses. *J Virol*. 2011;85(14):7384-7392. doi:10.1128/JVI.00382-11.

53. Neu U, Khan ZM, Schuch B, et al. Structures of B-lymphotropic polyomavirus VP1 in complex with oligosaccharide ligands. Schelhaas M, ed. *PLoS Pathog*. 2013;9(10):e1003714. doi:10.1371/journal.ppat.1003714.

54. Ströh LJ, Neu U, Blaum BS, Buch MHC, Garcea RL, Stehle T. Structure analysis of the major capsid proteins of human polyomaviruses 6 and 7 reveals an obstructed sialic acid binding site. *J Virol*. 2014;88(18):10831-10839. doi:10.1128/JVI.01084-14.

55. Norkin LC. Simian virus 40 infection via MHC class I molecules and caveolae. *Immunol Rev*. 1999;168(1):13-22. doi:10.1111/j.1600-065X.1999.tb01279.x.

56. Anderson HA, Chen Y, Norkin LC. MHC class I molecules are enriched in caveolae but do not enter with simian virus 40. *J Gen Virol*. 1998;79 (Pt 6)(6):1469-1477. doi:10.1099/0022-1317-79-6-1469.

57. Low J, Humes HD, Szczypka M, Imperiale M. BKV and SV40 infection of human kidney tubular epithelial cells in vitro. *Virology*. 2004;323(2):182-188. doi:10.1016/j.virol.2004.03.027.

58. Caruso M, Belloni L, Sthandier O, Amati P, Garcia M-I. Alpha4beta1 integrin acts as a cell receptor for murine polyomavirus at the postattachment level. *J Virol*. 2003;77(7):3913-3921. doi:10.1128/JVI.77.7.3913-3921.2003.

59. Stergiou L, Bauer M, Mair W, et al. Integrin-mediated signaling induced by simian virus 40 leads to transient uncoupling of cortical actin and the plasma membrane. *PLoS ONE*. 2013;8(2):e55799. doi:10.1371/journal.pone.0055799.

60. Maginnis MS, Haley SA, Gee GV, Atwood WJ. Role of N-linked glycosylation of the 5-HT2A receptor in JC virus infection. *J Virol*. 2010;84(19):9677-9684. doi:10.1128/JVI.00978-10.

61. You J, O'Hara SD, Velupillai P, et al. Ganglioside and Non-ganglioside Mediated Host

Responses to the Mouse Polyomavirus. Meyers C, ed. *PLoS Pathog*. 2015;11(10):e1005175. doi:10.1371/journal.ppat.1005175.

62. Norkin LC, Anderson HA, Wolfrom SA, Oppenheim A. Caveolar endocytosis of simian virus 40 is followed by Brefeldin A-sensitive transport to the endoplasmic reticulum, where the virus disassembles. *J Virol*. 2002;76(10):5156-5166. doi:10.1128/JVI.76.10.5156-5166.2002.

63. Richterová Z, Liebl D, Horák M, et al. Caveolae are involved in the trafficking of mouse polyomavirus virions and artificial VP1 pseudocapsids toward cell nuclei. *J Virol*. 2001;75(22):10880-10891. doi:10.1128/JVI.75.22.10880-10891.2001.

64. Damm E-M, Pelkmans L, Kartenbeck J, Mezzacasa A, Kurzchalia T, Helenius A. Clathrin- and caveolin-1-independent endocytosis: entry of simian virus 40 into cells devoid of caveolae. *J Cell Biol*. 2005;168(3):477-488. doi:10.1083/jcb.200407113.

65. Gilbert JM, Goldberg IG, Benjamin TL. Cell Penetration and Trafficking of Polyomavirus. *J Virol*. 2003;77(4):2615-2622. doi:10.1128/JVI.77.4.2615-2622.2003.

66. Liebl D, Difato F, Horníková L, Mannová P, Štokrová J, Forstová J. Mouse polyomavirus enters early endosomes, requires their acidic pH for productive infection, and meets transferrin cargo in Rab11-positive endosomes. *J Virol*. 2006;80(9):4610-4622. doi:10.1128/JVI.80.9.4610-4622.2006.

67. Pho MT, Ashok A, Atwood WJ. JC virus enters human glial cells by clathrin-dependent receptor-mediated endocytosis. *J Virol*. 2000;74(5):2288-2292.

68. Ewers H, Römer W, Smith AE, et al. GM1 structure determines SV40-induced membrane invagination and infection. *Nature Cell Biology*. 2010;12(1):11–8–suppp1–12. doi:10.1038/ncb1999.

69. Querbes W, Benmerah A, Tosoni D, Di Fiore PP. A JC virus-induced signal is required for infection of glial cells by a clathrin-and eps15-dependent pathway. *Journal of ....* 2004;78(1):250-256. doi:10.1128/JVI.78.1.250-256.2004.

70. Sanjuan N, Porrás A, Otero J. Microtubule-dependent intracellular transport of murine polyomavirus. *Virology*. 2003;313(1):105-116. doi:10.1016/S0042-6822(03)00309-X.

71. Eash S, Atwood WJ. Involvement of cytoskeletal components in BK virus infectious entry. *J Virol*. 2005;79(18):11734-11741. doi:10.1128/JVI.79.18.11734-11741.2005.

72. Hinshaw JE. Dynamin and its role in membrane fission. *Annu Rev Cell Dev Biol*. 2000;16(1):483-519. doi:10.1146/annurev.cellbio.16.1.483.

73. Gilbert JM, Benjamin TL. Early steps of polyomavirus entry into cells. *J Virol*. 2000;74(18):8582-8588. doi:10.1128/JVI.74.18.8582-8588.2000.

74.   Ferguson SM, De Camilli P. Dynamin, a membrane-remodelling GTPase. *Nature Reviews Molecular Cell Biology*. 2012;13(2):75-88. doi:10.1038/nrm3266.

75.   Hummeler K, Tomassini N, Sokol F. Morphological aspects of the uptake of simian virus 40 by permissive cells. *J Virol*. 1970;6(1):87-93.

76.   Kartenbeck J. Endocytosis of simian virus 40 into the endoplasmic reticulum. *J Cell Biol*. 1989;109(6):2721-2729. doi:10.1083/jcb.109.6.2721.

77.   Maraldi NM, Barbanti-Brodano G, Portolani M, La Placa M. Ultrastructural aspects of BK virus uptake and replication in human fibroblasts. *J Gen Virol*. 1975;27(1):71-80. doi:10.1099/0022-1317-27-1-71.

78.   Ashok A, Atwood WJ. Contrasting roles of endosomal pH and the cytoskeleton in infection of human glial cells by JC virus and simian virus 40. *J Virol*. 2003;77(2):1347-1356. doi:10.1128/JVI.77.2.1347-1356.2003.

79.   Querbes W, O'Hara BA, Williams G, Atwood WJ. Invasion of host cells by JC virus identifies a novel role for caveolae in endosomal sorting of noncaveolar ligands. *J Virol*. 2006;80(19):9402-9413. doi:10.1128/JVI.01086-06.

80.   Engel S, Heger T, Mancini R, et al. Role of endosomes in simian virus 40 entry and infection. *J Virol*. 2011;85(9):4198-4211. doi:10.1128/JVI.02179-10.

81.   Pelkmans L, Kartenbeck J, Helenius A. Caveolar endocytosis of simian virus 40 reveals a new two-step vesicular-transport pathway to the ER. *Nature Cell Biology*. 2001;3(5):473-483. doi:10.1038/35074539.

82.   Pelkmans L, Helenius A. Endocytosis Via Caveolae. *Traffic*. 2002;3(5):311-320. doi:10.1034/j.1600-0854.2002.30501.x.

83.   Jiang M, Abend JR, Tsai B, Imperiale MJ. Early events during BK virus entry and disassembly. *J Virol*. 2009;83(3):1350-1358. doi:10.1128/JVI.02169-08.

84.   Qian M, Cai D, Verhey KJ, Tsai B. A lipid receptor sorts polyomavirus from the endolysosome to the endoplasmic reticulum to cause infection. Galloway D, ed. *PLoS Pathog*. 2009;5(6):e1000465. doi:10.1371/journal.ppat.1000465.

85.   Moriyama T, Sorokin A. Intracellular trafficking pathway of BK Virus in human renal proximal tubular epithelial cells. *Virology*. 2008;371(2):336-349. doi:10.1016/j.virol.2007.09.030.

86.   Zila V, Difato F, Klimova L, Huerfano S, Forstová J. Involvement of microtubular network and its motors in productive endocytic trafficking of mouse polyomavirus. Salinas S, ed. *PLoS ONE*. 2014;9(5):e96922–. doi:10.1371/journal.pone.0096922.

87.   Inoue T, Tsai B. A nucleotide exchange factor promotes endoplasmic reticulum-to-

cytosol membrane penetration of the nonenveloped virus simian virus 40. *J Virol*. 2015;89(8):4069-4079. doi:10.1128/JVI.03552-14.

88.   Bagchi P, Walczak CP, Tsai B. The endoplasmic reticulum membrane J protein C18 executes a distinct role in promoting simian virus 40 membrane penetration. Dermody TS, ed. *J Virol*. 2015;89(8):4058-4068. doi:10.1128/JVI.03574-14.

89.   Chromy LR, Oltman A, Estes PA, Garcea RL. Chaperone-mediated in vitro disassembly of polyoma- and papillomaviruses. *J Virol*. 2006;80(10):5086-5091. doi:10.1128/JVI.80.10.5086-5091.2006.

90.   Rainey-Barger EK, Mkrtchian S, Tsai B. Dimerization of ERp29, a PDI-like protein, is essential for its diverse functions. *Mol Biol Cell*. 2007;18(4):1253-1260. doi:10.1091/mbc.E06-11-1004.

91.   Schelhaas M, Malmström J, Pelkmans L, et al. Simian Virus 40 depends on ER protein folding and quality control factors for entry into host cells. *Cell*. 2007;131(3):516-529. doi:10.1016/j.cell.2007.09.038.

92.   Walczak CP, Tsai B. A PDI family network acts distinctly and coordinately with ERp29 to facilitate polyomavirus infection. *J Virol*. 2011;85(5):2386-2396. doi:10.1128/JVI.01855-10.

93.   Nelson CDS, Ströh LJ, Gee GV, O'Hara BA, Stehle T, Atwood WJ. Modulation of a pore in the capsid of JC polyomavirus reduces infectivity and prevents exposure of the minor capsid proteins. Imperiale MJ, ed. *J Virol*. 2015;89(7):3910-3921. doi:10.1128/JVI.00089-15.

94.   Inoue T, Dosey A, Herbstman JF, Ravindran MS, Skiniotis G, Tsai B. ERdj5 reductase cooperates with protein disulfide isomerase to promote simian virus 40 endoplasmic reticulum membrane translocation. Dermody TS, ed. *J Virol*. 2015;89(17):8897-8908. doi:10.1128/JVI.00941-15.

95.   Daniels R, Rusan NM, Wadsworth P, Hebert DN. SV40 VP2 and VP3 insertion into ER membranes is controlled by the capsid protein VP1: implications for DNA translocation out of the ER. *Molecular Cell*. 2006;24(6):955-966. doi:10.1016/j.molcel.2006.11.001.

96.   Rainey-Barger EK, Magnuson B, Tsai B. A chaperone-activated nonenveloped virus perforates the physiologically relevant endoplasmic reticulum membrane. *J Virol*. 2007;81(23):12996-13004. doi:10.1128/JVI.01037-07.

97.   Bennett SM, Jiang M, Imperiale MJ. Role of cell-type-specific endoplasmic reticulum-associated degradation in polyomavirus trafficking. *J Virol*. 2013;87(16):8843-8852. doi:10.1128/JVI.00664-13.

98.   Inoue T, Tsai B. A large and intact viral particle penetrates the endoplasmic reticulum membrane to reach the cytosol. Galloway D, ed. *PLoS Pathog*. 2011;7(5):e1002037.

doi:10.1371/journal.ppat.1002037.

99.   Geiger R, Andritschke D, Friebe S, et al. BAP31 and BiP are essential for dislocation of SV40 from the endoplasmic reticulum to the cytosol. *Nature Cell Biology*. 2011;13(11):1305-1314. doi:10.1038/ncb2339.

100.   Nakanishi A, Shum D, Morioka H, Otsuka E, Kasamatsu H. Interaction of the Vp3 nuclear localization signal with the importin α2/β heterodimer directs nuclear entry of infecting simian virus 40. *J Virol*. 2002;76(18):9368-9377. doi:10.1128/JVI.76.18.9368-9377.2002.

101.   Nakanishi A, Itoh N, Li PP, Handa H, Liddington RC, Kasamatsu H. Minor capsid proteins of simian virus 40 are dispensable for nucleocapsid assembly and cell entry but are required for nuclear entry of the viral genome. *J Virol*. 2007;81(8):3778-3785. doi:10.1128/JVI.02664-06.

102.   Bennett SM, Zhao L, Bosard C, Imperiale MJ. Role of a nuclear localization signal on the minor capsid proteins VP2 and VP3 in BKPyV nuclear entry. *Virology*. 2015;474:110-116. doi:10.1016/j.virol.2014.10.013.

103.   Jiang M, Zhao L, Gamez M, Imperiale MJ. Roles of ATM and ATR-mediated DNA damage responses during lytic bk polyomavirus infection. Pipas J, ed. *PLoS Pathog*. 2012;8(8):e1002898. doi:10.1371/journal.ppat.1002898.

104.   Verhalen B, Justice JL, Imperiale MJ, Jiang M. Viral DNA replication-dependent DNA damage response activation during BK polyomavirus infection. Sandri-Goldin RM, ed. *J Virol*. 2015;89(9):5032-5039. doi:10.1128/JVI.03650-14.

105.   Eash S, Querbes W, Atwood WJ. Infection of vero cells by BK virus is dependent on caveolae. *J Virol*. 2004;78(21):11583-11590. doi:10.1128/JVI.78.21.11583-11590.2004.

106.   Shabalina SA, Koonin EV. Origins and evolution of eukaryotic RNA interference. *Trends Ecol Evol (Amst)*. 2008;23(10):578-587. doi:10.1016/j.tree.2008.06.005.

107.   Ecker JR, Davis RW. Inhibition of gene expression in plant cells by expression of antisense RNA. *PNAS*. 1986;83(15):5372-5376. doi:10.1073/pnas.83.15.5372.

108.   Fire A, Xu S, Montgomery MK, Kostas SA, Driver SE, Mello CC. Potent and specific genetic interference by double-stranded RNA in Caenorhabditis elegans. *Nature*. 1998;391(6):806-811. doi:10.1038/35888.

109.   Gönczy P, Echeverri C, Oegema K, et al. Functional genomic analysis of cell division in C. elegans using RNAi of genes on chromosome III. *Nature*. 2000;408(6810):331-336. doi:10.1038/35042526.

110.   Zhou H, Xu M, Huang Q, et al. Genome-scale RNAi screen for host factors required for HIV replication. *Cell Host Microbe*. 2008;4(5):495-504.

doi:10.1016/j.chom.2008.10.004.

111.   Krishnan MN, Ng A, Sukumaran B, et al. RNA interference screen for human genes associated with West Nile virus infection. *Nature*. 2008;455(7210):242-245. doi:10.1038/nature07207.

112.   Lipovsky A, Popa A, Pimienta G, et al. Genome-wide siRNA screen identifies the retromer as a cellular entry factor for human papillomavirus. *Proc Natl Acad Sci USA*. 2013;110(18):7452-7457. doi:10.1073/pnas.1302164110.

113.   Lee AS-Y, Burdeinick-Kerr R, Whelan SPJ. A genome-wide small interfering RNA screen identifies host factors required for vesicular stomatitis virus infection. *J Virol*. 2014;88(15):8355-8360. doi:10.1128/JVI.00642-14.

114.   Goodwin EC, Lipovsky A, Inoue T, et al. BiP and multiple DNAJ molecular chaperones in the endoplasmic reticulum are required for efficient simian virus 40 infection. *MBio*. 2011;2(3):e00101-e00111. doi:10.1128/mBio.00101-11.

CHAPTER II

Caveolin- and clathrin-independent entry of BKPyV into primary human proximal tubule epithelial cells

Abstract

BK polyomavirus (BKPyV) is a human pathogen that causes polyomavirus-associated nephropathy and hemorrhagic cystitis in transplant patients. Gangliosides and caveolin proteins have previously been reported to be required for BKPyV infection in animal cell models. Recent studies from our laboratory and others, however, have indicated that the identity of the cells used for infection studies can greatly influence the behavior of the virus. We therefore wished to re-examine BKPyV entry in a physiologically relevant primary cell culture model, human renal proximal tubule epithelial cells. Using siRNA knockdowns, we interfered with expression of UDP-glucose ceramide glucosyltransferase (UGCG), and the endocytic vesicle coat proteins caveolin 1, caveolin 2, and clathrin heavy chain. The results demonstrate that while BKPyV does require gangliosides for efficient infection, it can enter its natural host cells via a caveolin- and clathrin-independent pathway. The results emphasize the importance of studying viruses in a relevant cell culture model.

Introduction

BK polyomavirus (BKPyV) was initially isolated in 1971. Since then, the study of the BKPyV life cycle has been ongoing for more than 40 years. The polyomaviruses utilize both productive and non-productive pathways to be internalized [1]; therefore, morphological colocalization observations can be deceiving and inconsistent with functional studies. The first isolated polyomavirus, murine polyomavirus (MPyV), has been considered to infect host cells via a caveolin-mediated endocytic pathway [2]. However, subsequent experiments showed that MPyV could infect caveolin-deficient cell lines [3,4]. In addition, SV40, similar to the MPyV, was also reported to rely on caveolin proteins for viral entry [5]; however, SV40 is not only able to establish a successful infection in caveolin knockout cells, but is also capable of infecting caveolin knockout cells with additional clathrin knockdown [6]. Considering that the capsid genes of polyomavirus are partially conserved and the capsid structures of polyomaviruses are similar [7], all the previous findings prompt the possibility that BKPyV entry could be independent of caveolin and clathrin.

The current model for the BKPyV life cycle begins with viral attachment to the cell surface via an interaction between the major capsid protein VP1 and the BKPyV receptors, b-series gangliosides (GD1b/GT1b) [8,9]. Specific co-receptors for BKPyV have not been identified, but data suggest that an N-linked glycoprotein with (2,3)-linked sialic acid may function as a co-receptor [10]. Caveolin-dependent endocytosis has been previously implicated in BKPyV entry into host cells, and gangliosides are commonly enriched within lipid rafts where caveolin-dependent endocytosis frequently takes place [11]. After initial attachment to receptors, viral particles enter caveolin-coated plasma membrane invaginations named caveolae. The caveolae coat protein, caveolin, has been reported to further guide endocytosis during BKPyV entry [12,13], and

21

internalized individual BKPyV particles have been detected in tight-fitting vesicles [6,14]. Disturbing caveolin-dependent endocytosis through removal of cholesterol from the plasma membrane or through transfecting a dominant negative caveolin 1 mutant into cells significantly inhibited BKPyV infection [12,13], while disturbing actin polymerization did not affect the BKPyV endocytic process [15]. After internalization, it is believed that BKPyV-containing vesicles fuse with the endosome in the same way as other polyomaviruses [4,16,17]. Our laboratory demonstrated that acidification of the late endosome/lysosome is essential for infection [18]. BKPyV then traffics to the ER along microtubules [18,19]. After trafficking to the ER, the BKPyV capsid partially disassembles in the ER lumen, egresses from the ER via the endoplasmic reticulum associated protein degradation (ERAD) pathway, and enters the cytosol before it translocates into the nucleus using the importin α/β pathway [20,21].

Electron microscopic images of cells infected with BKPyV revealed that BKPyV particles were individually encapsulated in tight fitting vesicles after endocytosis [6,14]. Caveolin- and clathrin-dependent endocytic pathways are two major and well-studied pathways that form small endocytic vesicles [22]. Additionally, there are several caveolae- and clathrin-independent pathways that generate similar vesicles. Caveolin proteins are a family of cholesterol binding proteins comprised of three members [23], caveolin 1, caveolin 2, and caveolin 3. Caveolin 1 and caveolin 2 are ubiquitously expressed in cells including epithelial cells, while caveolin 3 is specifically expressed in muscle cells. Caveolin proteins were named because they all serve as caveolae coat proteins [24]; however, only caveolin 1 has been demonstrated to be required for caveolae formation, since caveolae formation is absent in caveolin 1-deficient but not in caveolin 2-deficient murine cells [25,26]. In addition to BKPyV, SV40 and MPyV are also thought to take advantage of caveolae-dependent endocytosis [2,27]. JC polyomavirus (JCPyV), on the other hand,

infects cells via clathrin-dependent endocytosis [28]. The clathrin protein complex is a triskelion comprised of three heavy chains and three light chains [29]. Clathrin complexes are not capable of directly interacting with the plasma membrane. Adaptor proteins are required to recruit clathrin complexes to clathrin pits on the membrane, where the legs of the clathrin triskelions further interdigitate to form a lattice. The clathrin-coated pit pinches off from the plasma membrane with the help of dynamin to form clathrin-coated vesicles. Silencing clathrin heavy chain expression with siRNA impairs clathrin-coated pit formation [30].

In order to address the possibility that BKPyV, SV40, and mouse polyomavirus may establish infection in the same pathway that is independent of caveolin and clathrin, we re-examined the BKPyV entry process in renal proximal tubule epithelial (RPTE) cells, the natural host cell for BKPyV. By treating cells with drugs and silencing caveolin 1, caveolin 2, clathrin heavy chain, and UDP-glucose ceramide glucosyltransferase (UGCG), we showed that BKPyV infection requires gangliosides but enters RPTE cells through a caveolin- and clathrin-independent pathway.

Results

Our lab has previously shown that BKPyV interacts with liposomes containing gangliosides GD1b and GT1b, and that adding these gangliosides to non-permissive LNCaP cells makes them permissive for BKPyV infection [8]. In order to continue examination of the role of gangliosides during BKPyV infection of human renal proximal tubule epithelial (RPTE) cells, an siRNA pool targeting UDP-glucose ceramide glucosyltransferase (UGCG) was transfected into human RPTE cells. UGCG catalyzes the first glycosylation step of its substrate, ceramide, and
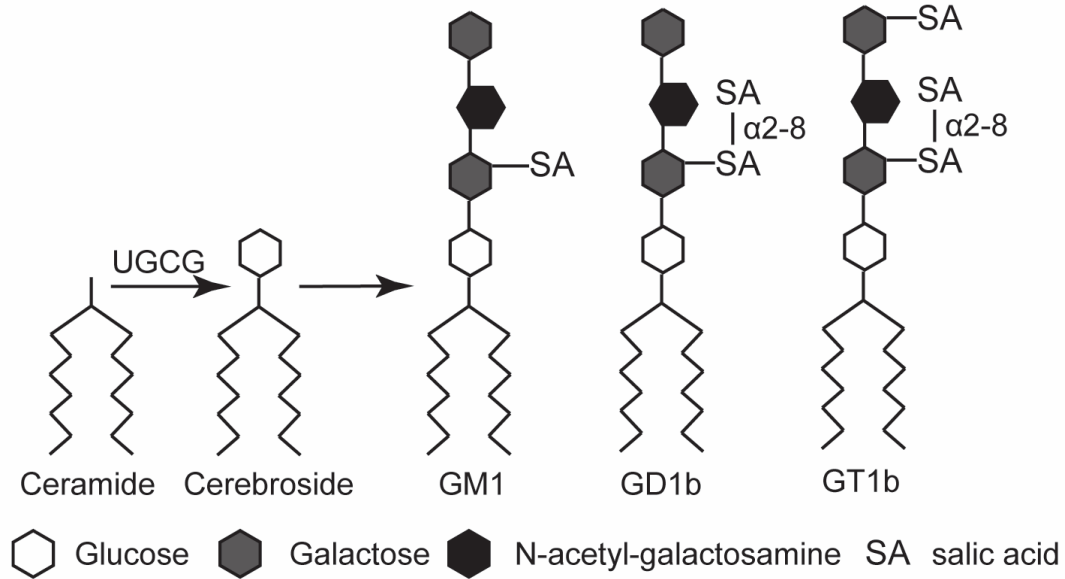
Figure 2.1: UGCG catalyzes cerebroside synthesis.
UGCG catalyzes the glycosylation step, transforming ceramide to cerebroside. Cerebroside is then used to synthesize gangliosides such as GM1, GD1b and GT1b. Sialic acids are α2-3 linked unless labeled otherwise.

transforms it into cerebroside, which is required for all ganglioside synthesis (Figure 2.1). Galactose, N-acetyl-galactosamine, and sialic acid are then added to cerebroside in order to synthesize gangliosides. Because a quality UGCG antibody was not available, RT-qPCR was performed to confirm efficient knockdown of UGCG. The RNA samples were harvested at two days post transfection, and UGCG mRNA expression was normalized to glyceraldehyde 3-phosphate dehydrogenase (GAPDH) mRNA. Compared to the no siRNA and the non-targeting siRNA controls, UGCG mRNA levels were reduced by more than 90% (Figure 2.2A).

We next tested the effect of knocking down UGCG on BKPyV infection. Human RPTE cells were transfected with no siRNA, a non-targeting siRNA pool, or a UGCG siRNA pool. Cells were infected with BKPyV at a MOI of 0.5 IU/cell, and at 48 hours post infection cell lysates were collected, resolved by SDS-PAGE, blotted, and assayed for TAg and GAPDH. The siRNA pool targeting UGCG reduced viral infection (Figure 2.2B). To further confirm that GD1b and GT1b are receptors for BKPyV infection in human RPTE cells, a rescue assay was performed. RPTE cells were transfected with the UGCG siRNA as described above. 10 hours prior to infection, gangliosides GM1, GD1b, or GT1b were added to the media, during which time the gangliosides incorporate into the cell membranes. Free gangliosides were removed by aspirating off the media and washing the cells with fresh media immediately before viral infection. Cells were infected and TAg expression was visualized by Western blotting. When siRNA that did not target UGCG was used and the gangliosides were subsequently added to the cells, the infection level stayed the same (Figure 2.2B). When the UGCG level was reduced, adding GM1, the receptor for SV40, did not restore infection as measured by TAg expression. However, when UGCG was reduced and GT1b or GD1b was added back, infection returned to

A

B
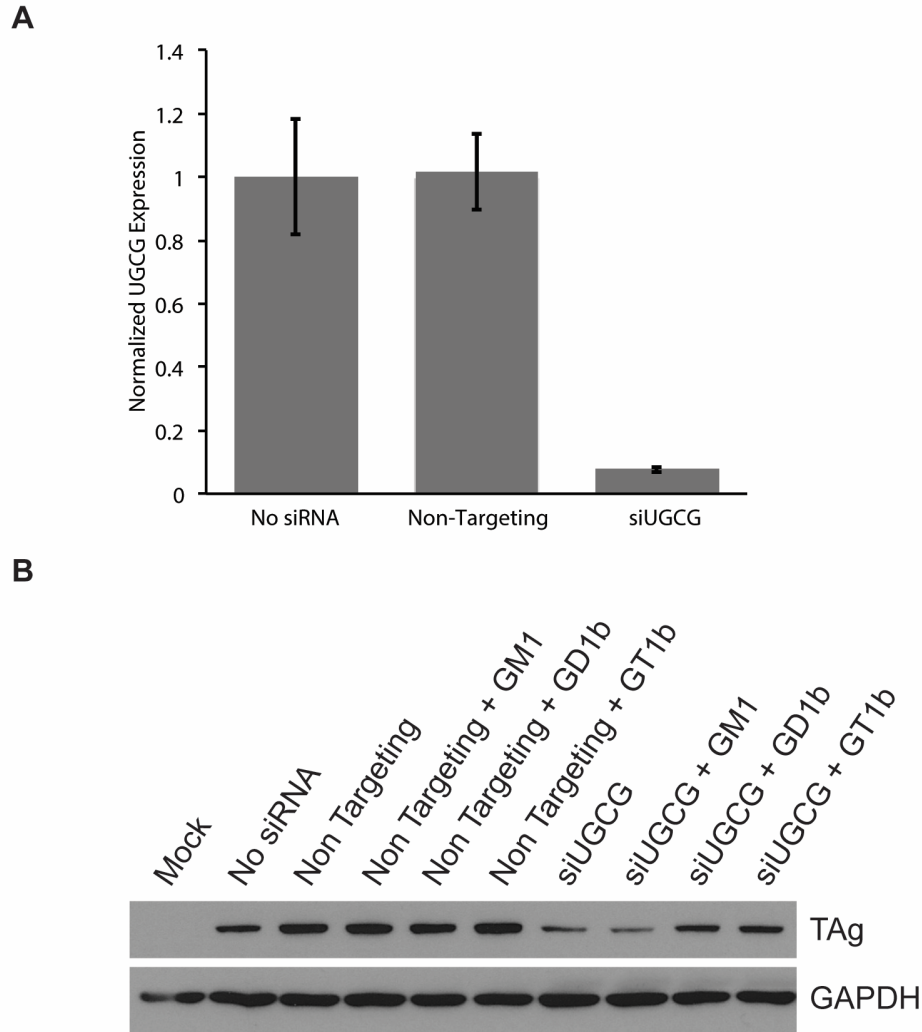
Figure 2.2: UGCG knockdown and rescue assays.
 (A) Normalized expression of UGCG mRNA (mean ± SEM). RPTE cells were transfected with non-targeting siRNAs or siRNAs targeting UGCG. Total RNA was collected, and reverse transcription and quantitative PCR were performed. UGCG mRNA expression was normalized to GAPDH mRNA. (B) RPTE cells were transfected with non-targeting siRNAs or siRNAs targeting UGCG. Gangliosides were added at 38 hours post transfection. At 48 hours post transfection, cells were infected with BKPyV at an MOI of 0.5 IU/cell. Western blotting was performed on protein samples harvested at 48 hours post infection.

the same level as the untransfected control. These results confirm the previous finding that

gangliosides GD1b and GT1b serve as receptors for BKPyV entry in human RPTE cells.

After examining the receptor used by BKPyV in RPTE cells, we next wanted to see if

cholesterol is required for BKPyV virus infection. Cholesterol regulates the conformation of

gangliosides in the plasma membrane [11,31], and the oligosaccharide orientation could be essential

for BKPyV attachment. A previous experiment showed that depleting cholesterol in Vero cells

blocked BKPyV infection [12]. In order to confirm this in RPTE cells, we tested the effect of

methyl-β-cyclodextrin (MβCD) and nystatin in RPTE cells. Both MβCD and nystatin are

cholesterol-depleting reagents that have been previously applied in polyomavirus studies. MβCD

and nystatin block cholesterol function in different ways: MβCD physically extracts cholesterol

from the plasma membrane and releases cholesterol into the media [32,33]; in contrast, nystatin only

binds to and forms a complex with cholesterol in the plasma membrane [34]. In order to test the

cytotoxicity of MβCD and nystatin, RPTE cells were treated with nystatin or MβCD at various

concentrations for two days (Figure 2.3C). Cell viability was evaluated with a cell viability assay

(WST-1 assay) after the treatment. Viable cells have a higher O.D. value in the viability assay.

RPTE cells were able to tolerate both nystatin and MβCD at most of concentrations except

treatment of MβCD at 5 mM. Next, RPTE cells were treated with nystatin or MβCD for 1 hour

prior to the BKPyV infection (MOI 0.5). Drugs were removed and cell were washed with fresh

media immediately before BKPyV infection. After virus absorption for one hour, nystatin or

MβCD were added back to the media. Infected cells were cultured for additional two days under

drug treatments, and protein samples were harvested at 48 hours post infection. Proteins were

separated with SDS-PAGE, blotted onto a nitrocellulose membrane, and probed for TAg.
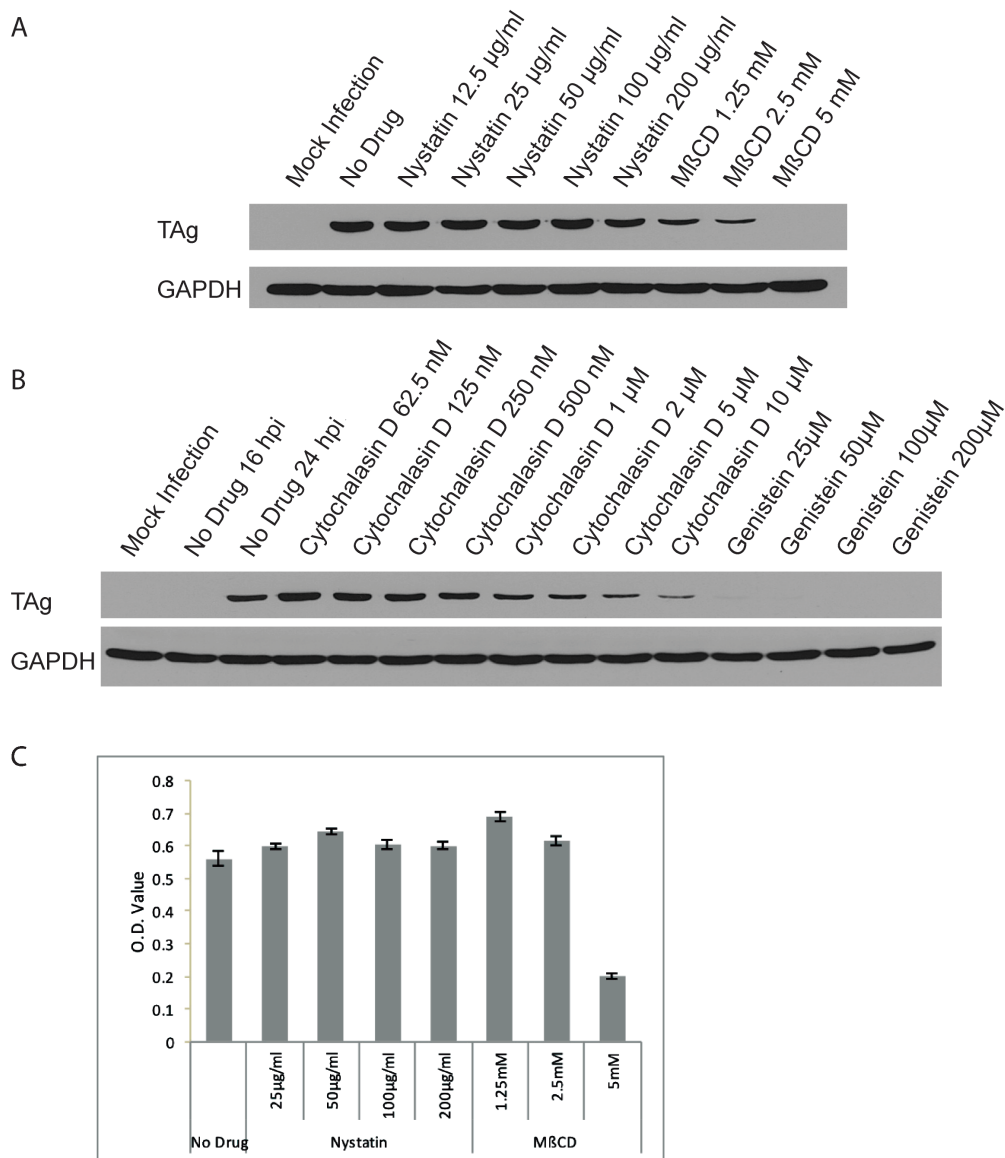
Figure 2.3: The effects of inhibitors on BKPyV infection.
(A) RPTE cells were treated with indicated drugs for 1 hour prior to BKPyV inoculation (MOI 0.5). Protein samples were collected at 48 hours post infection. Western blotting was performed on harvested protein samples. (B) RPTE cells were treated with indicated drugs for 1 hour prior to BKPyV inoculation (MOI 5). Protein samples were collected at 24 hours post infection (hpi) unless labeled otherwise. Western blotting was performed on harvested protein samples. (C) RPTE cells were treated as described above, and cell viability was evaluated with the WST-1 assay.

Interestingly, MβCD treatment significantly blocked BKPyV infection; however, nystatin did not affect BKPyV infection at all (Figure 2.3A).

Beside cholesterol, actin filaments also have an impact on BKPyV infection in Vero cells [15]. To confirm this in RPTE cells, actin filaments were disassembled with cytochalasin D, and actin filament disassembly was confirmed with phalloidin staining (Figure 2.4A-F). RPTE cells were then treated with cytochalasin D at various concentrations that had been tested to be non-toxic (Figure 2.4G). RPTE cells were infected with BKPyV (MOI 5) at 4˚C, and protein samples were harvested at 24 hours post infection unless indicated otherwise. When RPTE cells were treated at lower concentrations (lower than 500 nM) with cytochalasin D, phalloidin staining indicated that actin filaments were only partially disassembled (Figure 2.4A-D); however, BKPyV infection was slightly increased (Figure 2.3B). On the other hand, cytochalasin D at higher concentrations (500 nM or higher) significantly blocked actin filament assembly (Figure 2.4 E,F), and it also blocked BKPyV infection (Figure 2.3B). Genistein, a tyrosine kinase inhibitor, blocks BKPyV entry in Vero cells [12]. Its inhibitory effect in RPTE cells was also examined. At one day post infection, genistein completely blocked BKPyV entry in RPTE cells (Figure 2.3B). The experiments described above showed that BKPyV did not behave in exactly the same manner in natural host cells as it did in Vero cells. Next, whether BKPyV would follow a caveolin-dependent pathway in RPTE cells was tested. Caveolae have been reported to guide BKPyV entry in Vero cells [12]. In order to test whether BKPyV infects RPTE cells via the same endocytic pathway, caveolin 1 or caveolin 2 siRNA pools were transfected into cells. Each siRNA pool contained four unique siRNAs targeting the designated human mRNA. At 48 hours post-transfection, protein lysates were collected, resolved by SDS-PAGE, and probed for caveolin 1 or caveolin 2. Compared to the negative controls, samples with caveolin 1 or caveolin
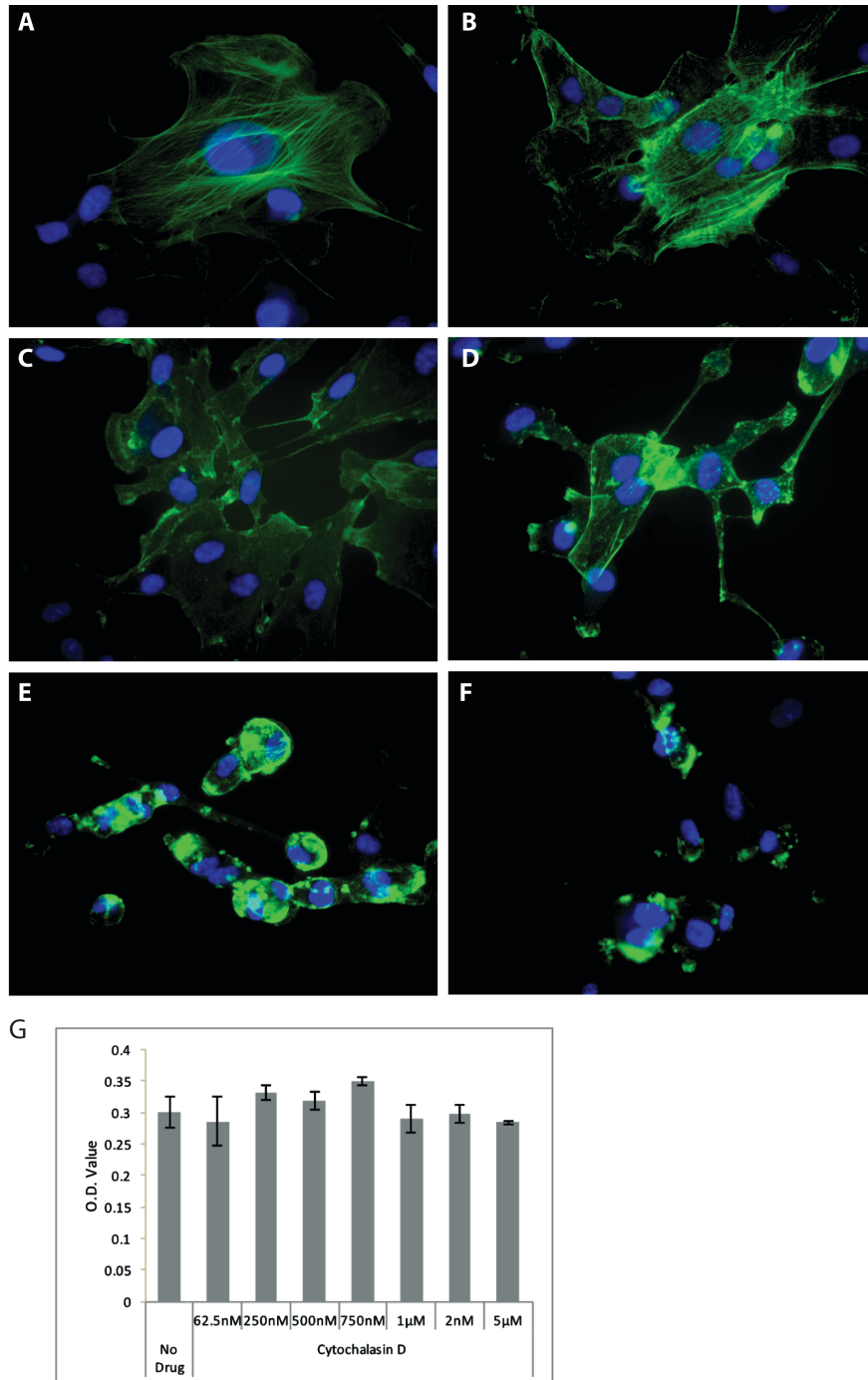
29

Figure 2.4: The effects of Cytochalasin D on actin filaments.
RPTE cells were treated for 1 hour with vehicle (DMSO, panel A) or 30 nM (B), 120 nM (C), 500 nM (D), 1 µM (E), or 2 µM (F) cytochalasin D, followed by staining with phalloidin. (G) RPTE cells were treated with cytochalasin D at indicated concentration for 24 hours, and cell viability was evaluated with the WST-1 assay.

2 siRNA transfection showed corresponding protein expression reduction, suggesting that the siRNA transfection was successful. However, an obvious off-target effect was also observed with caveolin 1-transfected RPTE cells. The caveolin 1 siRNA pool knocked down not only caveolin 1, but also caveolin 2 (Figure 2.5B). To eliminate the off-target effect from the caveolin 1 pool, the four siRNAs from this pool were transfected into RPTE cells individually to determine which siRNAs would knock down caveolin 1 but not caveolin 2. Analyzing protein samples from cells transfected with the individual siRNAs showed that siRNA #4 was the only siRNA that was capable of knocking down caveolin 1 without affecting caveolin 2 (Figure 2.5A).

To test the role of caveolin 1 or caveolin 2 during viral entry, caveolin 1 siRNA #4 or the caveolin 2 siRNA pool were transfected into RPTE cells. Transfection with no siRNA and the non-targeting siRNA pool were used as negative controls, and the siRNA pool targeting UGCG or an siRNA targeting TAg were positive controls. Cells were cultured for two days after transfection in order to deplete the targeted proteins and then infected with BKPyV. Two days post infection, cell lysates were collected and TAg and caveolin protein expression were evaluated by Western blotting. The Western blotting confirmed that the caveolin 1 siRNA #4 and the caveolin 2 siRNA pool successfully reduced caveolin 1 or caveolin 2 protein levels respectively (Figure 2.5B). The siUGCG pool and the siRNA targeting TAg both reduced TAg expression as expected. Surprisingly, knocking down caveolin did not increase or decrease BKPyV infection. These results suggest that BKPyV infection is independent of caveolin 1 or caveolin 2 in RPTE cells.

A

B
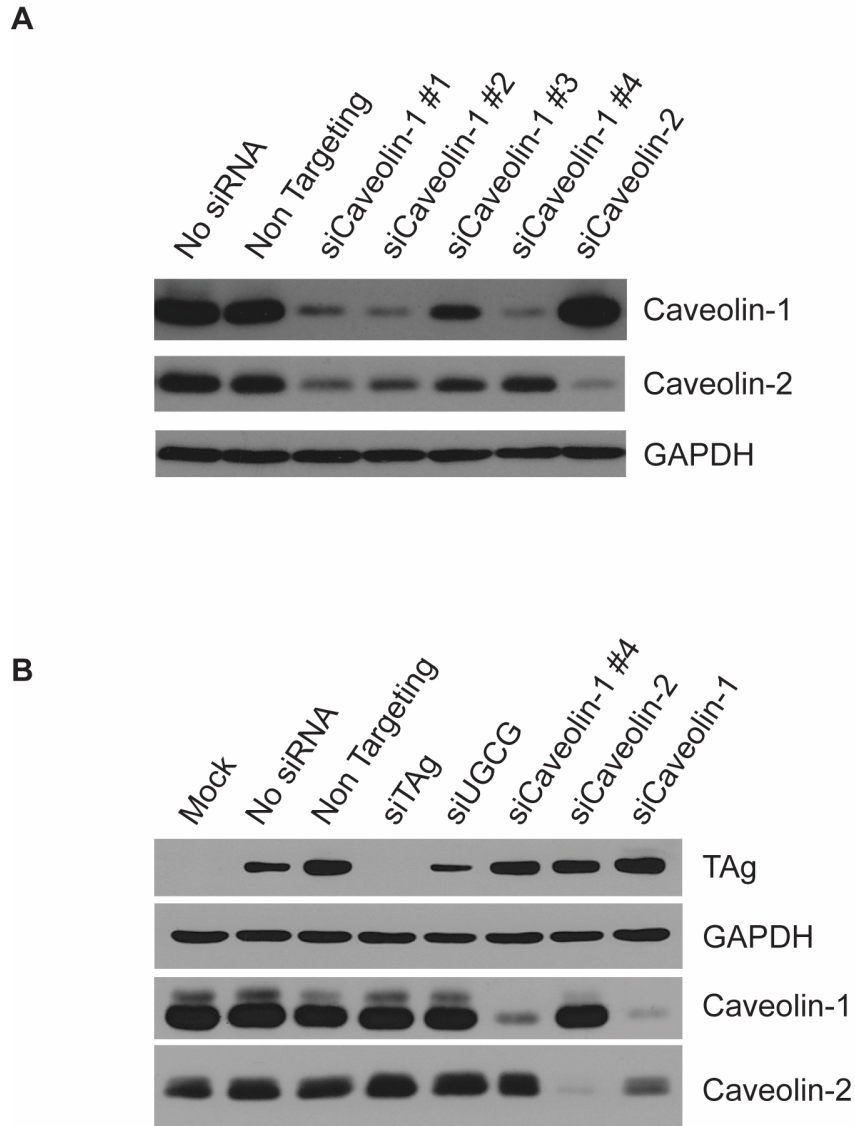
Figure 2.5: Caveolin protein knockdown and BKPyV entry.
(A) Cross-reactivity of siRNAs targeting caveolin 1 and caveolin 2. Individual siRNAs targeting caveolin 1 and an siRNA pool targeting caveolin 2 were transfected into RPTE cells. Caveolin expression at 2 days post infection was examined by Western blotting. (B) Caveolin protein knockdown does not affect BKPyV infection. RPTE cells were transfected with the indicated siRNAs. Viral infection and caveolin protein expression levels were examined by Western blotting.

Caveolin- and clathrin-dependent endocytic pathways are two major pathways that form small vesicles [22]. Clathrin-dependent endocytosis has been reported to be essential for JCPyV entry [28]. Since caveolins were not required for BKPyV entry into RPTE cells, we next examined if the clathrin-dependent pathway plays a role in BKPyV infection. To deplete clathrin, an siRNA pool targeting clathrin heavy chain was introduced into RPTE cells. BKPyV infection was evaluated as previously described. Compared to the no siRNA control and the non-targeting siRNA control, clathrin heavy chain was knocked down efficiently (Figure 2.6A). However, viral infection was not affected, indicating that BKPyV does not infect human RPTE cells by a clathrin-dependent pathway, consistent with the previous report from Moriyama et al [13]. In addition, we tested the possibility that both caveolin- and clathrin-dependent pathways could be involved during BKPyV endocytosis, and inhibiting one pathway can be compensated by the other pathway. To test this scenario, we transfected siRNA pools targeting clathrin heavy chain and the two caveolins into RPTE cells, and viral infection was evaluated. Similar to the single knockdowns, BKPyV infection was not affected compared to non-targeting control by knocking down caveolin 1, caveolin 2 and clathrin heavy chain at the same time (Figure 2.6B).

Norovirus also attaches to the plasma membrane with gangliosides [35] and enters host cells via a caveolin- and clathrin independent pathway [36]. In this study, Perry et al. demonstrated that dynamin II was involved in norovirus endocytosis. We therefore tested whether BKPyV entry is also dependent on dynamin II. RPTE cells were inoculated with BKPyV. After inoculation, NH_4Cl or Dynasore, a dynamin inhibitor [37], was added to infected cells at the indicated time points post infection. Protein samples were harvested and processed as previously described. The toxicity of NH4Cl or Dynasore was also tested (Figure 2.7B). Our laboratory has previously shown that NH4Cl blocks endosome acidification and thereby blocks BKPyV infection when

33

A

B
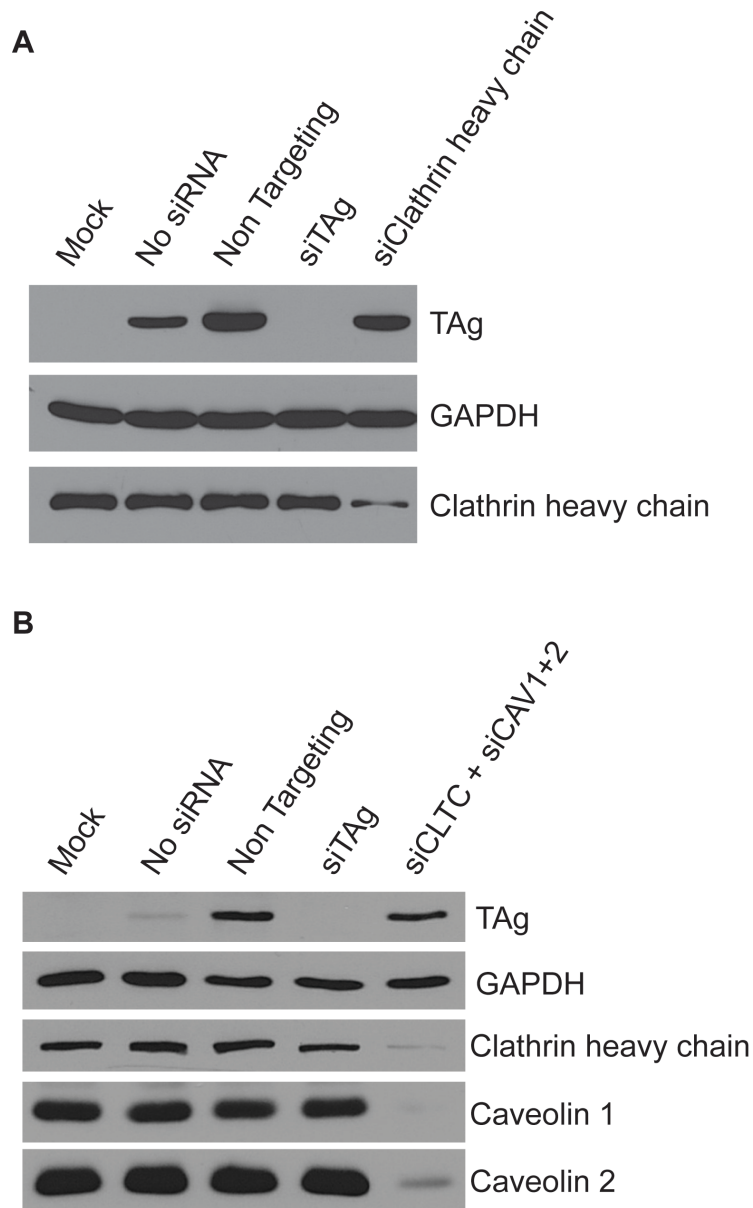
Figure 2.6: Clathrin heavy chain knockdown and BKPyV entry.
(A) RPTE cells were transfected with the indicated siRNAs, and viral infection and clathrin heavy chain expression levels were examined by Western blotting. (B) RPTE cells were transfected with the indicated combinations of siRNAs, and arranged as above.
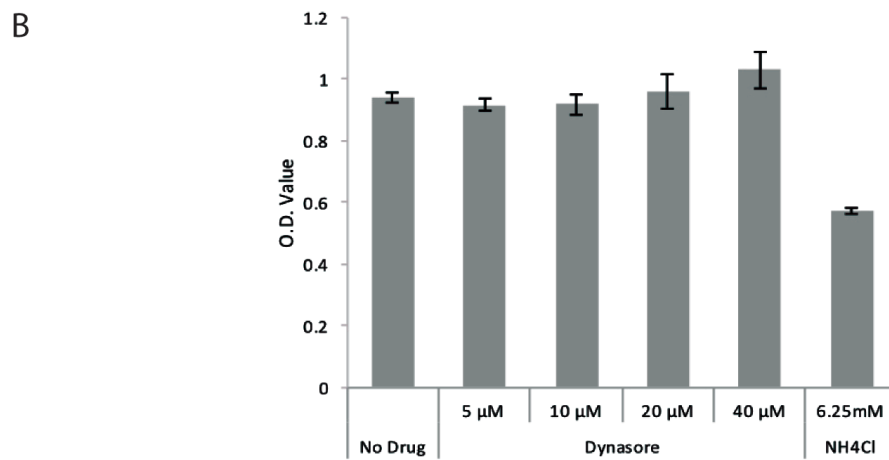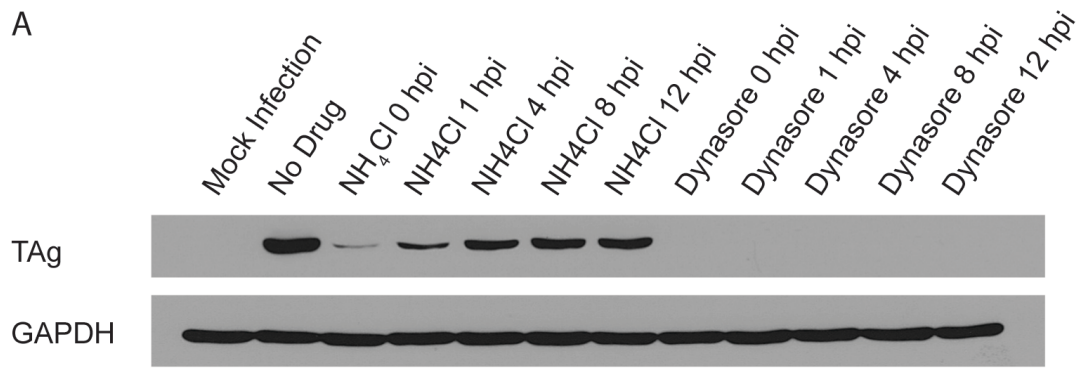
Figure 2.7: The effects of dynamin inhibitor on BKPyV infection.
(A) RPTE cells were inoculated with BKPyV (MOI 0.5). Dynasore (40µM) or NH$_4$Cl (6.25mM) were added at indicated time points. Protein samples were collected at 48 hours post infection. Western blotting was performed on harvested protein samples. (B) RPTE cells were treated with indicated drugs for 48 hours. Cell viability was evaluated with WST-1 assay.

added before 2 hours post infection [18], which was reproduced in this experiment (Figure 2.7A). Surprisingly, Dynasore blocked BKPyV infection when added up to 12 hours post infection (Figure 2.7A). At 12 hours post infection, BKPyV has already arrived at the ER, suggesting that Dynasore blocks a later step of BKPyV infection.

Discussion

BKPyV directly causes allograft failure among at least 1% of kidney transplant patients worldwide. Moreover, BKPyV can causes painful HC in hematopoietic cell transplant patients. Unfortunately, specific antiviral drugs are not currently available, and the only management available is withdrawing immunosuppression in PVAN patients, which risks acute rejection, or palliative care in HC patients. Due to the fact that BKPyV uses the host DNA synthesis machinery for its genome replication, one possible effective strategy to protect cells from infection would be targeting critical host factors required by BKPyV before it delivers its DNA genome into the nucleus of the host cell. Therefore, understanding the trafficking pathway that BKPyV undergoes is not only important for understanding viral biology but also potentially important for identifying drug targets.

The trafficking pathways of polyomaviruses have been extensively studied since the initial isolation of murine polyomavirus (MPyV) in 1953 [38]. Polyomaviruses have been shown to use three pathways to infect host cells: caveolin-dependent [12,13], clathrin-dependent [28], or caveolin- and clathrin-independent [4,6]. With BKPyV, most of the initial trafficking studies were carried out using non-human animal cell models because of a lack of relevant human cell models at the time. Those studies indicated that BKPyV infects monkey cells via a caveolin-dependent pathway [12]. However, several pieces of evidence caused us to examine whether the BKPyV entry

36

process might be cell type- or species-specific. First, SV40, MPyV, and cholera toxin B subunit had been originally considered to enter cells via a caveolin-dependent pathway [2,27,39,40], but subsequent studies showed that SV40, MPyV, and cholera toxin are able to enter caveolin 1-deficient cells [3,4,6,41,42]. Second, our lab showed that SV40 trafficking is cell type-dependent [20]. Third, an *in vitro* study showed that the 3-hydroxy-3-methyl-glutaryl coenzyme A (HMG-CoA) reductase inhibitor Pravastatin, which inhibits cholesterol synthesis, prevents BKPyV infection by depleting caveolin 1 protein in RPTE cells [43]; however, a clinical trial using Pravastatin failed to protect patients from PVAN at the maximum effective dose [44]. Lastly, a study focused on BKPyV trafficking in human kidney cells supported the previous animal model that BKPyV entry is caveolin-dependent [13]; however, we were unable to reproduce the results of Moriyama et al. by exactly following their reported protocol. In fact, our caveolin depletion was at least two fold more efficient than theirs, and viral infection was evaluated as early as one-day post infection versus five days post infection as they tested. Considering that 100 nM siRNA was applied in their experiment setting, the phenotype they observed could be an off-target effect of the concentrated siRNA.

These findings inspired us to re-examine BKPyV entry into RPTE cells. Our results demonstrate that BKPyV does behave differently when infecting RPTE cells than it does in monkey cells. The cholesterol-depleting reagent MβCD blocked BKPyV infection as previously tested in Vero cells [12], however, another cholesterol depleting reagent, nystatin, did not block BKPyV infection in RPTE cells at all. Actin filament disassembly upon latrunculin A treatment did not affect BKPyV infection in Vero cells. However, another actin assembly inhibitor, cytochalasin D, slightly increased BKPyV infection of RPTE cells at lower concentrations (lower than 500 nM), and decreased infection at higher concentrations (500 nM or higher).

Dynasore, a dynamin II inhibitor, blocked viral entry as expected, however, it could still block BKPyV infection even after viruses reached the ER. The effects of inhibitor treatments were more complicated than our original expectations, and drugs that have similar function showed totally conflicting effects on BKPyV entry. Although we confirmed the inhibitory effect of genistein in RPTE cells, genistein regulates too many pathways to make any conclusion about a particular pathway [45,46]. It suggests that more care is required when interpreting drug treatment results.

By transfecting siRNAs targeting caveolin 1 or caveolin 2, we reduced caveolin 1 or caveolin 2 expression in RPTE cells without affecting BKPyV infection. We also tested if BKPyV infects RPTE cells using clathrin-coated vesicles, as JCPyV does in the human glial cell line SVG [28]. Similar to the caveolin knockdown, there was no obvious difference in infection between clathrin heavy chain-depleted cells versus control cells. In order to eliminate the possibility that BKPyV enters RPTE cells via both caveolin- and clathrin-dependent pathways, the two caveolins and clathrin heavy chain were knocked down together, and when we challenged the transfected cells with BKPyV, no change in BKPyV infection was observed. In addition, our UGCG knockdown data confirmed previous findings from our lab that gangliosides GD1b and GT1b serve as receptors for BKPyV in primary RPTE cells. We saw a reproducible slight increase in infection in cells transfected with the non-targeting siRNA pool. It suggests that the non-targeting siRNA pool also has an off-targeting effect.

Several caveolin- and clathrin-independent pathways that could assist BKPyV entry have been reported, such as RhoA/Rac1 [47], Cdc42 [48,49], ARF6 [50], and flotillin [51] mediated endocytosis. Considering that polyomavirus enters tight fitting vesicles after endocytosis [6,14,52], and actin polymerization may not be required for BKPyV entry [15] , we speculate that BKPyV is more

likely to infect RPTE cells by a yet uncharacterized endocytic pathway, since most of the endocytic pathways listed above are associated with actin polymerization [53-56].

In addition to protein-dependent endocytic pathways, it is possible that BKPyV enters host cells using a lipid-mediated endocytosis pathway in which cholesterol and gangliosides alone may be sufficient to initiate entry. An in vitro assay showed that artificial liposomes with cholesterol and gangliosides, called giant unilamellar vesicles, can form caveolae-like vesicles without the addition of any host proteins [57]. A later study showed that SV40 was able to induce deep invaginations on the surface of these vesicles [58], suggesting that entry could be vesicle coat protein-independent. In that scenario, the virus-containing tight fitting vesicles might be formed by multiple direct interactions between gangliosides and the VP1 capsid protein, with cholesterol stabilizing the vesicle membrane invagination. Further studies are required to fully define the BKPyV endocytosis process.

In summary, we have demonstrated that BKPyV enters its natural host cell via a caveolin- and clathrin-independent pathway, and we have confirmed that gangliosides GD1b/GT1b serve as receptors. Additional studies will be required to determine the role of additional cellular proteins in the viral entry and trafficking processes.

Materials and Methods

Cell culture. Primary renal proximal tubule epithelial cells (RPTE) (Lonza) were grown in renal epithelial basal growth medium (REBM) (Lonza) with renal epithelial cell growth medium (REGM) supplement (Lonza) at 37˚C with 5% CO_2 in a humidified incubator.

Drug treatment. Nystatin (Sigma) and methyl-β-cyclodextrin (MβCD, Sigma) were kindly provided by Christiane Wobus (University of Michigan). Nystatin was suspended at 50 mg/ml in cell culture grade water. MβCD was dissolved in cell culture grade water at 30 mM. Dynasore (Sigma) was dissolved in DMSO at 20 mM. Cytochalasin D (Sigma) was dissolved in DMSO at 1 mM. NH_4Cl (Fisher) was dissolved in cell grade water at 1 M and filtered with a 0.22 μm filter. Genistein (Sigma) was dissolved in DMSO at 50 mM. Drugs or vehicle were directly added to the cell culture media at indicated concentrations and time points.

Phalloidin staining. RPTE cells were grown on coverslips in a 12 well plate. After drug treatment, cells were fixed with 4% paraformaldehyde (PFA) in PBS at room temperature for 10 minutes. After fixation, cells were permeabilized with 0.1% Triton X-100 in PBS at room temperature for 5 minutes. Next, cells were stained with 1 unit Alexa Fluor 488 phalloidin (Thermo) in 200 μl PBS for 20 minutes at room temperature. The coverslips were mounted in Prolong Gold with DAPI (Thermo) onto microscope slides (Thermo). Cells were washed with PBS three times between each staining step.

Transfection. siGENOME siRNA pools and individual siRNAs were purchased from Dharmacon: Non-targeting control (D-001206-14); Caveolin 1 (M-003467-01); Caveolin 2 (M-010958-00); UGCG (M-006441-02); Caveolin 1 #1 (D-003467-01); Caveolin 1 #2 (D-003467-02); Caveolin 1 #3 (D-003467-03); Caveolin 1 #4 (D-003467-05); Clathrin heavy chain (M-004001-00). siRNA targeting large T antigen was custom synthesized with the sequence (5' AUCUGAGACUUGGGAAGAGCAU 3'), which corresponds to the natural BKPyV 5p miRNA [59]. siRNAs were rehydrated at 20 μM according to the Basic siRNA Resuspension protocol from

Dharmacon. RPTE cells were transfected according to the Lipofectamine RNAiMAX (Thermo Fisher Scientific) manual. Transfection complexes were prepared by mixing 1 µl of 20 µM siRNA with 400 µl of diluted transfection reagent (0.7% RNAiMAX reagent v/v in REBM/REGM without antibiotics) in each well of a 12 well plate. The complexes were incubated at room temperature for 20 min before adding 70,000 cells suspended in 400 µl REBM/REGM without antibiotics to each well.

Infection. BKPyV (Dunlop) was cultured, purified with a cesium chloride linear gradient, and titered as described previously [18,60]. RPTE cells were infected as follows at 2 days post transfection. Cells were pre-chilled for 15 min at 4˚C. Purified viruses were diluted to 87,500 IU/ml (MOI 0.5) or 875,000 IU/ml (MOI 5) in REBM/REGM. 400 µl of the diluted virus were added to the wells and incubated at 4˚C for 1 hour with shaking every 15 minutes to distribute the inoculum over the entire well. The plate was transferred to 37˚C after the 1-hour incubation.

Ganglioside treatment. Gangliosides GM1, GD1b, and GT1b (Matreya) were kindly provided by Billy Tsai (University of Michigan). Gangliosides were rehydrated at 1 mM in cell culture grade water. 10 hours prior to infection, gangliosides were added directly to the media at 1 µM. At the time of infection, media with gangliosides was removed and cells were washed with fresh media to remove the unincorporated gangliosides.

Preparation of protein lysates. Cells were lysed at 48 hours post infection with E1A buffer (50 mM HEPES [pH 7], 250 mM NaCl, and 0.1% NP-40, with inhibitors: 5 µg/ml PMSF,

5 µg/ml aprotinin, 5 µg/ml leupeptin, 50 mM sodium fluoride and 0.2 mM sodium orthovanadate added right before use). Protein concentration was quantified with the Bradford assay (Bio-Rad).

Western blotting. Protein samples were separated on 12% SDS-PAGE gels. After electrophoresis, the proteins were transferred to a nitrocellulose membrane (pore size 0.2 µm) with a Bio-rad Trans-Blot Cell in Towbin transfer buffer (25 mM Tris, 192 mM glycine, 20% methanol), at 60 V overnight. Membranes were blocked with 2% nonfat milk in PBS-T buffer (144 mg/L KH_2PO_4, 9 g/L NaCl, 795 mg/L Na_2HPO_4, pH 7.4, 0.1% Tween 20) for 1 hour. Membranes were probed with primary and secondary antibodies diluted in 2% milk in PBS-T as follows: TAg (pAb416) at 1:5,000 dilution [61]; GAPDH (Abcam ab9484) at 1:10,000; caveolin 1 (Santa Cruz SC-894) at 1:20,000; caveolin 2 (Cell signaling #8522) at 1:5,000; clathrin heavy chain (Thermo Fisher Scientific, MA1-065) was kindly provided by Christiane Wobus (University of Michigan), used at 1:10,000, horseradish peroxidase (HRP)-conjugated ECL sheep anti-mouse (GE healthcare NA931V) at 1:5,000; and HRP-conjugated ECL donkey anti-rabbit antibody (GE healthcare NA934V) at 1:5,000. Protein bands were further visualized with HRP substrate (Millipore, WBLUF0100) and exposure to films.

Reverse transcription and quantitative PCR (RT-qPCR). At 48 hours post transfection, cellular RNA was harvested with TRIzol RNA isolation reagent (Thermo Fisher Scientific) and further purified according to the manual for the Zymo Research Direct-zol RNA MiniPrep kit. 100 ng of RNA was treated with 1 unit of DNase I (Promega) and cDNA was prepared according to the SuperScript II Reverse Transcriptase (Thermo Fisher Scientific) manual. qPCR was performed on the cDNA with either of the following primer pairs: GAPDH

(5' GCCTCAAGATCATCAGCAAT 3') and (5' CTGTGGTCATGAGTCCTTCC 3'), UGCG

(5' AGACACCTGGGAGCTTGCTA 3') and (5' TTCGTCCTCTTCTTGGTGCT 3'). UGCG or

GAPDH expression in each cDNA sample was quantified in 25 µl reactions and in triplicate.

Each reaction was comprised of 2.5 µl of cDNA, 12.5 µl of Power SYBR green PCR master mix

(Applied Biosystems), 300 nM of each primer, and nuclease free water (Promega). Amplification

was performed using the iCycler iQ5 real-time detection system (Bio-Rad) with the following

PCR protocol settings: 2 min at 50°C, 10 min at 95°C, 40 cycles of 15 s at 95°C and 30 s at

57°C. SYBR green signal intensity was read immediately after each 57˚C extension.

Note

Parts of this chapter were previously published: Zhao L, Marciano AT, Rivet CR,

Imperiale MJ. 2016. Caveolin- and clathrin-independent entry of BKPyV into primary human

proximal tubule epithelial cells. *Virology*. 492:66-72.

References

1. You J, O'Hara SD, Velupillai P, et al. Ganglioside and non-ganglioside mediated host responses to the mouse polyomavirus. Meyers C, ed. *PLoS Pathog*. 2015;11(10):e1005175. doi:10.1371/journal.ppat.1005175.

2. Richterová Z, Liebl D, Horák M, et al. Caveolae are involved in the trafficking of mouse polyomavirus virions and artificial VP1 pseudocapsids toward cell nuclei. *J Virol*. 2001;75(22):10880-10891. doi:10.1128/JVI.75.22.10880-10891.2001.

3. Gilbert JM, Goldberg IG, Benjamin TL. Cell penetration and trafficking of polyomavirus. *J Virol*. 2003;77(4):2615-2622. doi:10.1128/JVI.77.4.2615-2622.2003.

4. Liebl D, Difato F, Horníková L, Mannová P, Štokrová J, Forstová J. Mouse polyomavirus enters early endosomes, requires their acidic pH for productive infection, and meets transferrin cargo in Rab11-positive endosomes. *J Virol*. 2006;80(9):4610-4622. doi:10.1128/JVI.80.9.4610-4622.2006.

5. Norkin LC. Simian virus 40 infection via MHC class I molecules and caveolae. *Immunol Rev*. 1999;168(1):13-22. doi:10.1111/j.1600-065X.1999.tb01279.x.

6.   Damm E-M, Pelkmans L, Kartenbeck J, Mezzacasa A, Kurzchalia T, Helenius A. Clathrin- and caveolin-1-independent endocytosis: entry of simian virus 40 into cells devoid of caveolae. *J Cell Biol*. 2005;168(3):477-488. doi:10.1083/jcb.200407113.

7.   Ströh LJ, Gee GV, Blaum BS, et al. Trichodysplasia spinulosa-associated polyomavirus uses a displaced binding site on VP1 to engage sialylated glycolipids. *PLoS Pathog*. 2015;11(8):e1005112. doi:10.1371/journal.ppat.1005112.

8.   Low JA, Magnuson B, Tsai B, Imperiale MJ. Identification of gangliosides GD1b and GT1b as receptors for BK virus. *J Virol*. 2006;80(3):1361-1366. doi:10.1128/JVI.80.3.1361-1366.2006.

9.   Neu U, Allen S-AA, Blaum BS, et al. A structure-guided mutation in the major capsid protein retargets BK polyomavirus. Galloway DA, ed. *PLoS Pathog*. 2013;9(10):e1003688. doi:10.1371/journal.ppat.1003688.

10.   Dugan AS, Eash S, Atwood WJ. An N-linked glycoprotein with alpha(2,3)-linked sialic acid is a receptor for BK virus. *J Virol*. 2005;79(22):14442-14445. doi:10.1128/JVI.79.22.14442-14445.2005.

11.   Lingwood D, Simons K. Lipid rafts as a membrane-organizing principle. *Science*. 2010;327(5961):46-50. doi:10.1126/science.1174621.

12.   Eash S, Querbes W, Atwood WJ. Infection of vero cells by BK virus is dependent on caveolae. *J Virol*. 2004;78(21):11583-11590. doi:10.1128/JVI.78.21.11583-11590.2004.

13.   Moriyama T, Marquez JP, Wakatsuki T, Sorokin A. Caveolar endocytosis is critical for BK virus infection of human renal proximal tubular epithelial cells. *J Virol*. 2007;81(16):8552-8562. doi:10.1128/JVI.00924-07.

14.   Maraldi NM, Barbanti-Brodano G, Portolani M, La Placa M. Ultrastructural aspects of BK virus uptake and replication in human fibroblasts. *J Gen Virol*. 1975;27(1):71-80. doi:10.1099/0022-1317-27-1-71.

15.   Eash S, Atwood WJ. Involvement of cytoskeletal components in BK virus infectious entry. *J Virol*. 2005;79(18):11734-11741. doi:10.1128/JVI.79.18.11734-11741.2005.

16.   Querbes W, O'Hara BA, Williams G, Atwood WJ. Invasion of host cells by JC virus identifies a novel role for caveolae in endosomal sorting of noncaveolar ligands. *J Virol*. 2006;80(19):9402-9413. doi:10.1128/JVI.01086-06.

17.   Engel S, Heger T, Mancini R, et al. Role of endosomes in simian virus 40 entry and infection. *J Virol*. 2011;85(9):4198-4211. doi:10.1128/JVI.02179-10.

18.   Jiang M, Abend JR, Tsai B, Imperiale MJ. Early events during BK virus entry and disassembly. *J Virol*. 2009;83(3):1350-1358. doi:10.1128/JVI.02169-08.

19. Moriyama T, Sorokin A. Intracellular trafficking pathway of BK Virus in human renal proximal tubular epithelial cells. *Virology*. 2008;371(2):336-349. doi:10.1016/j.virol.2007.09.030.

20. Bennett SM, Jiang M, Imperiale MJ. Role of cell-type-specific endoplasmic reticulum-associated degradation in polyomavirus trafficking. *J Virol*. 2013;87(16):8843-8852. doi:10.1128/JVI.00664-13.

21. Bennett SM, Zhao L, Bosard C, Imperiale MJ. Role of a nuclear localization signal on the minor capsid proteins VP2 and VP3 in BKPyV nuclear entry. *Virology*. 2015;474:110-116. doi:10.1016/j.virol.2014.10.013.

22. Mayor S, Pagano RE. Pathways of clathrin-independent endocytosis. *Nat Rev Mol Cell Biol*. 2007;8(8):603-612. doi:10.1038/nrm2216.

23. Murata M, Peränen J, Schreiner R, Wieland F, Kurzchalia TV, Simons K. VIP21/caveolin is a cholesterol-binding protein. *PNAS*. 1995;92(22):10339-10343.

24. Rothberg KG, Heuser JE, Donzell WC, Ying YS, Glenney JR, Anderson RG. Caveolin, a protein component of caveolae membrane coats. *Cell*. 1992;68(4):673-682.

25. Drab M, Verkade P, Elger M, et al. Loss of caveolae, vascular dysfunction, and pulmonary defects in caveolin-1 gene-disrupted mice. *Science*. 2001;293(5539):2449-2452. doi:10.1126/science.1062688.

26. Razani B, Wang XB, Engelman JA, et al. Caveolin-2-deficient mice show evidence of severe pulmonary dysfunction without disruption of caveolae. *Mol Cell Biol*. 2002;22(7):2329-2344. doi:10.1128/MCB.22.7.2329-2344.2002.

27. Pelkmans L, Kartenbeck J, Helenius A. Caveolar endocytosis of simian virus 40 reveals a new two-step vesicular-transport pathway to the ER. *Nature Cell Biology*. 2001;3(5):473-483. doi:10.1038/35074539.

28. Pho MT, Ashok A, Atwood WJ. JC virus enters human glial cells by clathrin-dependent receptor-mediated endocytosis. *J Virol*. 2000;74(5):2288-2292.

29. Fotin A, Cheng Y, Sliz P, et al. Molecular model for a complete clathrin lattice from electron cryomicroscopy. *Nature*. 2004;432(7017):573-579. doi:10.1038/nature03079.

30. Hinrichsen L, Harborth J, Andrees L, Weber K, Ungewickell EJ. Effect of clathrin heavy chain- and alpha-adaptin-specific small inhibitory RNAs on endocytic accessory proteins and receptor trafficking in HeLa cells. *J Biol Chem*. 2003;278(46):45160-45170. doi:10.1074/jbc.M307290200.

31. Lingwood CA, Manis A, Mahfoud R, Khan F, Binnington B, Mylvaganam M. New aspects of the regulation of glycosphingolipid receptor function. *Chem Phys Lipids*. 2010;163(1):27-35. doi:10.1016/j.chemphyslip.2009.09.001.

32. López CA, de Vries AH, Marrink SJ. Molecular mechanism of cyclodextrin mediated cholesterol extraction. Berkowitz M, ed. *PLoS Comput Biol*. 2011;7(3):e1002020–. doi:10.1371/journal.pcbi.1002020.

33. Ohtani Y, Irie T, Uekama K, Fukunaga K, Pitha J. Differential effects of alpha-, beta- and gamma-cyclodextrins on human erythrocytes. *Eur J Biochem*. 1989;186(1-2):17-22.

34. Bittman R, Fischkoff SA. Fluorescence studies of the binding of the polyene antibiotics filipin 3, amphotericin B, nystatin, and lagosin to cholesterol. *PNAS*. 1972;69(12):3795-3799.

35. Taube S, Perry JW, Yetming K, et al. Ganglioside-linked terminal sialic acid moieties on murine macrophages function as attachment receptors for murine noroviruses. *J Virol*. 2009;83(9):4092-4101. doi:10.1128/JVI.02245-08.

36. Perry JW, Wobus CE. Endocytosis of murine norovirus 1 into murine macrophages is dependent on dynamin II and cholesterol. *J Virol*. 2010;84(12):6163-6176. doi:10.1128/JVI.00331-10.

37. Macia E, Ehrlich M, Massol R, Boucrot E, Brunner C, Kirchhausen T. Dynasore, a cell-permeable inhibitor of dynamin. *Dev Cell*. 2006;10(6):839-850. doi:10.1016/j.devcel.2006.04.002.

38. Gross L. A filterable agent, recovered from Ak leukemic extracts, causing salivary gland carcinomas in C3H mice. *Experimental Biology and Medicine*. 1953;83(2):414-421. doi:10.3181/00379727-83-20376.

39. Orlandi PA, Fishman PH. Filipin-dependent inhibition of cholera toxin: evidence for toxin internalization and activation through caveolae-like domains. *J Cell Biol*. 1998;141(4):905-915. doi:10.1083/jcb.141.4.905.

40. Parton RG. Regulated internalization of caveolae. *J Cell Biol*. 1994;127(5):1199-1215. doi:10.1083/jcb.127.5.1199.

41. Shogomori H, Futerman AH. Cholera toxin is found in detergent-insoluble rafts/domains at the cell surface of hippocampal neurons but is internalized via a raft-independent mechanism. *J Biol Chem*. 2001;276(12):9182-9188. doi:10.1074/jbc.M009414200.

42. Torgersen ML, Skretting G, van Deurs B, Sandvig K. Internalization of cholera toxin by different endocytic mechanisms. *J Cell Sci*. 2001;114(Pt 20):3737-3747.

43. Moriyama T, Sorokin A. Repression of BK virus infection of human renal proximal tubular epithelial cells by pravastatin. *Transplantation*. 2008;85(9):1311-1317. doi:10.1097/TP.0b013e31816c4ec5.

44. Gabardi S, Ramasamy S, Kim M, et al. Impact of HMG-CoA reductase inhibitors on the incidence of polyomavirus-associated nephropathy in renal transplant recipients with

human BK polyomavirus viremia. *Transpl Infect Dis*. 2015;17(4):536-543. doi:10.1111/tid.12402.

45. Banerjee S, Li Y, Wang Z, Sarkar FH. Multi-targeted therapy of cancer by genistein. *Cancer Lett*. 2008;269(2):226-242. doi:10.1016/j.canlet.2008.03.052.

46. Andres A, Donovan SM, Kuhlenschmidt MS. Soy isoflavones and virus infections. *J Nutr Biochem*. 2009;20(8):563-569. doi:10.1016/j.jnutbio.2009.04.004.

47. Lamaze C, Dujeancourt A, Baba T, Lo CG, Benmerah A, Dautry-Varsat A. Interleukin 2 receptors and detergent-resistant membrane domains define a clathrin-independent endocytic pathway. *Molecular Cell*. 2001;7(3):661-671. doi:10.1016/S1097-2765(01)00212-X.

48. Sabharanjak S, Sharma P, Parton RG, Mayor S. GPI-anchored proteins are delivered to recycling endosomes via a distinct cdc42-regulated, clathrin-independent pinocytic pathway. *Dev Cell*. 2002;2(4):411-423.

49. Chadda R, Howes MT, Plowman SJ, Hancock JF, Parton RG, Mayor S. Cholesterol-sensitive Cdc42 activation regulates actin polymerization for endocytosis via the GEEC pathway. *Traffic*. 2007;8(6):702-717. doi:10.1111/j.1600-0854.2007.00565.x.

50. Radhakrishna H, Donaldson JG. ADP-ribosylation factor 6 regulates a novel plasma membrane recycling pathway. *J Cell Biol*. 1997;139(1):49-61. doi:10.1083/jcb.139.1.49.

51. Glebov OO, Bright NA, Nichols BJ. Flotillin-1 defines a clathrin-independent endocytic pathway in mammalian cells. *Nature Cell Biology*. 2006;8(1):46-54. doi:10.1038/ncb1342.

52. Drachenberg CB, Papadimitriou JC, Wali R, Cubitt CL, Ramos E. BK polyoma virus allograft nephropathy: ultrastructural features from viral cell entry to lysis. *Am J Transplant*. 2003;3(11):1383-1392.

53. Ilangumaran S, Hoessli DC. Effects of cholesterol depletion by cyclodextrin on the sphingolipid microdomains of the plasma membrane. *Biochem J*. 1998;335 (Pt 2):433-440.

54. Burridge K, Wennerberg K. Rho and Rac take center stage. *Cell*. 2004;116(2):167-179.

55. Doherty GJ, McMahon HT. Mechanisms of endocytosis. *Annual review of biochemistry*. 2009;78:857-902. doi:10.1146/annurev.biochem.78.081307.110540.

56. Chinnapen DJ-F, Hsieh W-T, Welscher te YM, et al. Lipid sorting by ceramide structure from plasma membrane to ER for the cholera toxin receptor ganglioside GM1. *Dev Cell*. 2012;23(3):573-586. doi:10.1016/j.devcel.2012.08.002.

57. Bacia K, Schwille P, Kurzchalia T. Sterol structure determines the separation of phases

and the curvature of the liquid-ordered phase in model membranes. *PNAS*. 2005;102(9):3272-3277. doi:10.1073/pnas.0408215102.

58. Ewers H, Römer W, Smith AE, et al. GM1 structure determines SV40-induced membrane invagination and infection. *Nature Cell Biology*. 2010;12(1):11–8–suppp1–12. doi:10.1038/ncb1999.

59. Seo GJ, Fink LHL, O'Hara B, Atwood WJ, Sullivan CS. Evolutionarily conserved function of a viral microRNA. *J Virol*. 2008;82(20):9823-9828. doi:10.1128/JVI.01144-08.

60. Abend JR, Low JA, Imperiale MJ. Inhibitory effect of gamma interferon on BK virus gene expression and replication. *J Virol*. 2007;81(1):272-279. doi:10.1128/JVI.01571-06.

61. Harlow E, Whyte P, Franza BR, Schley C. Association of adenovirus early-region 1A proteins with cellular polypeptides. *Mol Cell Biol*. 1986;6(5):1579-1589.

CHAPTER III

Whole genome RNA interference screen for host genes associated with BKPyV infection

Abstract

BK polyomavirus (BKPyV) is a human pathogen first isolated in 1971. The mature BKPyV particle is about 45 nm in diameter and contains a 5.2 kb circular dsDNA genome. BKPyV infection is ubiquitous in the human population, with over 80% of the adult population worldwide seropositive for BKPyV. BKPyV infection is usually asymptomatic; however, BKPyV reactivates in immunosuppressed transplant patients and causes two diseases, polyomavirus associated nephropathy (PVAN) and hemorrhagic cystitis. Due to a lack of specific antiviral drugs, the first-line treatment for BKPyV reactivation is to reduce immunosuppression in PVAN patients, thereby increasing the likelihood of graft rejection; therefore, elucidating details of the BKPyV life cycle will potentially benefit clinical practice and therapy development in addition to uncovering interesting viral and cell biology.

In order to establish a productive infection, viruses have developed multiple strategies to set up a permissive environment for replication. This requires interactions between various viral components and host cell proteins. Whole-genome high-throughput siRNA screening provides a tool to investigate potential virus-host interactions. By silencing every single human gene with an siRNA pool, and then assessing the effects of the knockdown on BKPyV infection, we will be

able to dissect the functions of individual host proteins during the viral life cycle. To further identify host factors associated with BKPyV entry and intracellular trafficking, a whole genome siRNA screen was performed on BKPyV in human primary renal proximal tubular epithelial (RPTE) cells. DNAJ B14, which has previously been implicated in BKPyV entry, is our top hit, and DNAJ B12 is also among our top 100 hits. The other hits we identified have not been previously reported; however, many of them are involved in vesicular transport. After validation, Rab18, STX18 protein, and the NRZ protein complex are identified to be essential for BKPyV infection. Considering that all of these proteins form a complex on the ER membrane and participate in Golgi to ER trafficking, the Golgi to ER pathway may play an important previously-undiscovered role in BKPyV infection.

Introduction

BK polyomavirus (BKPyV) is a small DNA icosahedral virus measuring about 45 nm in diameter, and was first isolated in 1971[1]. Subsequent serology surveys revealed that up to 80% of the world's population has been infected with BKPyV [2], and most of the initial infections occur in early childhood [3]. Fortunately for most healthy individuals, the immune system limits BKPyV infection, and BKPyV infection is usually asymptomatic. After initial exposure, BKPyV establishes a persistent infection in the urinary tract with periodic shedding into the urine [4]. BKPyV reactivates when the immune system is compromised in transplant patients, and it causes two diseases: polyomavirus-associated nephropathy (PVAN) and hemorrhagic cystitis (HC). PVAN is one of the major causes of graft failure after kidney transplantation [5]. In addition, BKPyV can be detected in the urine of 90% of allogeneic hematopoietic cell transplant patients who suffered from HC, according to a recent study [6].

50

Despite the fact that BKPyV was initially isolated more than 40 years ago, the choices for clinical management of BKPyV reactivation are limited. Because the viral genome does not encode any polymerase, BKPyV relies exclusively on the host DNA replication machinery for viral genome replication; therefore, most common therapeutic strategies targeting viral polymerases are not applicable. The first-line treatment for PVAN is lowering the dosage of immunosuppressants, which inevitably increases the risk of acute rejection and graft failure [5]. Other options for treating BKPyV besides withdrawing immunosuppressants are cidofovir, leflunomide, and fluoroquinolones, drugs that inhibit BKPyV infection through modulating the host cell DNA replication machinery. However, they are not good options because of their cytotoxicity. Therefore, no specific antiviral drug is currently available for BKPyV reactivation.

To establish a successful infection, BKPyV must deliver its DNA genome into the nucleus in order to access the host DNA replication machinery, which means penetrating the plasma membrane, the ER membrane, and the nuclear envelope. In addition, BKPyV has to traffic to the ER through a crowded cytoplasm. Without any help from host factors, this process would seem impossible. In order to block BKPyV infection, one possible strategy would be to target host factors that assist viral entry or intracellular trafficking before the virus manages to deliver its genome to the nucleus.

Many host factors have been demonstrated as playing important roles after BKPyV delivers its genome into the nucleus, such as p53 [7], pRB [8], ATM, and ATR [9]. However, few host factors have been identified as assisting viral entry and intracellular trafficking. Polyomavirus takes advantage of multiple pathways to enter the host cell, and some of the pathways are non-productive [10]. Distinguishing the critical pathway that BKPyV takes to establish successful infection from all of the pathways that BKPyV uses remains a challenge. Owing to non-

51

productive pathways and limited specific inhibitors, some experiments performed with immunofluorescent staining and drug treatments are unreliable and misleading.

Both SV40 and murine polyomavirus (MPyV) have been considered to enter the cell via a caveolin-mediated pathway [11,12], however, subsequent experiments revealed that caveolin was completely dispensable for successful infection [13-15]. In the previous chapter, evidence is provided suggesting that BKPyV, as had been also reported for SV40 and MPyV, does not require caveolin to infect renal proximal tubular epithelial (RPTE) cells. In order to reveal the true pathway that BKPyV takes in the early stages of infection, another approach to identify host factors involved in the early stages of BKPyV infection that avoids the limitations of the previous experiments, which were based on morphological changes and drug treatments, is needed.

Numerous assays have been developed for the purpose of identifying host factors associated with viral infections, including one of the most widely used assays: genome-wide siRNA screening. RNA interference (RNAi) was first discovered in plant cells in 1986 [16]. Twelve years later, siRNA, a short double stranded RNA, was reported as a potential tool for biological research [17]. Barely two years after the introduction of siRNA methods, genomic siRNA screens were performed in *C. elegans* [18]. After the completion of the human genome project in 2006, whole genome siRNA screening in humans became possible. By silencing every single human gene with an siRNA pool, and then assessing the effects of the knockdown on infection, it is possible to dissect the functions of individual host proteins during the viral life cycle. siRNA screening has been extensively applied to research on virus, such as HIV [19], West Nile virus [20], HPV [21], VSV [22], and another polyomavirus, SV40 [23]. However, no genome-wide siRNA screen has been reported for BKPyV. With the help of a whole genome siRNA screen,

we identified a series of potential host factors that may be involved in BKPyV infection. By further validating our primary hits, RAB18, STX18, and two members of the NRZ complex were identified as host factors that are essential for BKPyV infection.

Rab18 is a Ras-like GTPase that regulates retrograde trafficking from the Golgi to the ER [24,25]. Rab18 usually localizes to the membrane of the ER and the Golgi apparatus [24]. Upon overexpression, Rab18 also localizes to lipid droplets and may localize to the endosome [26]. Rab18 interacts with STX18 protein and the NRZ protein complex in cells [27]. STX18 protein functions as a t-SNARE on the ER membrane where the NRZ complex works as a tether complex assisting retrograde vesicle docking [28,29]. All of these proteins work together in capturing targeted vesicles and in initiating the fusion process on the ER membrane. Our screen results suggest that BKPyV enters the ER via a vesicle fusion step, and trafficking from the Golgi to the ER may play an important role in efficient BKPyV infection.

Results

siRNA screen assay development.

Morphology studies have only suggested a basic model of the BK polyomavirus (BKPyV) life cycle, and therefore details of the early stages of the BKPyV life cycle remain to be elucidated. In order to identify host factors involved in viral entry and intracellular trafficking, a whole genome siRNA screen was developed for the BKPyV Dunlop strain in its natural host cell line, human primary renal proximal tubule epithelial (RPTE) cells.

A two-step screen approach is commonly used for this type of screen. In the first step, host cells are transfected with siRNA pools from an siRNA library, and targeted proteins are depleted in the 48-hours after the introduction of siRNA. For the second step, transfected cells

are challenged with virus and viral infection is evaluated with a proper readout suitable for large-scale experimentation.

Our lab previously showed that BKPyV induces G2/M arrest in order to fully take advantage of the host cell DNA replication machinery [9], which provides us with a cost efficient approach to evaluate viral infection in siRNA-transfected cells. By applying a simple Hoechst DNA stain, cells in G2/M phase can be easily distinguished from the rest of the cells based on the difference in DNA content in each nucleus. The percentage of G2/M arrested cells (G2%) in the whole cell population can then be calculated and serve as a readout for the screen assay.

To optimize the primary screen assay, RPTE cells were transfected with non-targeting siRNA or a custom synthesized siRNA targeting the TAg mRNA (siTAg), which corresponds to the natural BKPyV 5p miRNA [30]. After a 48-hour culture, transfected RPTE cells were challenged with purified BKPyV. At 48 hours post infection, cells were fixed and permeabilized with Triton X-100. The nuclei were visualized with Hoechst stain. Cell images were acquired with a high-throughput microscope and analyzed with a cell cycle module from ImageXpress high-content image analysis software. Using the software, cells arrested in G2/M phase were identified based on nuclear DNA content. (G2% values were calculated and illustrated in Figure 3.1A). Compared to mock infected cells, BKPyV infection significantly increased the present of G2/M cells. This was completely abolished by introducing siTAg to RPTE cells. The Z' factor is used to describe the quality of an assay. The Z' factor is usually smaller than 1.0, with 1.0 being the optimum. A minimal Z' factor of 0.5 is required for an siRNA screen assay [31]. After further optimizing transfection and infection conditions, our assay reached a Z' factor of 0.77, which is sufficient for siRNA screening.
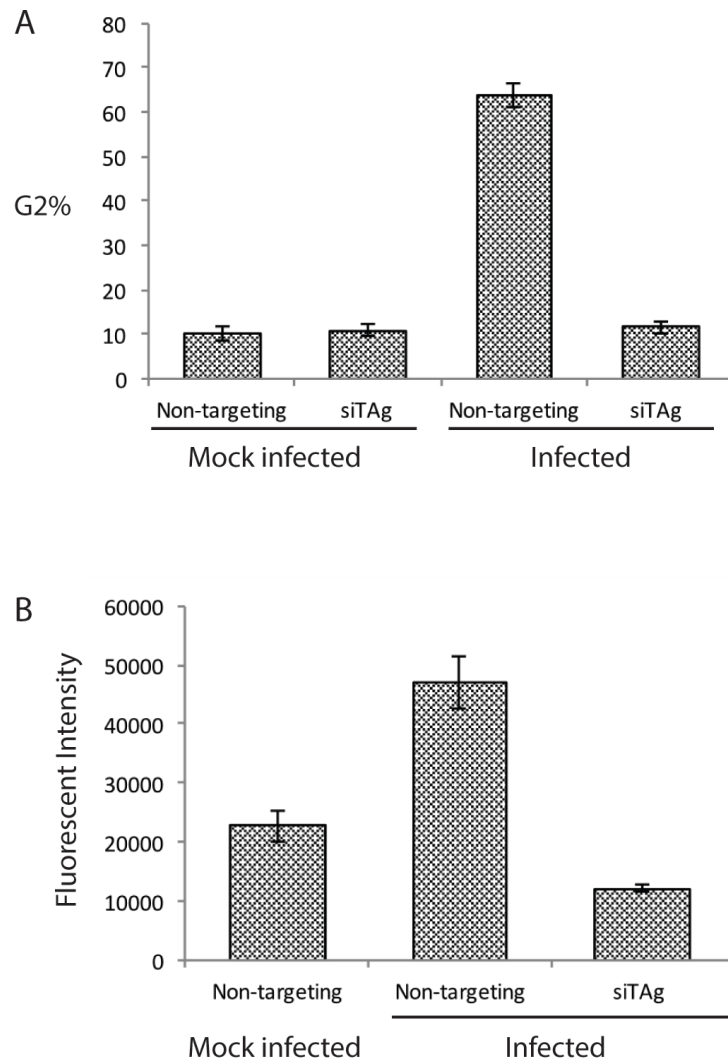
Figure 3.1: Primary screen assay development.
(A) RPTE cells were transfected with a non-targeting siRNA control or an siRNA targeting viral early protein large tumor antigen. Cells were infected with BKPyV at 48 hours post transfection, then fixed and stained with Hoechst at 48 hours post infection. Cells in G2/M phase were identified with image analysis software and the percentage of cells arrested in G2/M phase (G2%) was calculated. (B) RPTE cells were transfected with a non-targeting siRNA control or an siRNA targeting viral early protein TAg. Cells were inoculated with BKPyV at 48 hours post transfection, and then fixed and immunofluorescently stained for TAg at 48 hours post infection. Fluorescent intensity per nucleus was quantified with image analysis software.

To optimize the validation assay, RPTE cells were transfected, infected, and fixed as described above. After fixation, cells were immunofluorescently stained for TAg. Images of the cells were acquired and analyzed with the multi-wavelength cell scoring module from ImageXpress analysis software. Average fluorescent intensity per nucleus was quantified (Figure 3.1B). A Z' factor of 0.55 was achieved after optimization. Both rounds of screening met the sensitivity and accuracy requirements for siRNA screening in triplicate [31].

Primary whole genome siRNA screen on BKPyV in RPTE cells.

After the development of both assays, the primary screen protocol was adapted to an automated workstation. Each siRNA pool from the siGENOME siRNA library, containing 18,100 human genes, was aliquoted and transferred to three clear-bottom 384 well plates. RPTE cells were transfected and cultured for 48 hours to deplete the targeted proteins. Next, cells were infected with BKPyV. The G2% values were quantified, recorded, and uploaded to the MScreen web tool developed by the Center for Chemical Genomics (University of Michigan). To begin the analysis, we arbitrarily set the inhibitory effect of the siTAg as 100%, and the inhibitory effect of non-targeting siRNA control as 0%. The inhibitory effect of each siRNA pool was calculated accordingly. A larger value represents a stronger inhibitory effect on BKPyV infection when an siRNA pool is introduced into RPTE cells, which also means that the targeted host factor is more likely to be required for BKPyV infection. After testing over 18,100 siRNA pools contained in the siGENOME library in triplicate, all the acquired data were plotted onto a histogram and a heat map (Figure 3.2). In this heat map (Figure 3.2B), the darkness of a colored bar indicates the inhibitory (blue) or enhancement (red) effect of an siRNA pool on BKPyV infection. Every three bars in the same row illustrate the results of one siRNA pool in triplicate. 18,100 genes are illustrated in four columns, and each column represents results from
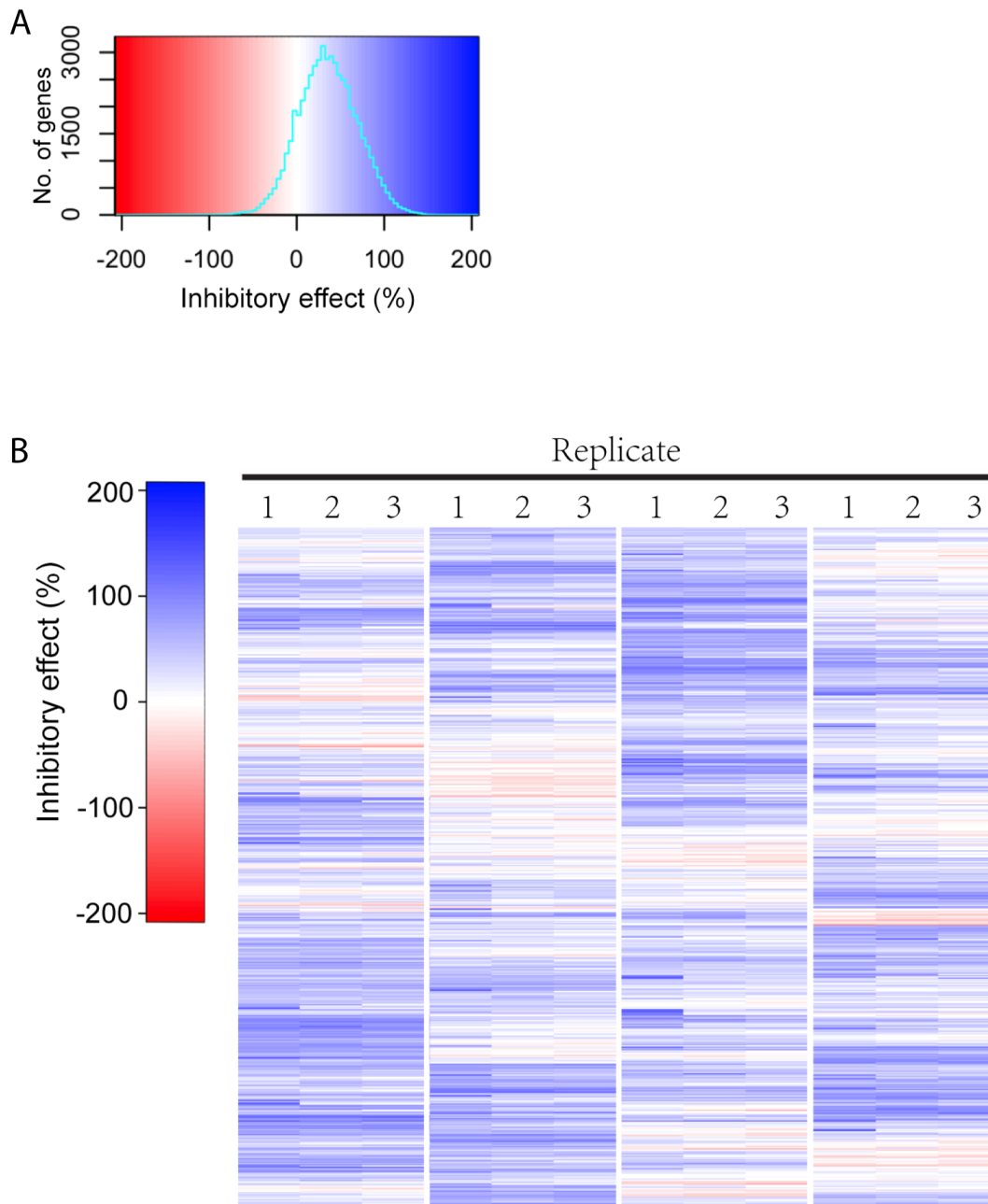
Figure 3.2: Histogram and heat map of the whole genome siRNA screen data.
RPTE cells were transfected with a non-targeting siRNA control, siTAg control, or an siRNA pool in siGENOME library. Transfected cells were challenged with BKPyV. The percentage of cells arrested in G2/M phase (G2%) was calculated and converted into a scale in which siTAg transfected control was arbitrarily set as 100%, and the non-targeting control was set as 0%. (A) Histogram of the primary screen data. (B) Heat map of the primary screen data. Primary screen results of ~18,100 genes are illustrated in four columns, with each column representing approximately 4,500 genes. Each colored bar represents a data point. Three bars in the same row of a column illustrate the effects of one siRNA pool tested in triplicate.

approximately 4,500 genes in triplicates. The histogram (Figure 3.2A) shows that the G2% data

fit into a normal distribution centered at approximately 35%. Moreover, 70% of the siRNA pools

tested inhibited BKPyV infection to some degree when compared to the non-targeting siRNA

control. Similar results were also observed in an siRNA screen using the same siRNA library on

papillomavirus infection [21].

In order to illustrate the primary screen data in greater detail, the 300 top hits from both

tails of the distribution were also plotted onto a separate heat map (Figure 3.3). Each colored bar

represents a data point, and every three bars in the same row illustrate the inhibitory effect of one

siRNA pool in triplicate. The heat map shows that the three replicates correlates well. The

overall Z' factor achieved in the primary screen is 0.6 and the Pearson product-moment

correlation coefficient factors are 0.8-0.9 between replicates. DNAJ B14, which has previously

been implicated in BKPyV entry, is our top hit, and DNAJ B12 is also among our top 100 hits

[23,32]. Most of the other identified hits we have identified have not been previously reported,

however, and many of them are involved in vesicular transport.

DAVID enrichment analysis and validation

The top 800 host factors that were most likely to affect BKPyV infection were uploaded

to the Database for Annotation, Visualization and Integrated Discovery (DAVID) enrichment

analysis tool (https://david.ncifcrf.gov). The analysis showed that translation-related genes were

among the most enriched groups of genes that assist viral infection among the candidate genes

(Table 3.1). Considering that BKPyV exclusively relies on the host protein synthesis machinery,

this result is consistent with our expectation.

Other than translation-related genes, several clusters of genes that may assist viral

infection were also significantly enriched (Table 3.1), especially intracellular transport proteins
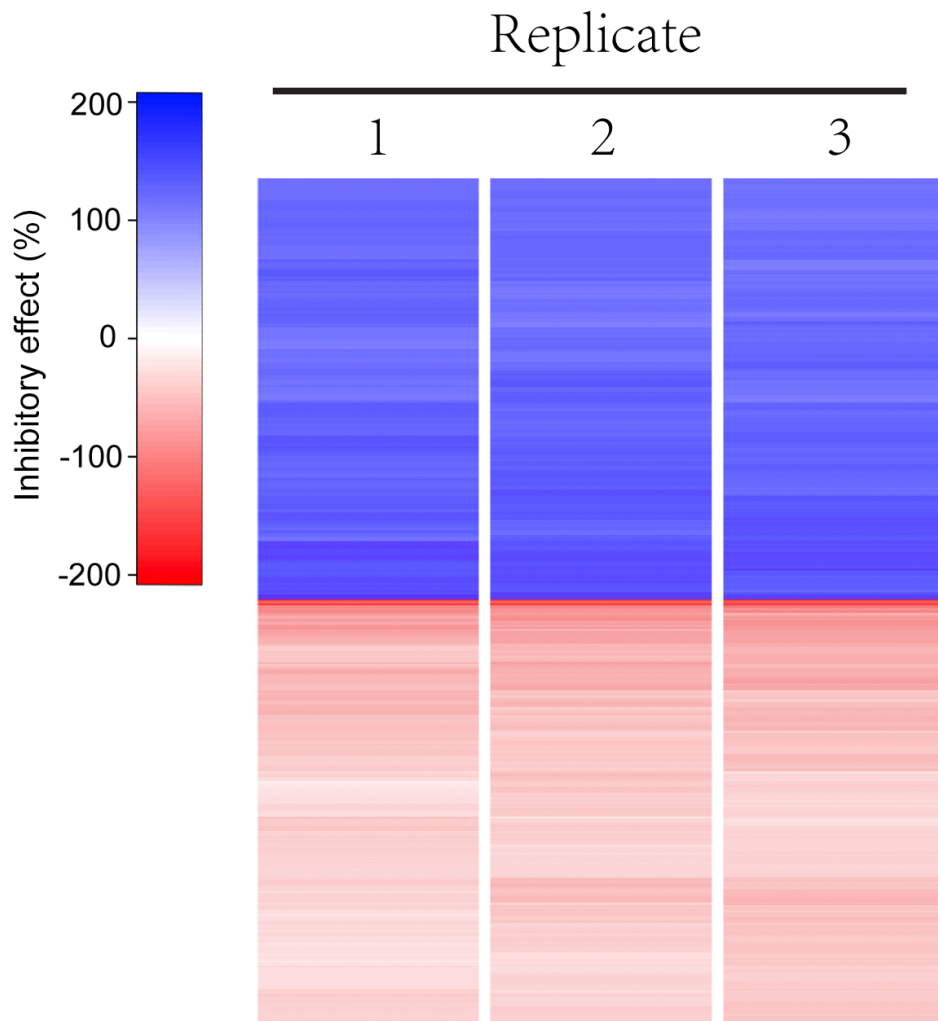
Figure 3.3: Heat map of the top hits from both tails.
Top 300 genes from both tails (600 genes in total) are illustrated in this heat map. Each colored bar represents a data point. Three bars in the same row illustrate the effects of one siRNA pool in triplicate. The non-targeting siRNA control is set as 0%, and siTAg is set as 100%.

associated with vesicle budding, and coat proteins located in the Golgi apparatus. Based on the enrichment analysis results and our interest, we manually selected 147 genes for validation (Table 3.2).

G2% is an indirect readout for BKPyV infection as knockdown of cell cycle regulatory proteins may induce G2/M arrest spontaneously even without viral infection; thus false positive or false negative candidates could be introduced into the results. To eliminate these false candidates, we next applied a direct readout of virus infection during validation. As we previously developed and optimized, TAg immunostaining fluorescent intensity was applied as a direct readout to validate the 147 genes. RPTE cells were transfected with a custom siRNA library in triplicate (Table 3.2). Next, the transfected cells were cultured for 48 hours to deplete the targeted proteins. At 48 hours post transfection, cells were infected with BKPyV. Infected cells were fixed at 48 hours post infection and probed for TAg with primary antibody and FITC-labeled secondary antibody. After acquiring images, integrated TAg fluorescent intensity per nucleus was recorded and the percentage of inhibition compared to the controls was calculated (Table 3.3). As previously described, the non-targeting control was set as 0%, and siTAg was set as 100%. Validation was performed in triplicate, and results from two repeats of the validation of 147 genes were obtained (Figure 3.4). Every six colored bars in the same row illustrate validation results of one siRNA pool. In general, replicates in validation experiments are less correlated compared to the primary screen (Figure 3.3), probably due to variation introduced by the extra steps required for immunofluorescent staining versus Hoechst staining. Compared to the primary screening results (Figure 3.2B), the siRNA pools in the validation test were significantly more inhibitory to BKPyV.

60

Table 3.1: DAVID enrichment analysis result. List of top enriched categories.

Term	P Values	Fold Enrichment
Translational elongation	2.68E-13	6.94
Translation	2.07E-08	3.06
Vesicle coating	8.47E-06	12.81
Membrane budding	1.31E-05	12.01
Golgi transport vesicle coating	1.35E-05	16.47
COPI coating of Golgi vesicle	1.35E-05	16.47
Golgi vesicle budding	1.35E-05	16.47
Vesicle targeting, to, from or within Golgi	3.99E-05	13.73
Vesicle targeting	1.02E-04	8.73
Vesicle organization	4.63E-04	4.84
Retrograde vesicle-mediated transport, Golgi to ER	7.80E-04	7.84
Establishment of vesicle localization	1.07E-03	5.82
Intracellular transport	1.38E-03	1.69
Cellular protein localization	1.76E-03	1.90
Cellular macromolecule localization	1.97E-03	1.89
Vesicle localization	1.99E-03	5.19
Intracellular protein transport	2.06E-03	1.94

Table 3.2: List of genes selected for validation.

| Entrez ID	Gene symbol	Entrez ID	Gene symbol	Entrez ID	Gene symbol
87	ACTN1	5584	PRKCI	26270	FBXO6
162	AP1B1	5611	DNAJC3	26272	FBXO4
163	AP2B1	5683	PSMA2	27090	ST6GALNAC4
363	AQP6	5704	PSMC4	27339	PRPF19
375	ARF1	5912	RAP2B	30837	SOCS7
468	ATF4	6419	SETMAR	51226	COPZ2
578	BAK1	6464	SHC1	51617	HMP19
638	BIK	6480	ST6GAL1	51725	FBXO40
648	BMI1	6605	SMARCE1	53407	STX18
660	BMX	6667	SP1	54014	BRWD1
677	ZFP36L1	7098	TLR3	54788	DNAJB12
1130	LYST	7157	TP53	54984	PINX1
1175	AP2S1	7168	TPM1	55215	FANCI
1211	CLTA	7294	TXK	55300	PI4K2B
1314	COPA	7415	VCP	55843	ARHGAP15
2002	ELK1	7903	ST8SIA4	55973	BCAP29
2070	EYA4	8396	PIP4K2B	56254	RNF20
2178	FANCE	8702	B4GALT4	56949	XAB2
2186	BPTF	8835	SOCS2	57192	MCOLN1
2297	FOXD1	8904	CPNE1	57569	ARHGAP20
2316	FLNA	9021	SOCS3	58513	EPS15L1
2624	GATA2	9026	HIP1R	64215	DNAJC1
2626	GATA4	9230	RAB11B	64326	RFWD2
3151	HMGN2	9829	DNAJC6	79595	SAP130
3298	HSF2	10017	BCL2L10	79784	MYH14
3309	HSPA5	10026	PIGK	79856	SNX22
3359	HTR3A	10039	PARP3	79874	RABEP2
3554	IL1R1	10111	RAD50	79982	DNAJB14
3799	KIF5B	10131	TRAP1	80230	RUFY1
4000	LMNA	10155	TRIM28	81609	SNX27
4001	LMNB1	10268	RAMP3	83933	HDAC10
4084	MXD1	10454	TAB1	84148	KAT8
4091	SMAD6	10475	TRIM38	85439	STON2
4144	MAT2A	10524	KAT5	90196	SYS1
4188	MDFI	10612	TRIM3	92591	ASB16
4204	MECP2	10791	VAMP5	116988	AGAP3
4248	MGAT3	10847	SRCAP	135892	TRIM50
4281	MID1	10947	AP3M2	140460	ASB7
4335	MNT	11143	KAT7	221002	RASGEF1A
4478	MSN	22818	COPZ1	221395	GPR116
4601	MXI1	22820	COPG1	221687	RNF182
4637	MYL6	22931	RAB18	283383	GPR133
4758	NEU1	23090	ZNF423	284131	ENDOV
4928	NUP98	23192	ATG4B	287015	TRIM42
5002	SLC22A18	23317	DNAJC13	347240	KIF24
5058	PAK1	23511	NUP188	388552	BLOC1S3
5296	PIK3R2	25788	RAD54B	440730	TRIM67
5310	PKD1	25897	RNF19A		
5514	PPP1R10	26118	WSB1		
5567	PRKACB	26224	FBXL3		
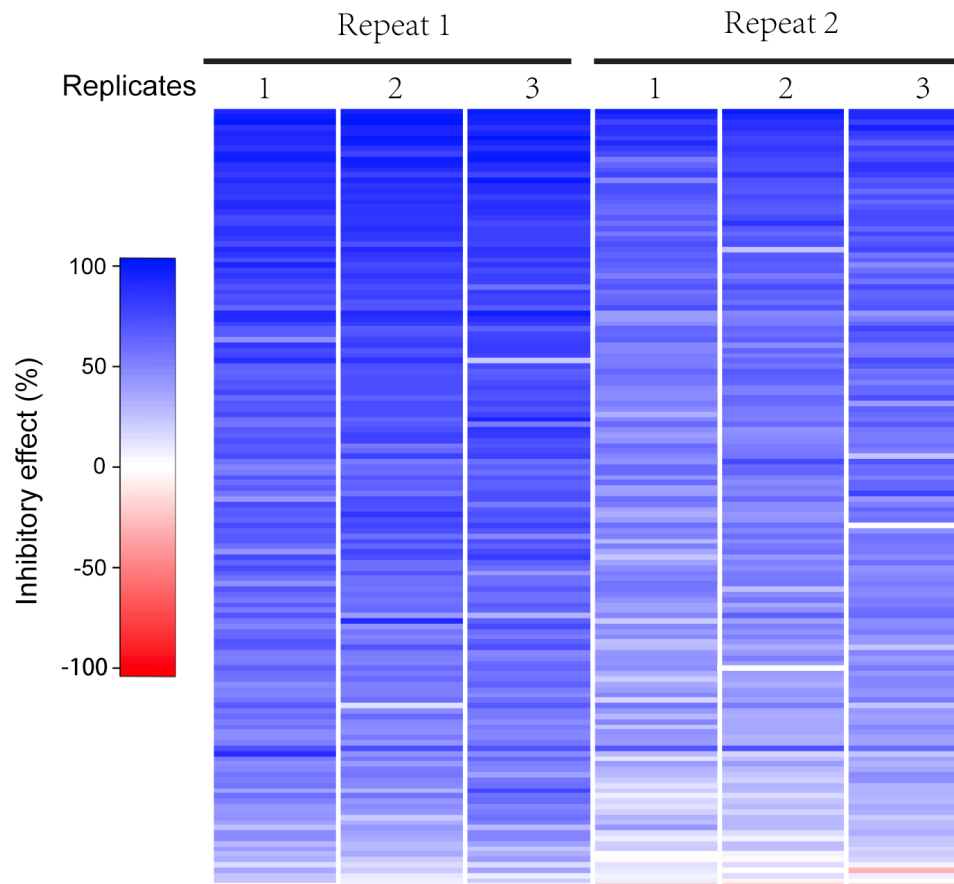
Figure 3.4: Heat map of the validation results.
Two repeats of the validation of 147 genes in triplicate are illustrated in this heat map. Each colored bar represents a data point. Six bars in the same row illustrate the effects of one siRNA pool on BKPyV infection. Non-targeting transfected control is set as 0%, and siTAg control is set as 100%.

Table 3.3: Results from the validation. Percentage of inhibition of each siRNA pool is listed.

Gene	%	Gene	%	Gene	%
DNAJB14	103.67	SETMAR	69.31	KAT8	54.17
DNAJC3	101.61	FBXO6	68.96	ZNF423	53.16
XAB2	97.15	LMNA	68.33	TRIM38	52.55
RAB18	96.77	FLNA	68.30	SOCS2	52.49
SP1	94.96	MNT	68.07	RASGEF1A	52.40
DNAJB12	93.72	PARP3	67.74	TRIM50	52.15
SOCS3	92.50	MDFI	67.60	FANCE	51.31
SNX22	89.33	AP2B1	66.79	KIF5B	50.97
ASB16	89.21	RAB11B	66.69	EYA4	50.85
SAP130	89.02	SMARCE1	66.38	RUFY1	50.81
HSPA5	88.13	IL1R1	66.25	ENDOV	50.71
LMNB1	87.23	PKD1	65.88	ZFP36L1	50.66
SRCAP	85.20	PIGK	65.78	VAMP5	50.41
COPZ2	84.79	TPM1	65.33	BCAP29	49.91
FBXO4	84.71	ST6GALNAC4	65.16	GPR133	49.40
BLOC1S3	82.81	HMGN2	65.09	AP3M2	49.09
CPNE1	82.40	EPS15L1	64.88	LYST	47.75
PSMA2	82.34	DNAJC13	64.25	TRAP1	47.63
DNAJC1	82.02	RAD50	63.74	TXK	46.79
AP2S1	81.82	COPZ1	63.73	HDAC10	46.40
BPTF	81.76	GPR116	63.71	FANCI	45.37
GATA2	81.27	NUP98	63.49	TRIM42	44.65
RNF20	80.93	GATA4	63.38	BIK	44.31
ELK1	79.58	SHC1	63.06	RAMP3	44.24
KAT5	79.53	TLR3	63.00	BMX	44.15
RABEP2	78.59	MGAT3	62.95	ASB7	44.08
MXD1	78.37	FOXD1	62.94	BAK1	44.02
COPG1	78.20	AQP6	62.73	PPP1R10	42.60
MYH14	77.49	SOCS7	62.62	BMI1	40.72
VCP	77.35	ST6GAL1	62.35	PAK1	40.68
ARHGAP20	75.69	PIP4K2B	61.96	RNF182	40.48
ACTN1	75.67	MECP2	61.88	NEU1	38.21
NUP188	75.53	B4GALT4	61.82	PRKACB	37.81
TP53	75.17	MAT2A	61.55	PRPF19	37.24
PI4K2B	74.32	FBXO40	60.68	TAB1	36.98
PSMC4	74.29	ARF1	60.26	TRIM28	35.88
AGAP3	74.23	WSB1	59.42	MXI1	34.96
PINX1	74.10	KAT7	58.96	AP1B1	30.69
HMP19	73.70	SYS1	58.78	ARHGAP15	29.60
DNAJC6	73.25	BCL2L10	58.70	ST8SIA4	28.52
CLTA	72.83	SNX27	58.40	HSF2	21.99
MCOLN1	72.53	ATG4B	58.10	MID1	19.37
KIF24	72.15	SMAD6	58.06	FBXL3	14.37
BRWD1	72.05	MSN	57.44	TRIM67	13.50
COPA	71.35	SLC22A18	57.31	RFWD2	12.26
STX18	70.44	TRIM3	57.26	MYL6	10.04
STON2	69.88	PIK3R2	56.97	PRKCI	-6.69
ATF4	69.56	HIP1R	56.64		
RAP2B	69.47	HTR3A	56.37		
RAD54B	69.34	RNF19A	55.53		

As a second validation, RPTE cells were transfected with the indicated siRNA pools in 12 well plates, and challenged with BKPyV at 2 days post transfection as described above. Protein samples were harvested at 2 days post infection and analyzed via Western blotting. The membranes were probed with TAg antibody and an internal loading control, GAPDH. The Western blotting result of PI4K2B, AP2S1, ASB16, DNAJC3, SOCS3, SOCS7, TP53, RAB18, TLR3, BLOC1S3, VAMP5, VCP, and STON2 were consistent with TAg fluorescent intensity analysis (Table 3.3, Figure 3.5A, 3.5B). In addition, Western blotting results suggest that genes with an inhibitory value of 65 or higher in Table 3.3 might be essential for BKPyV infection.

Eliminating candidate obtained due to off-target effects.

RNA interference is notorious for its off-target effects [33-36]. Although only 25nM siRNA was applied in our screen, it is impossible to completely avoid off-target effects. To eliminate false positive candidates in our validated hits, individual siRNAs from the pools of the top hits in which we were most interested were tested. Because we identified many more hits than we could study individually, 12 genes, AP2M1, AP2S1, CLTA, PI4K2B, BLOC1S3, STX18, RAB18, SNX22, TLR3, ASB16, SOCS3, and SOCS7 were selected for the individual siRNA validation assay. Protein samples were prepared after siRNA knockdown and BKPyV infection, and assayed for TAg expression by Western blotting as previously described. Interestingly, the majority of the individual siRNAs did not inhibit BKPyV infection in the same manner they did as pools (Figure 3.6A and Figure 3.6B). All of the four individual siRNAs in the AP2M1 pool reduced AP2M1 expression; however, only two of the individual siRNAs inhibited BKPyV infection (Figure 3.6A). This indicates that one siRNA (or more) that has a strong
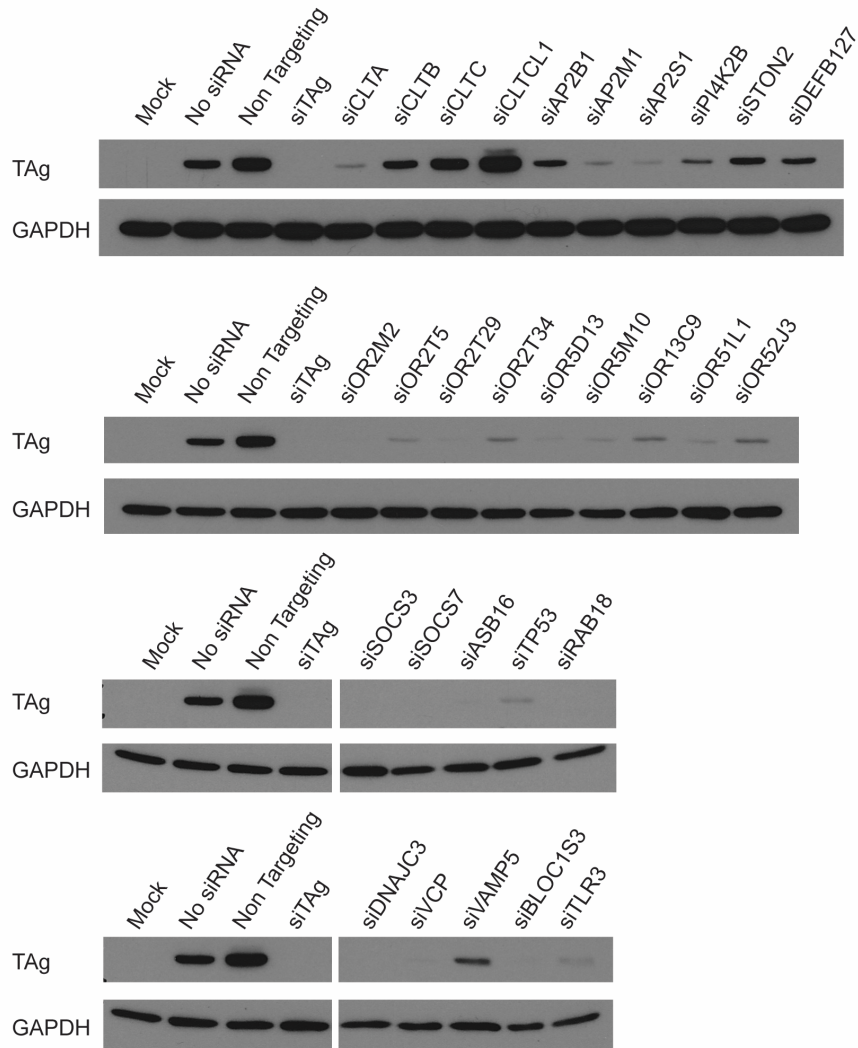
Figure 3.5A: Screen hit validation via Western blot.
RPTE cells were transfected with the indicated siRNA pools, infected by BKPyV, and viral infection (TAg) and GAPDH levels were examined by Western blotting.

Figure 3.5B: Screen hit validation via Western blot. (continued).
RPTE cells were transfected with the indicated siRNA pools, infected by BKPyV, and viral infection (TAg) and GAPDH levels were examined by Western blotting.
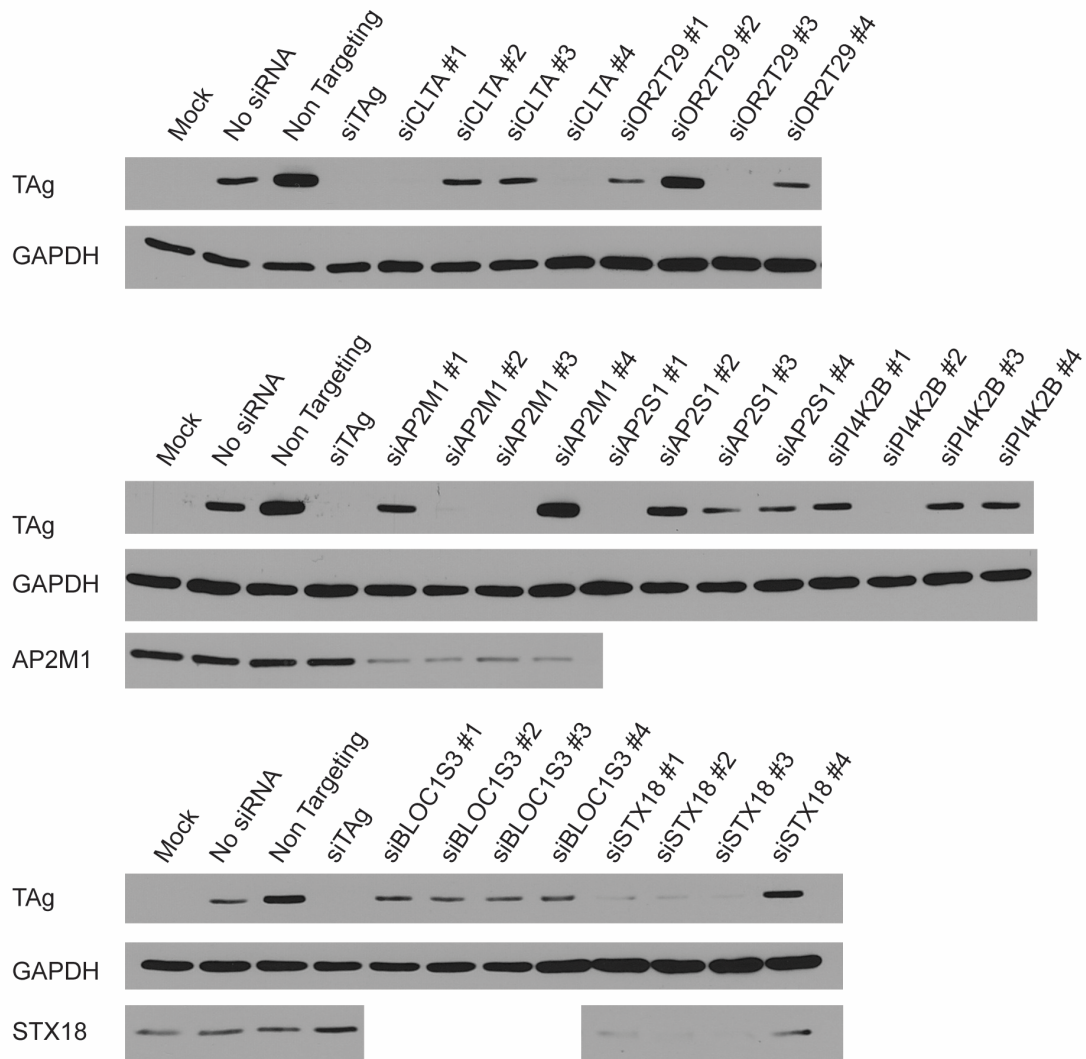
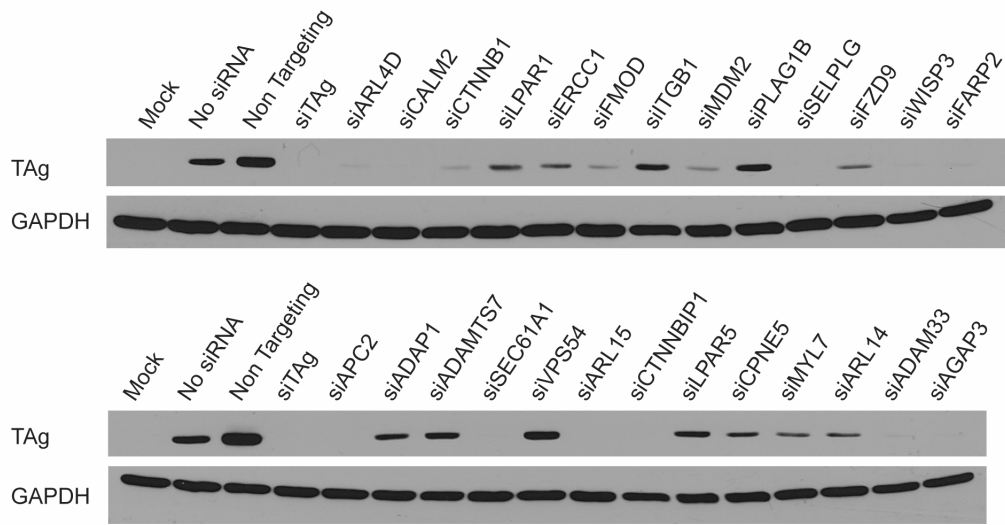**Figure 3.6A:** Individual siRNA testing to eliminate false positives.
RPTE cells were transfected with the indicated siRNAs and then infected with BKPyV. Viral
infection (TAg), GAPDH expression levels, and knockdown efficiency were examined by
Western blot.
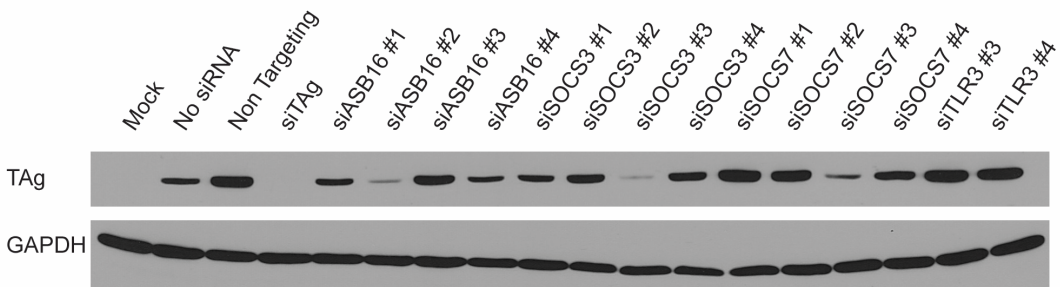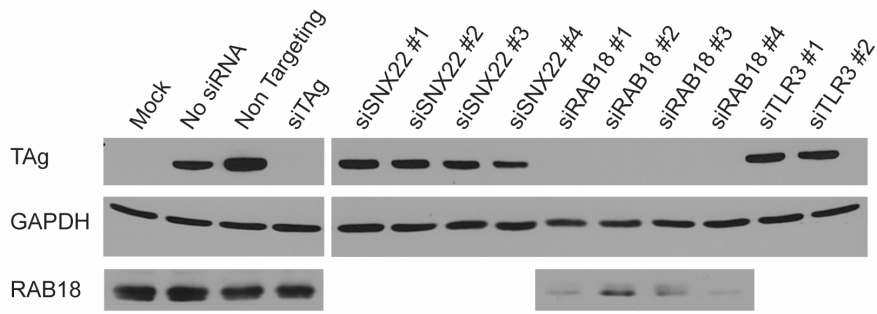
Figure 3.6B: Individual siRNA testing to eliminate false positive hits (continued). RPTE cells were transfected with the indicated siRNAs and then infected with BKPyV. Viral infection (TAg), GAPDH expression levels, and knockdown efficiency were examined by Western blot.

off-target effect in the siRNA pool, thereby determining the phenotype of the pool. After testing

all of the individual siRNAs for the 12 genes, there were still two viable candidates left: RAB18

and STX18. Knocking down RAB18 or STX18 significantly inhibited BKPyV infection in

RPTE cells. Three to four individual siRNAs, out of four, from each siRNA pool were capable of

reducing both the targeted protein level and the TAg protein level (Figure 3.6A, 3.6B).

NRZ complex and BKPyV intracellular trafficking.

RAB18 and STX18 interact with each other and also the NRZ protein complex (Figure

3.7), which regulates Golgi to ER trafficking in cells [24,27,29]. There are several additional

members of the RAB18/STX18/NRZ protein complex, including Zwilch, ZW10, RINT1,

SCFD1, and KNTC1[27]. In order to determine if these members of the complex were also

involved in BKPyV infection, we tested individual siRNAs targeting these proteins. RPTE cells

were transfected and infected, and protein samples were prepared as previously described.

Compared to the non-targeting siRNA control, knockdown of ZW10 and RINT1 also

significantly inhibited BKPyV infection (Figure 3.8). All of these data suggest that the NRZ

complex plays a role during virus intracellular trafficking.

Discussion

BK polyomavirus (BKPyV) was initially isolated more than 40 years ago [1], however,

understanding the BKPyV life cycle remains a huge challenge. Due to the small size of almost

all viruses, most available biological tools have certain limitations when applied to viral

research. Under the electron microscope, internalized BKPyV particles are commonly observed

to be individually packaged in tight fitting vesicles [13,37]. Considering the diameter of BKPyV,

these vesicles are far beyond the resolution limit of optical microscopes. In addition, BKPyV

70

Figure 3.7: A schematic view of the Rab18, STX18, and NRZ complex with a vesicle containing a BKPyV particle.

Figure 3.8: The effects of knocking down members of NRZ complex on BKPyV infection. RPTE cells were transfected with the indicated siRNAs, and viral infection (TAg) and GAPDH levels were examined by Western blotting.
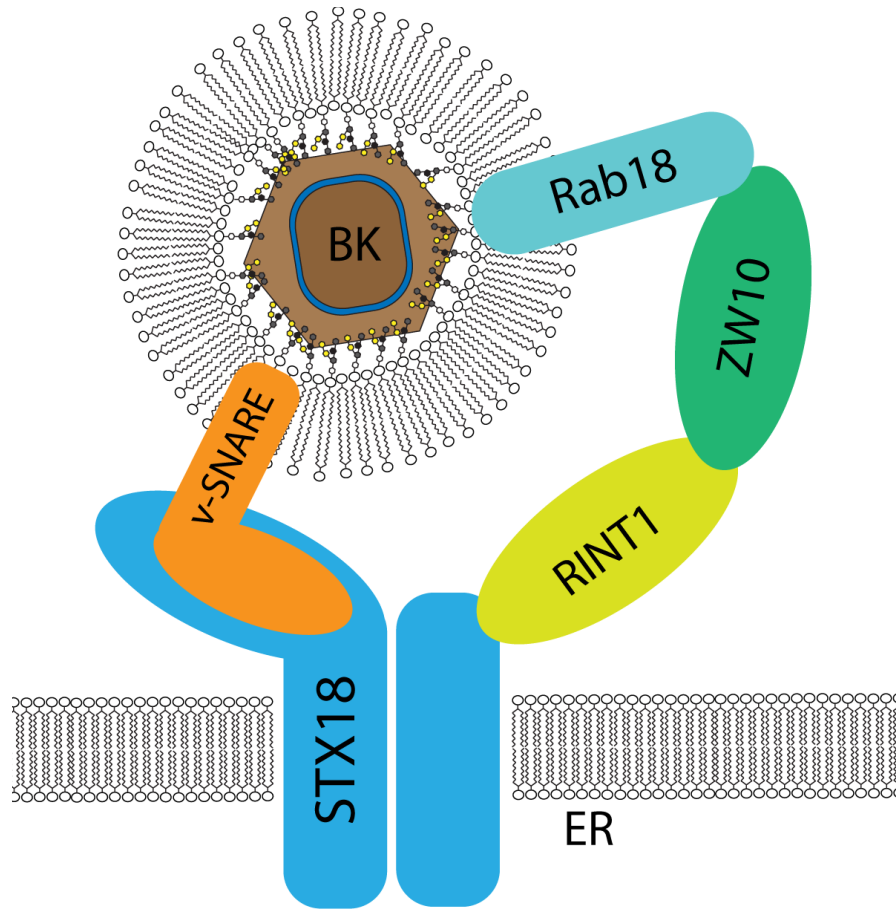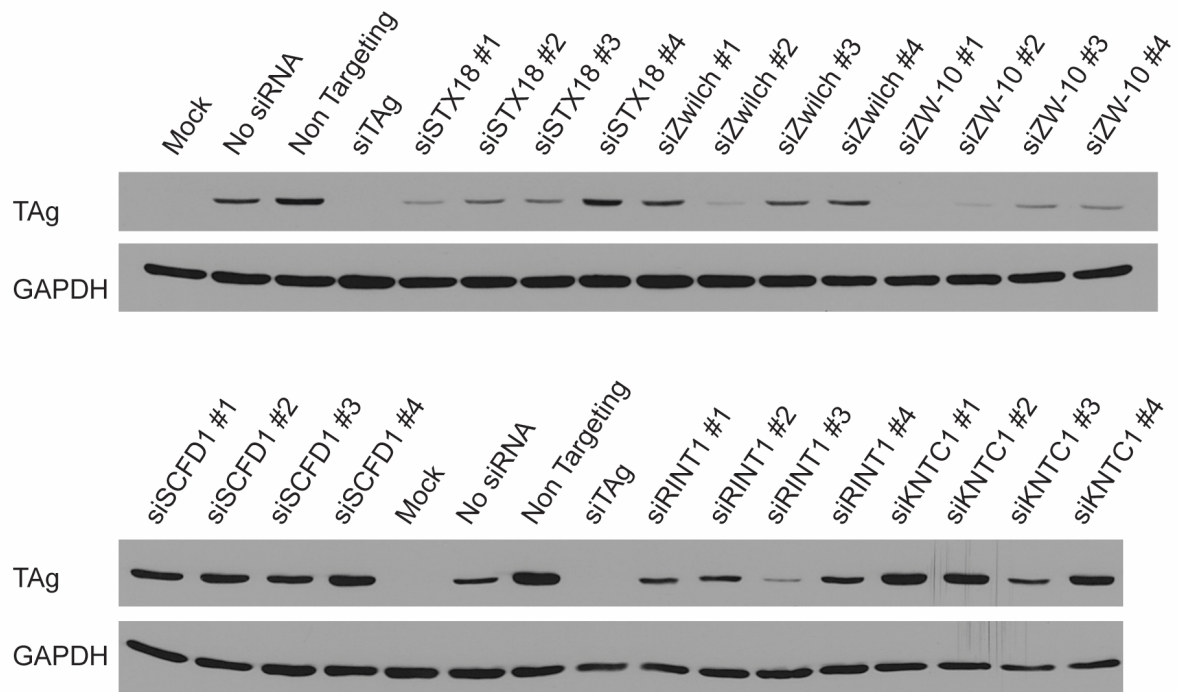
appears to take advantage of multiple endocytic pathways to enter host cell. More importantly, some of the endocytic pathways that BKPyV uses are non-productive [10], which suggests that morphological observations, especially protein localization evidence, may be deceiving. As previously discussed in chapter 2, SV40, BKPyV, murine polyomavirus (MPyV), and cholera toxin have been considered to enter the cell via a caveolin-mediated pathway [12,38-42]. However, subsequent experiments including our results presented in Chapter 2 have demonstrated that caveolin is actually completely dispensable [13-15,43-45]. Because of the limitations of the existing biological tools, research of the earliest stages of the polyomavirus life cycle has progressed slowly in the last 40 years. Many questions remain to be answered.

Whole genome siRNA screening provides us a tool to study the remaining questions. However, one of the major challenges of developing an siRNA screen assay is finding a readout that is sensitive, cost efficient, and also suitable for high throughput automation. One of the most common readouts for a viral siRNA screen is cell viability, however, BKPyV does not lyse host cells within a reasonable period of time compared to the duration of the RNAi effect in cells. Another common strategy to evaluate viral infection is by incorporating reporter genes into the viral genome. Because BKPyV is highly sensitive to genomic modification, several approaches attempting to incorporate reporter genes into the BKPyV genome have failed. Moreover, our unpublished data indicate that pseudovirus particles containing modified genomes traffic differently in host cells compared to wild type virus (Bennett and Imperiale, unpublished data). Therefore, constructing a pseudovirus containing a reporter gene was not a viable method for us. In addition, immunofluorescent staining for viral protein expression is neither cost- nor time-efficient for a whole genome screen. For all of these reasons, we needed a novel readout for evaluating viral infection.

BKPyV does not encode a DNA polymerase in its genome, thus the host DNA replication machinery is indispensable for viral replication. In order to fully activate the DNA replication machinery, BKPyV subverts cell cycle control and induces G2/M arrest [9]. Cells in the G2/M phase have at least two times more DNA content compared to G0/G1 cells; thus, they can be easily differentiated from non-G2/M cells by DNA staining. Most uninfected RPTE cells in cell culture remain in the G0/G1 phase. Because BKPyV infection dramatically increases the percentage of G2/M cells, the change in the DNA content can be easily detected and quantified, this provided us with a cost-efficient approach to evaluate viral infection in siRNA transfected cells. Based on this idea, we developed and used a screening assay that evaluates viral infectivity by measuring the percentage of cells in G2/M phase.

Our primary screen results showed that knocking down 70% of the human genes in RPTE cells, inhibited BKPyV infection when compared to the non-targeting control. A similar data distribution was also observed in an siRNA screen for HPV infection using the same siRNA library [21]. All of the siRNA data in our screen formed a normal distribution centered at around ~35% inhibition compared to the non-targeting control and the siTAg control. Ideally, it is expected that most genes would not impact the BKPyV life cycle, and the normal distribution should be centered at 0. There are several reasons why the distribution is not centered at 0. One reason is that the siTAg transfected cells, the positive control, were not completely immune to BKPyV infection. If a mock infected control was used to calculate the inhibitory effect, then the average inhibitory effect of the whole screen would have been lower, the normal distribution would have been narrower, and the average inhibitory effect would have been closer to zero. Another reason is that knocking down a functional protein inside of a live cell will impact the cell viability in general; therefore, siRNA introduction makes the cell less permissive for viral

replication and shifts the normal distribution to the right. A more important reason is that the non-targeting siRNA, the negative control, reproducibly increased BKPyV infection in RPTE cells (discussed below). Although the normal distribution is not centered at 0, the final ranking of genes in the primary screen is what is most important for the analysis.

The increased BKPyV infection induced by non-targeting siRNA control could be an off-target effect of RNAi. Dharmacon reported that another non-targeting pool reduces EGFR mRNA expression by more than 50% in an assay- and cell line-dependent manner, which indicates that a non-targeting siRNA pool also has off-target effects. In fact, each siRNA in the siGENOME library carries a complimentary strand (passenger strand) to enhance the stability of siRNA molecules, and the siGENOME siRNA passenger strand is not chemically modified to prevent it from incorporating into the RNA-induced silencing complex (RISC); therefore, passenger strand integration into RISC possibly increases off-target effects. More importantly, even if only the correct guide strand enters the RISC complex, RISC only uses the 2nd to the 8th nucleotides of the guide strand, called the seed region, to recognize targeted mRNAs [33-36,46]. Considering this characteristic of RNAi, the seven-nucleotide seed region can only have $4^7=16,384$ possible combinations, which is even fewer than the number of total human genes (around 20,000~25,000 according to the current estimation). As a result, it appears that off-target effects of RNAi are inevitable for whole genome siRNA screens, and a true 'non-targeting' siRNA pool does not exist [36]. This is one of the major limitations of an siRNA screen, and off-target effects can dramatically increase the expense of validation and lower the efficiency of screening.

There are two common strategies to minimize off-target effects of RNAi. The first strategy is to use siRNA pools instead of individual siRNAs. By pooling four unique siRNAs

targeting the same gene, the off-target effect of each siRNA is reduced 75%; meanwhile, the effective siRNA concentration for the targeted protein stays the same. This strategy has been applied to our primary screen. Another strategy to further minimize off-target effects is to reduce the total concentration of siRNA. In fact, we reduced the siRNA concentration to the minimum concentration that could be handled by the automated system for the primary screen. After applying both strategies to our siRNA screen on BKPyV, we still could not completely avoid off-target effects.

We arbitrarily tested knockdown of several genes that we thought were relevant to BKPyV infection, such as endocytosis or innate immunity, using TAg expression (assayed by Western blotting) for the readout (Figure 3.5A and 3.5B). About half of the genes tested were validated in this assay. Extrapolating from this, it is estimated that roughly half of the total primary hits could be validated with Western blot. I speculate that knocking down 300-400 genes from our primary top hits would also significantly inhibit BKPyV infection when assayed by Western blot. However, further validating the effect of each individual siRNA on BKPyV infection revealed that individual siRNAs did not always behave in the same way as pooled siRNAs. In fact, one siRNA (or more) with a strong off-target effect can determine the overall effect of an entire siRNA pool. False positive hits induced by off-target effect are common in siRNA screens, and this issue has previously been discussed [35,46-48]. In an analysis from Franceschini et al., two siRNA screens on the same pathogen, in the same cell line, using two different siRNA libraries from different vendors, are completely uncorrelated [49]. Due to the ubiquitous off-target effects, seed region analysis of the current primary screen data with a proper bioinformatics algorithm may be necessary to reveal more true hits in the future [49,50]. Because each siRNA pool contains up to four seed region sequences, it is difficult to calculate

the accurate inhibitory effect of each seed region sequence, which indicates that the siRNA

screening would be more powerful if the primary screen were done with individual siRNAs.

This, however, is not practical due to its high expense. Moreover, it suggests that the current

whole genome siRNA library design in general could be updated. Designing the siRNA library

based on seed regions would greatly benefit the process of identifying host factors and simplify

future bioinformatics analysis.

After validation, Rab18, STX18, ZW10, and RINT1 were identified as essential host

factors for BKPyV infection. Rab18 protein usually localizes to several cellular compartments,

such as the ER, the Golgi apparatus, lipid droplets, and the endosome[26]. Rab18 can interact and

form protein complex with STX18, ZW10, and RINT1 proteins in cells (Figure 3.7) [27]. ZW10

and RINT1 interact each other with their N termini and form an NRZ protein complex with an

additional protein, NAG. The NRZ complex indirectly interacts with the t-SNARE protein

STX18 on the ER membrane [28,29,51]. Rab18 is a Ras-like GTPase, and its interaction with the

NRZ complex is GTP-dependent [24,25,27]. STX18 and the NRZ complex form a protrusion about

20 nm in length from the surface of the ER membrane [52], and this complex is expected to tether

activated Rab18 on the coat protein I (COPI) vesicle surface and to mediate vesicle fusion with

the ER membrane. A model of the Rab18/STX18/NRZ protein complex assisting BKPyV

trafficking is proposed (Figure 3.9) [26]. Rab18 on the membrane of the Golgi apparatus or the

endosome buds and traffics together with virus containing vesicles (Figure 3.9A). The NRZ

complex on the ER membrane captures vesicles by binding to Rab18-GTP on the vesicle

membrane (Figure 3.9B). STX18 further interacts with v-SNARE on the vesicles (Figure 3.9C),

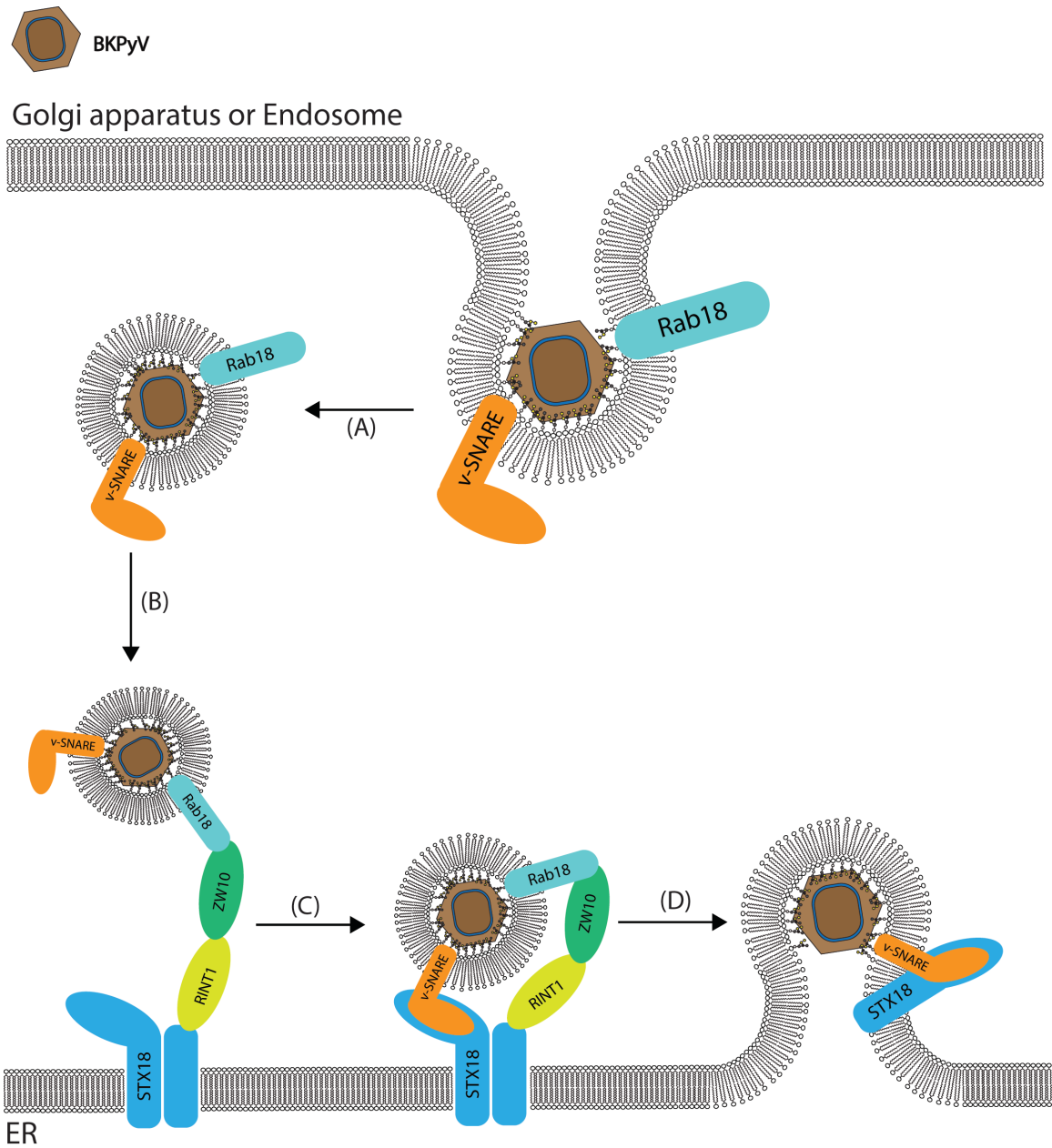and the STX18/v-SNARE complex mediates vesicle fusion to the ER membrane. After these

Figure 3.9: A schematic view of BKPyV vesicular trafficking.
(A) BKPyV forms vesicle on membrane of the Golgi apparatus or the endosome. (B) The GTP binding Rab18 interacts with ZW10 of the NRZ tethering complex. (C) STX18 on the ER membrane interacts with v-SNARE. (D) STX18 and v-SNARE mediate vesicle fusion.

steps, BKPyV successfully enters the ER. Our finding supports the speculation that Golgi to ER trafficking may play a role in BKPyV infection.

Materials and Methods

Cell culture. Primary renal proximal tubule epithelial (RPTE) cells purchased from Lonza were maintained in the medium recommended, REGM BulletKit (REGM/REBM, Lonza, CC-3190), at 37°C with 5% CO2 in a humidified incubator. Cells recovered from the frozen vial directly from Lonza (Passage 2) were cultured and expanded for 3 passages. Afterwards, expended cells (Passage 5) were passaged one more time and plated for the screening, or aliquoted and frozen in liquid nitrogen for later experiments. For all experiments besides screens, frozen aliquots (Passage 5) were recovered about one week prior to each experiment, and cells were then plated for experiments.

siRNA and siRNA library. The whole-genome human siGENOME smart pool siRNA library from Dharmacon was acquired and prepared by the Center for Chemical Genomics (University of Michigan). All other siGENOME siRNAs were also purchased from Dharmacon: Non-targeting control (D-001206-14); siRNA targeting large T antigen (custom synthesized with the sequence 5' AUCUGAGACUUGGGAAGAGCAU 3'), which corresponds to the natural BKPyV 5p miRNA [30].

Primary siRNA screening in 384 well plates. BKPyV (Dunlop) was cultured, purified with a cesium chloride linear gradient, and titered as described previously [53,54]. The siRNA library was rehydrated at 500 nM in siRNA buffer (Dharmacon, B-002000-UB-100) according to

the Basic siRNA Resuspension protocol from Dharmacon. 1 μl 500nM siRNA suspension was spotted into each well of 384-well PE viewplates on Biomek laboratory automation workstation. RPTE cells were transfected according to the Lipofectamine RNAiMAX (Thermo Fisher Scientific) manual. Briefly, transfection complexes were prepared by adding 9 μl of diluted transfection reagent (0.78% RNAiMAX reagent v/v in REBM/REGM without antibiotics) to each well of 384-well plates with siRNA spotted. The transfection complexes were incubated at room temperature for 20 min before adding 1,800 cells suspended in 10 μl REBM/REGM without antibiotics to each well. Transfected cells were cultured at 37˚C for 48 h. After the 48 hours culture, cells were infected with following procedures: incubate plates at 4˚C for 15 min; dilute purified BKPyV Dunlop in cold REGM/REBM; dispense 5 μl 1,800,000 IU/ml virus to each well with Multidrop Combi reagent dispenser (Thermo Fisher); incubate plates at 4˚C for 1 hour; transfer plates to 37˚C for additional 48 hours culture. Next, cells were fixed with 4% paraformaldehyde (Electron Microscopy Sciences) at room temperature for 20 min, permeabilized with 0.1% triton x-100 in PBS for 5 min at room temperature, and stained with 2 μg/ml Hoechst 33342 (Thermo Fisher, H3570) in PBS for 15 min at room temperature. Cells were washed for 3 times with PBS after each staining step. Images of wells were taken with ImageXpress Micro XLS high-throughput microscope and analyzed with MetaXpress High-Content Image Acquisition and Analysis software. The quantified data generated from MetaXpress were upload and further analyzed with MScreen, a high-throughput analysis system developed by the Center for Chemical Genomics (University of Michigan).

Validation in 96 well plates. BKPyV (Dunlop) was cultured, purified with a cesium chloride linear gradient, and titered as described previously [53,54]. The custom siRNA library was

rehydrated at 500 nM in siRNA buffer (Dharmacon, B-002000-UB-100), according to the Basic

siRNA Resuspension protocol from Dharmacon. 3 µl 500 nM siRNA suspension was spotted

into each well of 96-well PE viewplates on Biomek laboratory automation workstation.

Transfection complexes were prepared by adding 27 µl of diluted transfection reagent (0.78%

RNAiMAX reagent v/v in REBM/REGM without antibiotics) in each well of a 96-well plates

with siRNA spotted. The transfection complexes were incubated at room temperature for 20 min

before adding 5,400 cells suspended in 30 µl REBM/REGM without antibiotics to each well.

Transfected cells were cultured at 37˚C for 48 h. After the 48 hours culture, cells were infected

with following procedures: incubate plates at 4˚C for 15 min; dilute purified BKPyV Dunlop in

cold REGM/REBM; dispense 15 µl 1,800,000 IU/ml virus to each well with Multidrop Combi

reagent dispenser (Thermo Fisher); incubate plates at 4˚C for 1 hour; transfer plates to 37˚C for

additional 48 hours culture. Next, cells were fixed with 4% paraformaldehyde (Electron

Microscopy Sciences) at room temperature for 20 min; permeabilized with 0.1% triton x-100 in

PBS for 5 min at room temperature. The cells were then blocked with 5% goat serum in PBS at

room temperature for 1 hour and probed with with TAg antibody [55] at a 1:150 dilution and 1:200

FITC labeled goat anti-mouse IgG antibody (Sigma) successively for 1 hour each at room

temperature. All antibodies were diluted in 5% goat serum. At last, nuclei were visualized with 2

µg/ml Hoechst 33342 (Thermo Fisher, H3570) in PBS for 15 min at room temperature. Cells

were washed for 3 times with PBS after each staining step. Images of wells were taken with

ImageXpress Micro XLS high-throughput microscope and analyzed with MetaXpress High-

Content Image Acquisition and Analysis software. The averages of integrated FITC fluorescence

intensity per nucleus were calculated automatically by software.

Secondary validation in 12 well plates. siRNAs were rehydrated at 1 µM in siRNA buffer (Dharmacon, B-002000-UB-100). Transfection complexes were prepared by mixing 20 µl of 1 µM siRNA with 380 µl of diluted transfection reagent (0.74% RNAiMAX reagent v/v in REBM/REGM without antibiotics) in each well of 12-well plates. The transfection complexes were incubated at room temperature for 20 min before adding 70,000 cells suspended in 400 µl REBM/REGM without antibiotics to each well. RPTE cells were infected as follows at 2 days post transfection. Cells were pre-chilled for 15 min at 4˚C. Purified viruses were diluted to 87,500 IU/ml (MOI 0.5) in REBM/REGM. 400 µl of the diluted virus were added to the wells and incubated at 4˚C for 1 hour with shaking every 15 minutes to distribute the inoculum over the entire well. The plate was transferred to 37˚C after the 1 hour incubation.

Preparation of protein lysates. Cells were lysed at 48 hours post infection with E1A buffer (50 mM HEPES [pH 7], 250 mM NaCl, and 0.1% NP-40, with inhibitors: 5 µg/ml PMSF, 5 µg/ml aprotinin, 5 µg/ml leupeptin, 50 mM sodium fluoride and 0.2 mM sodium orthovanadate added right before use). Protein concentration was quantified with the Bradford assay (Bio-Rad).

Western blotting. Protein samples were separated on 12% SDS-PAGE gels. After electrophoresis, the proteins were transferred to a nitrocellulose membrane (pore size 0.2 µm) with a Bio-Rad Trans-Blot Cell in Towbin transfer buffer (25 mM Tris, 192 mM glycine, 20% methanol) at 60 V overnight. Membranes were blocked with 2% nonfat milk in PBS-T buffer (144 mg/L KH_2PO_4, 9 g/L NaCl, 795 mg/L Na_2HPO_4, pH 7.4, 0.1% Tween 20) for 1 hour. Membranes were probed with primary and secondary antibodies diluted in 2% milk in PBS-T as follows: TAg (pAb416) at 1:5,000 dilution [55]; STX18 (Abcam ab156017) at 1:1,000; Rab18

(Sigma SAB4200173) at 1:10,000, AP2M1 (Abcam ab75995) at 1:10,000; GAPDH (Abcam ab9484) at 1: 10,000; horseradish peroxidase (HRP)-conjugated ECL sheep anti-mouse (GE healthcare NA931V) at 1: 5,000; and HRP-conjugated ECL donkey anti-rabbit antibody (GE healthcare NA934V) at 1: 5,000. Protein bands were further visualized with HRP substrate (Millipore, WBLUF0100) and exposure to x-ray film.

References

1. Gardner SD, Field AM, Coleman DV, Hulme B. New human papovavirus (B.K.) isolated from urine after renal transplantation. *The Lancet*. 1971;1(7712):1253-1257. doi:10.1016/s0140-6736(71)91776-4.

2. Egli A, Infanti L, Dumoulin A, et al. Prevalence of polyomavirus BK and JC Infection and replication in 400 healthy blood donors. *J Infect Dis*. 2009;199(6):837-846. doi:10.1086/597126.

3. Kean JM, Rao S, Wang M, Garcea RL. Seroepidemiology of human polyomaviruses. Atwood WJ, ed. *PLoS Pathog*. 2009;5(3):e1000363. doi:10.1371/journal.ppat.1000363.

4. Ahsan N, Shah KV. Polyomaviruses and human diseases. *Adv Exp Med Biol*. 2006;577(Chapter 1):1-18. doi:10.1007/0-387-32957-9_1.

5. Kuypers DRJ. Management of polyomavirus-associated nephropathy in renal transplant recipients. *Nat Rev Nephrol*. 2012;8(7):390-402. doi:10.1038/nrneph.2012.64.

6. Lunde LE, Dasaraju S, Cao Q, et al. Hemorrhagic cystitis after allogeneic hematopoietic cell transplantation: risk factors, graft source and survival. *Bone Marrow Transplant*. 2015;50(11):1432-1437. doi:10.1038/bmt.2015.162.

7. Shivakumar CV, Das GC. Interaction of human polyomavirus BK with the tumor-suppressor protein p53. *Oncogene*. 1996;13(2):323-332.

8. Harris KF, Christensen JB, Imperiale MJ. BK virus large T antigen: interactions with the retinoblastoma family of tumor suppressor proteins and effects on cellular growth control. *J Virol*. 1996;70(4):2378-2386.

9. Jiang M, Zhao L, Gamez M, Imperiale MJ. Roles of ATM and ATR-mediated DNA damage responses during lytic BK polyomavirus infection. Pipas J, ed. *PLoS Pathog*. 2012;8(8):e1002898. doi:10.1371/journal.ppat.1002898.

10.   You J, O'Hara SD, Velupillai P, et al. Ganglioside and non-ganglioside mediated host responses to the mouse polyomavirus. Meyers C, ed. *PLoS Pathog*. 2015;11(10):e1005175. doi:10.1371/journal.ppat.1005175.

11.   Norkin LC. Simian virus 40 infection via MHC class I molecules and caveolae. *Immunol Rev*. 1999;168(1):13-22. doi:10.1111/j.1600-065X.1999.tb01279.x.

12.   Richterová Z, Liebl D, Horák M, et al. Caveolae are involved in the trafficking of mouse polyomavirus virions and artificial VP1 pseudocapsids toward cell nuclei. *J Virol*. 2001;75(22):10880-10891. doi:10.1128/JVI.75.22.10880-10891.2001.

13.   Damm E-M, Pelkmans L, Kartenbeck J, Mezzacasa A, Kurzchalia T, Helenius A. Clathrin- and caveolin-1-independent endocytosis: entry of simian virus 40 into cells devoid of caveolae. *J Cell Biol*. 2005;168(3):477-488. doi:10.1083/jcb.200407113.

14.   Gilbert JM, Goldberg IG, Benjamin TL. Cell penetration and trafficking of polyomavirus. *J Virol*. 2003;77(4):2615-2622. doi:10.1128/JVI.77.4.2615-2622.2003.

15.   Liebl D, Difato F, Horníková L, Mannová P, Štokrová J, Forstová J. Mouse polyomavirus enters early endosomes, requires their acidic pH for productive infection, and meets transferrin cargo in Rab11-positive endosomes. *J Virol*. 2006;80(9):4610-4622. doi:10.1128/JVI.80.9.4610-4622.2006.

16.   Ecker JR, Davis RW. Inhibition of gene expression in plant cells by expression of antisense RNA. *PNAS*. 1986;83(15):5372-5376. doi:10.1073/pnas.83.15.5372.

17.   Fire A, Xu S, Montgomery MK, Kostas SA, Driver SE, Mello CC. Potent and specific genetic interference by double-stranded RNA in Caenorhabditis elegans. *Nature*. 1998;391(6):806-811. doi:10.1038/35888.

18.   Gönczy P, Echeverri C, Oegema K, et al. Functional genomic analysis of cell division in C. elegans using RNAi of genes on chromosome III. *Nature*. 2000;408(6810):331-336. doi:10.1038/35042526.

19.   Zhou H, Xu M, Huang Q, et al. Genome-scale RNAi screen for host factors required for HIV replication. *Cell Host Microbe*. 2008;4(5):495-504. doi:10.1016/j.chom.2008.10.004.

20.   Krishnan MN, Ng A, Sukumaran B, et al. RNA interference screen for human genes associated with West Nile virus infection. *Nature*. 2008;455(7210):242-245. doi:10.1038/nature07207.

21.   Lipovsky A, Popa A, Pimienta G, et al. Genome-wide siRNA screen identifies the retromer as a cellular entry factor for human papillomavirus. *Proc Natl Acad Sci USA*. 2013;110(18):7452-7457. doi:10.1073/pnas.1302164110.

22.   Lee AS-Y, Burdeinick-Kerr R, Whelan SPJ. A genome-wide small interfering RNA screen identifies host factors required for vesicular stomatitis virus infection. *J Virol*.

2014;88(15):8355-8360. doi:10.1128/JVI.00642-14.

23. Goodwin EC, Lipovsky A, Inoue T, et al. BiP and multiple DNAJ molecular chaperones in the endoplasmic reticulum are required for efficient simian virus 40 infection. *MBio*. 2011;2(3):e00101-e00111. doi:10.1128/mBio.00101-11.

24. Dejgaard SY, Murshid A, Erman A, et al. Rab18 and Rab43 have key roles in ER-Golgi trafficking. *J Cell Sci*. 2008;121(Pt 16):2768-2781. doi:10.1242/jcs.021808.

25. Liu S, Storrie B. Are Rab proteins the link between Golgi organization and membrane trafficking? *Cell Mol Life Sci*. 2012;69(24):4093-4106. doi:10.1007/s00018-012-1021-6.

26. Martin S, Driessen K, Nixon SJ, Zerial M, Parton RG. Regulated localization of Rab18 to lipid droplets: effects of lipolytic stimulation and inhibition of lipid droplet catabolism. *J Biol Chem*. 2005;280(51):42325-42335. doi:10.1074/jbc.M506651200.

27. Gillingham AK, Sinka R, Torres IL, Lilley KS, Munro S. Toward a comprehensive map of the effectors of rab GTPases. *Dev Cell*. 2014;31(3):358-373. doi:10.1016/j.devcel.2014.10.007.

28. Hirose H, Arasaki K, Dohmae N, et al. Implication of ZW10 in membrane trafficking between the endoplasmic reticulum and Golgi. *EMBO J*. 2004;23(6):1267-1278. doi:10.1038/sj.emboj.7600135.

29. Tagaya M, Arasaki K, Inoue H, Kimura H. Moonlighting functions of the NRZ (mammalian Dsl1) complex. *Front Cell Dev Biol*. 2014;2(286):25. doi:10.3389/fcell.2014.00025.

30. Seo GJ, Fink LHL, O'Hara B, Atwood WJ, Sullivan CS. Evolutionarily conserved function of a viral microRNA. *J Virol*. 2008;82(20):9823-9828. doi:10.1128/JVI.01144-08.

31. Zhang J, Chung T, Oldenburg K. A simple statistical parameter for use in evaluation and validation of high throughput screening assays. *J Biomol Screen*. 1999;4(2):67-73.

32. Bagchi P, Walczak CP, Tsai B. The endoplasmic reticulum membrane j protein C18 executes a distinct role in promoting simian virus 40 membrane penetration. Dermody TS, ed. *J Virol*. 2015;89(8):4058-4068. doi:10.1128/JVI.03574-14.

33. Jackson AL, Bartz SR, Schelter J, et al. Expression profiling reveals off-target gene regulation by RNAi. *Nat Biotechnol*. 2003;21(6):635-637. doi:10.1038/nbt831.

34. Jackson AL, Burchard J, Schelter J, et al. Widespread siRNA "off-target" transcript silencing mediated by seed region sequence complementarity. *RNA*. 2006;12(7):1179-1187. doi:10.1261/rna.25706.

35. Birmingham A, Anderson EM, Reynolds A, et al. 3' UTR seed matches, but not overall

identity, are associated with RNAi off-targets. *Nat Meth*. 2006;3(3):199-204. doi:10.1038/nmeth854.

36. Tschuch C, Schulz A, Pscherer A, et al. Off-target effects of siRNA specific for GFP. *BMC Mol Biol*. 2008;9(1):60. doi:10.1186/1471-2199-9-60.

37. Maraldi NM, Barbanti-Brodano G, Portolani M, La Placa M. Ultrastructural aspects of BK virus uptake and replication in human fibroblasts. *J Gen Virol*. 1975;27(1):71-80. doi:10.1099/0022-1317-27-1-71.

38. Parton RG. Regulated internalization of caveolae. *J Cell Biol*. 1994;127(5):1199-1215. doi:10.1083/jcb.127.5.1199.

39. Orlandi PA, Fishman PH. Filipin-dependent inhibition of cholera toxin: evidence for toxin internalization and activation through caveolae-like domains. *J Cell Biol*. 1998;141(4):905-915. doi:10.1083/jcb.141.4.905.

40. Pelkmans L, Kartenbeck J, Helenius A. Caveolar endocytosis of simian virus 40 reveals a new two-step vesicular-transport pathway to the ER. *Nature Cell Biology*. 2001;3(5):473-483. doi:10.1038/35074539.

41. Eash S, Querbes W, Atwood WJ. Infection of vero cells by BK virus is dependent on caveolae. *J Virol*. 2004;78(21):11583-11590. doi:10.1128/JVI.78.21.11583-11590.2004.

42. Moriyama T, Marquez JP, Wakatsuki T, Sorokin A. Caveolar endocytosis is critical for BK virus infection of human renal proximal tubular epithelial cells. *J Virol*. 2007;81(16):8552-8562. doi:10.1128/JVI.00924-07.

43. Shogomori H, Futerman AH. Cholera toxin is found in detergent-insoluble rafts/domains at the cell surface of hippocampal neurons but is internalized via a raft-independent mechanism. *J Biol Chem*. 2001;276(12):9182-9188. doi:10.1074/jbc.M009414200.

44. Torgersen ML, Skretting G, van Deurs B, Sandvig K. Internalization of cholera toxin by different endocytic mechanisms. *J Cell Sci*. 2001;114(Pt 20):3737-3747.

45. Zhao L, Marciano AT, Rivet CR, Imperiale MJ. Caveolin- and clathrin-independent entry of BKPyV into primary human proximal tubule epithelial cells. *Virology*. 2016;492:66-72. doi:10.1016/j.virol.2016.02.007.

46. Mohr S, Bakal C, Perrimon N. Genomic screening with RNAi: results and challenges. *Annual review of biochemistry*. 2010;79:37-64. doi:10.1146/annurev-biochem-060408-092949.

47. Mohr SE, Smith JA, Shamu CE, Neumüller RA, Perrimon N. RNAi screening comes of age: improved techniques and complementary approaches. *Nature Reviews Molecular Cell Biology*. 2014;15(9):591-600. doi:10.1038/nrm3860.

48. Hofer U. Techniques and applications: RNAi "off-targets" pathogen infection. *Nat Rev Microbiol*. March 2014. doi:10.1038/nrmicro3252.

49. Franceschini A, Meier R, Casanova A, et al. Specific inhibition of diverse pathogens in human cells by synthetic microRNA-like oligonucleotides inferred from RNAi screens. In: Vol 111. 2014:4548-4553. doi:10.1073/pnas.1402353111.

50. Sigoillot FD, Lyman S, Huckins JF, et al. A bioinformatics method identifies prominent off-targeted transcripts in RNAi screens. *Nat Meth*. 2012;9(4):363-366. doi:10.1038/nmeth.1898.

51. Civril F, Wehenkel A, Giorgi FM, et al. Structural analysis of the RZZ complex reveals common ancestry with multisubunit vesicle tethering machinery. *Structure*. 2010;18(5):616-626. doi:10.1016/j.str.2010.02.014.

52. Ren Y, Yip CK, Tripathi A, et al. A structure-based mechanism for vesicle capture by the multisubunit tethering complex Dsl1. *Cell*. 2009;139(6):1119-1129. doi:10.1016/j.cell.2009.11.002.

53. Abend JR, Low JA, Imperiale MJ. Inhibitory effect of gamma interferon on BK virus gene expression and replication. *J Virol*. 2007;81(1):272-279. doi:10.1128/JVI.01571-06.

54. Jiang M, Abend JR, Tsai B, Imperiale MJ. Early events during BK virus entry and disassembly. *J Virol*. 2009;83(3):1350-1358. doi:10.1128/JVI.02169-08.

55. Harlow E, Whyte P, Franza BR, Schley C. Association of adenovirus early-region 1A proteins with cellular polypeptides. *Mol Cell Biol*. 1986;6(5):1579-1589.

CHAPTER IV

Discussion

Summary

Although polyomaviruses are genetically similar, it has been reported that polyomaviruses use different pathways to infect host cells. Conflicting reports have been published on the endocytic process of SV40 and murine polyomavirus (MPyV). In order to investigate BKPyV infection in greater detail, caveolin 1, caveolin 2, and clathrin heavy chain were silenced by transfecting RPTE cells with siRNA pools; however, BKPyV infection was not affected. My results provided in this dissertation (Chapter 2, ref [1]) together with other reports demonstrate that caveolin is dispensable for SV40, MPyV, and BKPyV infection [1-6]. In addition, by silencing UDP-glucose ceramide glucosyltransferase (UGCG) and performing a ganglioside rescue assay, we confirmed functionally that BKPyV infection requires ganglioside receptors. In order to identify the host factors associated with a BKPyV infection, we developed and performed an automated whole genome siRNA screen for factors important for BKPyV infection in primary human renal proximal tubule epithelial (RPTE) cells. We used the percentage of cells arrested in G2/M phase as a readout. After validation, we showed that RAB18 and STX18 along with two proteins of the NRZ complex may have an essential role in BKPyV infection.

Whole genome siRNA screening

Since siRNA was introduced as a biological tool, it has been extensively applied to research on viruses, and thousands of host factors required for infection have been identified for various viruses, directly or indirectly. Each siRNA screen performed on HIV identified hundreds of host factors distributed into various pathways [7-9]. In a hepatitis C virus (HCV) screen, PI4KIIIα was identified to interact with the nonstructural protein 5A, and PI4KIIIα is important to form viral replication complexes [10]. Moreover, using an siRNA screen, SON DNA binding protein was identified as a critical protein regulating influenza virion trafficking to the late endosomes [11]. Vacuolar ATPase and calcium/calmodulin-dependent protein kinase IIb were also identified as essential host factors for influenza virus in a separate siRNA screen [12]. In addition, the ubiquitin ligase CBLL1 was found to be important for West Nile virus (WNV) internalization, thereby revealing the role of the endoplasmic reticulum associated protein degradation (ERAD) pathway in WNV infection [13]. The role of the Golgi apparatus in human papillomavirus (HPV) lifecycle had been a mystery until an siRNA screen performed on HPV revealed that the retromer and endosome-to-Golgi apparatus trafficking is essential to HPV infection [14,15]. An siRNA screen performed on another polyomavirus, SV40, showed that DNAJ proteins are important for SV40 to exit the ER [16,17]. All these host factors would have been difficult to identify by educated guesses, and these host factors listed are only a fraction of host factors identified with the help of siRNA screen.

However, the siRNA screen has its own limitations. When siRNA was first introduced, RNAi was believed to be highly specific [18]. However, subsequent studies demonstrate that the specificity of RNAi is much lower than originally speculated. Each siRNA screen on HIV identified 200~300 genes; however, less than 10 hits overlapped between these screens [19-21],

89

which suggests that off-target effects could be responsible for some of the non-overlapping hits. The RNA-induced silencing complex (RISC) only uses the 2nd to the 8th nucleotides of the guide strand, called the seed region, to recognize targeted mRNAs [22-26]. Considering this characteristic of RNAi, the seven nucleotide seed region can have 4^7=16,384 possible combinations. Moreover, there are only 10,868 total seed regions in total in the whole genome siRNA library that we used for our primary screen. This number is about half the total number of human genes (around 20,000~25,000 according to the current estimation). As a result, off-target effects of RNAi are inevitable for a whole genome siRNA screen, and it is estimated that hundreds of genes would be affected by any siRNA pool, including the non-targeting siRNA control [23]. During the validation, I found that one siRNA with a strong off-target effect in many of the pools could eventually determine the phenotype of the pool. This is one of the major limitations of an siRNA screen. Sorting out off-target effects can dramatically increase the expense of validation and lower the yield of screening.

Bioinformatics analysis is a useful way to eliminate some false positives. Analyzing screening data based on individual seed region sequences instead of siRNA pools can dramatically increase the correlation between siRNA screens on the same pathogen, thereby increase validation efficiency [27,28]. However, because siRNA pools were used for our primary siRNA screen on BKPyV, and up to four seed region sequences were mixed in the same siRNA pool, the accurate inhibitory effect of each seed region sequence could not be calculated, which would partially compromise the accuracy of the seed region analysis. This indicates that applying individual siRNAs to the primary screen could dramatically simplify the bioinformatics analysis and may enhance the screen efficiency, and also suggests that designing siRNA libraries based

90

on seed regions and performing bioinformatics analysis afterward may enhance the accuracy and efficiency of future screens. This approach also results in added expenses, however.

BKPyV receptor and attachment

BKPyV attachment to the host cell is the most well studied early step of BKPyV infection. Subsequent to the finding that gangliosides GD1b and GT1b are BKPyV receptors [29], structures of the BKPyV capsid and the capsid protein-receptor complex have also been carefully studied based on crystal structures of other polyomaviruses [30-36]. In the case of BKPyV, GD1b and GT1b bind to the shallow grooves on the surface of VP1, and each VP1 pentamer is capable of interacting with five ganglioside molecules [31]. Gangliosides are commonly enriched in cholesterol-rich regions of the plasma membrane referred to as lipid rafts. Cholesterol assists the positioning of gangliosides so that the oligosaccharide chains are pointing in the correct direction for the initial attachment [37,38].

Co-receptors for polyomavirus are mostly unknown. JC polyomavirus uses serotonin receptors to infect cells [39], and integrin mediates endocytosis of murine polyomavirus (MPyV) after attachment [40]. After initial attachment, BKPyV may also use protein co-receptors to coordinate the entry process. Dugan et al. reported that cleaving oligosaccharide chains on the cell membrane with neuraminidase blocks BKPyV virus entry, and restoring N-linked glycoproteins with $\alpha(2,3)$-(N)-sialyltransferase rescues BKPyV infection [41], which suggests that a N-linked glycoprotein may serve as BKPyV co-receptor. Because BKPyV interacts with its receptors, gangliosides GT1b and GD1b, via the $\alpha2,8$-linked N-acetylneuraminic acid (sialic acid) on those two gangliosides [31], and because $\alpha2,3$-linked sialic acid alone cannot reach the binding pocket [31]. It indicates that if an N-linked glycoprotein co-receptor exists for BKPyV

infection, it must interact with the capsid protein VP1 using a different domain than the ganglioside binding domain. On the other hand, digestion of membrane proteins with proteinase K enhanced MPyV infection [42], which suggests that glycoproteins on the plasma membrane serve as traps for polyomavirus. Another study from Benjamin et al. supports the same idea, that eliminating gangliosides alone is sufficient to fully block MPyV infection, and polyomavirus particles all enter non-productive pathways when gangliosides are not used as a receptor [43]. In my opinion, all of the evidence point to the same idea that gangliosides instead of membrane proteins are required for polyomavirus entry. In other words, protein co-receptors may not be required or even exist for polyomaviruses.

BKPyV Endocytosis

The process of BKPyV endocytosis has been extensively investigated. The current model indicates that BKPyV enters the caveolae endocytic pathway after initial attachment to receptors GD1b/GT1b and eventually enters the host cells in tight-fitting vesicles [44,45]. In Vero cells, depleting the membrane cholesterol with methyl-β-cyclodextrin (MβCD) blocked cholera toxin endocytosis as well as BKPyV infection [46,47]. In addition, overexpressing mutant caveolin 1 or inhibiting tyrosine kinases with genistein blocked viral infection. Genistein is well known for its effect as a tyrosine kinase inhibitor, and it is also considered as an inhibitor of the caveolin-mediated pathway [46]. However, genistein regulates too many pathways to draw any conclusions about its effect on BKPyV endocytosis [48,49]. In RPTE cells, one group reported that interfering with cholesterol function with both MβCD and nystatin or knocking down caveolin 1 inhibited BKPyV infection [47]. Furthermore, their confocal images indicate that BKPyV co-localizes with

caveolin protein in both Vero and RPTE cells immediately after endocytosis, which led to their conclusion that caveolae plays a role in BKPyV entry.

There are several strategies that can be used to interfere with cholesterol function, and most of these strategies have limitations [50]. In vitro, MβCD directly extracts cholesterol from the plasma membrane and releases cholesterol to the culture media [50]. Because caveolin 1 directly interacts with cholesterol, caveolae cannot form under MβCD treatment [51]. However, MβCD treatment not only releases cholesterol from the plasma membrane but also releases gangliosides and other transmembrane proteins [50]. Therefore, the inhibitory effect is more likely to be the result of losing BKPyV receptors rather than caveolae. Moreover, nystatin binds to and forms a complex with cholesterol on the cell membrane [52], which can be toxic to the cells. Nystatin is insoluble in aqueous solutions, however, Sigma still recommends a 50 mg/ml stock suspension in water because nystatin is effective in a suspension. After treatment, we easily observed nystatin crystal precipitation in our experiments; therefore, it is surprising that nystatin would cause a dose-dependent effect in RPTE cells [47]. According to the solubility information listed on the Sigma website, nystatin is soluble in DMSO at 5 mg/ml. If DMSO were used as a vehicle for nystatin delivery, then 100 µg/ml of nystatin means addition of 2% of DMSO to the cell culture media, which is toxic to cells. I made an attempt to reproduce the reported inhibitory effect of nystatin on BKPyV in RPTE cells [47]. However, I could not reproduce the published result: nystatin did not impact BKPyV infection in my experiments (Figure 2.3A). In any case, cholesterol is important for many biological activities including clathrin-mediated endocytosis [53]; therefore, one cannot conclude that caveolae assists BKPyV entry from cholesterol depletion assays.

Overexpressing mutant caveolin-1 has multiple effects on cells in addition to reducing caveolin activity. When viewed under the microscope, the overexpressed mutant caveolin 1 accumulated in the perinuclear region [46,54]. This accumulation may completely block the exit of the virus from the Golgi apparatus or other trafficking pathways [55]. Therefore, the fact that mutant caveolin 1 blocked infection does not necessarily mean that caveolin is important for BKPyV entry. In addition, my siRNA knockdown experiments showed that caveolin 1 is dispensable for BKPyV infection; thus the inhibitory effect of mutant caveolin 1 is more likely to be a side effect.

Because gangliosides are enriched in lipid rafts containing abundant cholesterol [56], and because caveolin as a cholesterol interacting protein also accumulates in lipid rafts, caveolin and gangliosides must colocalize on the plasma membrane. Because gangliosides serve as receptors for BKPyV, BKPyV must colocalize with caveolin at early stages of the virus-host cell interaction. Additionally, polyomavirus enter cells via multiple pathways including non-productive pathways; therefore, colocalization results cannot be used to prove that caveolae are required for BKPyV infection.

All of the experiments described above indirectly tested the function of caveolin 1 on BKPyV infection. Moriyama et al. also reported that knocking down caveolin 1 inhibited BKPyV infection [47]. In their experiment, RPTE cells were transfected with concentrated siRNA pool targeting caveolin 1 (100nM), which may enhance off-target effects. Transfected cells were infected with BKPyV at 48 hours post transfection and protein samples were harvested at 5 days post infection. At 5 days post infection, BKPyV would have already undergone two infection cycles. An over 80% reduction of TAg expression was observed when there was a 50% knockdown of caveolin 1. However, I failed to reproduce these data, despite following their

94

protocol exactly. In addition, I achieved significantly more than 50% caveolin 1 knockdown with my optimized protocol, yet I observed no TAg expression reduction. This suggests that the caveolin 1 protein is dispensable for BKPyV infection in RPTE cells. Caveolin proteins have long been considered to mediate SV40, MPyV, and BKPyV infection; however, subsequent experiments showed that SV40, MPyV, and even cholera toxin can invade caveolin-deficient cells. My results are consistent with these later observations [1-6]. The major capsid protein VP1 of MPyV, SV40, Merkel cell polyomavirus, and JC polyomavirus are well conserved except for the ganglioside interacting domain [31,57]. It makes the most sense that although polyomaviruses bind to different gangliosides, they may follow the same endocytic pathway when entering host cells.

Results described in Chapter 2 demonstrate that gangliosides are essential for BKPyV infection, and that caveolin and clathrin are both dispensable for BKPyV entry. Knocking down caveolin 1, caveolin 2, and clathrin heavy chain did not affect BKPyV infection. Partial disassembly of the actin filaments with cytochalasin D increased virus infection when used at a low concentration. All of the above findings suggest that BKPyV may infect host cells via a novel endocytic pathway.

Many in vitro plasma membrane models have been developed and widely applied to the study of endocytosis. One of the model systems is giant unilamellar vesicles (GUVs) [58,59], which have been used to study the attachment and endocytic processes of toxins and viruses. Because GUV is an artificial, protein-free system, the impact of protein can be eliminated and the composition of the membrane can be easily manipulated. It has been reported that cholera toxin, a toxin that binds ganglioside GM1, alone can induce phase separation in GUVs. In addition, cholera toxin can induce the formation of budding vesicles from GUVs, and cholesterol plays a regulatory role during this process [60]. Subsequent experiments testing the interaction between

95

SV40 and GUVs showed that SV40 is capable of inducing deep invaginations without the help of any host proteins or cholesterol [61]. In the process of invagination formation, the length of ceramide tails of the ganglioside is important [61], suggesting that the binding force between gangliosides and capsid proteins is responsible for formation of the deep invagination. Morphologically, this deep invagination would look like a single polyomavirus encapsulated in a tight-fitting vesicle if a cross section of the invagination were observed under the EM [2,44]. Moreover, a single viral particle may be sufficient to induce an invagination, as previously observed under EM during SV40 entry [2].

In summary, I propose that cholesterol in the plasma membrane regulates the position of the gangliosides and facilitates initial attachment (Figure 4.1) [38]. After the initial attachment to the gangliosides on the cell membrane, the BKPyV capsid recruits more gangliosides to the attachment site. By recruiting more gangliosides, the interaction between VP1 and gangliosides with long ceramide tails forms invaginations on the cell membrane, and no host proteins are required for this process. Cholesterol is not required for formation of this invagination [61]. However, cholesterol regulates budding in GUVs and in retrograde trafficking [60,66], and cholesterol interacts with ceramide tails, which will stabilize the entire deep invagination structure and may benefit the final fission step of virus-containing vesicles.

Lastly, how the virus-containing vesicle pinches off from the invagination is still unknown. There are two possible ways. First, it may get pinched off with the help of other host proteins in the same way as other vesicles. Dynamin assists vesicle fission in many vesicular trafficking pathways [62]. Dynasore, a dynamin inhibitor, inhibited BKPyV infection in RPTE cells (Figure 2.7A). However, the inhibitory effect of Dynasore was not specific, and it blocked BKPyV infection even when added at 12 hours post infection; therefore, whether the fission step

needs host protein assistance is still unknown. Alternatively, because each BKPyV virion can interact with 360 ganglioside molecules, the fission step may be solely dependent on the interaction between gangliosides and capsid proteins, and independent of host proteins. In addition, our primary screen showed that knocking down dynamin did not affect G2/M arrest induced by BKPyV. The real role of dynamin in BKPyV infection is still unclear and the machinery involved in vesicle fission remains to be revealed.

Endosome to ER retrograde transport

After endocytosis, there is no direct evidence that shows colocalization of BKPyV with the endosome [63], however evidence showing other polyomaviruses entering the endosome is abundant [4,54,64]. After entering the endosome, BKPyV particles undergo a sorting step in the late endosome/lysosome and traffic along with gangliosides [65,66]. Acidification of the late endosome is essential to activate this sorting machinery [63]. NH_4Cl blocks the acidification step and completely abolishes virus infection. After 2 hours post infection, NH_4Cl no longer inhibits viral infection, suggesting that all infectious viral particles have moved into a secondary vesicle and have already trafficked through the late endosome/lysosome at that time. After passing through the endosome, the majority of the details regarding viral trafficking are missing, and only an incomplete model with few time points is available. At 4 hours post infection, a few viral particles have already reached a destination at which microtubules are important for trafficking; meanwhile, it takes the majority of viral particles 10~12 hours to reach this destination [63]. Because BKPyV trafficking is not synchronized after the endosome step, it is possible that BKPyV takes several different routes to reach the ER. At 8 hours post infection, BKPyV capsids start to disassemble and VP1 cleavage products can be detected. Viral particles have already

passed from the endosome when VP1 cleavage products could be detected. I speculate that BKPyV capsid does not disassociate from gangliosides or undergo conformation changes in the late endosome or lysosome. This speculation is also consistent with subsequent reports that gangliosides sort the BKPyV particle to the ER, and capsid conformational changes are not required before BKPyV enters the ER [65,66]. Vesicles containing BKPyV are proposed to fuse with the ER membrane; however, the details of this process are still unclear. BKPyV particles are expected to disassemble in the ER with the help of several ER proteins including protein disulfide isomerases [63,67-70].

Gangliosides have been reported to assist the sorting process and regulate endosome to ER trafficking [65]. In addition, the ceramide structure is a determinant of sorting and the transport destination [61,66]. Because oligosaccharide chains of gangliosides interact with VP1 and are buried in the shallow groove of VP1, the only part of the gangliosides that the cell can use to identify, categorize, and sort are the ceramide tails. Because polyomaviruses use the gangliosides for receptors, I speculate that although different polyomaviruses bind to different gangliosides to enter the cell, they fall into the same ganglioside-dependent retrograde transport pathway, which transports the virus to the ER with the help of Rab proteins. After acidification and maturation of the endosome, the late endosome/lysosome sorts the gangliosides into different secondary vesicles that traffic to different cell compartments based on the ceramide structure [66]. Because BKPyV associates with gangliosides [65], BKPyV particles should traffic to different compartments along with the gangliosides. In addition, gangliosides that do not traffic to the ER may also serve as a trap for BKPyV in addition to glycoproteins on the plasma membrane [42]. It also has been found that cholera toxin binding to gangliosides is dispensable for ganglioside retrograde trafficking to the ER [66]. This suggests that the retrograde trafficking of gangliosides is

intrinsic and is independent of toxin or virus binding. In other words, BKPyV may act as a "hitchhiker" during the retrotranslocation of gangliosides to the ER; therefore, a protein co-receptor may not be required for polyomavirus infection [66]. Lastly, it is proposed that gangliosides traffic to the ER via several routes [66], which may explain why BKPyV trafficking in RPTE cells is not synchronized after BKPyV passes through the endosome. The fast trafficking viral particles may traffic directly from the late endosome to the ER; in contrast, the slow trafficking particles may traffic to the Golgi apparatus before trafficking to the ER.

Two more questions regarding the process of BKPyV trafficking from the endosome to the ER are whether or not BKPyV traffics through the Golgi apparatus at all, and whether or not trafficking through the Golgi apparatus is necessary for successful infection. Few studies have been performed attempting to address this question [71]. Most of the reports claim that viral intracellular traffic bypasses the Golgi apparatus; however, some the reports support the idea that BKPyV traffics to Golgi apparatus. First, brefeldin A, an inhibitor that blocks coat protein I (COPI) vesicle formation on the Golgi apparatus [72], inhibits BKPyV infection [63,73]. Second, cholera toxin, shiga toxin, HPV, and BKPyV undergo retrograde transport to the ER, and this retrograde transportation can be blocked with the chemicals retro-1 and retro-2 [74,75], suggesting that they share similar trafficking pathways. Cholera toxin, shiga toxin, and HPV have been demonstrated to visit the Golgi apparatus during intracellular trafficking [14,52,76,77], suggesting that BKPyV may also traffic to the Golgi apparatus. Third, there is one report that showed the colocalization of BKPyV and the Golgi apparatus [71]. Fourth, as previously discussed, gangliosides mediate the sorting process of polyomavirus during retrograde traffic and gangliosides traffic to the Golgi apparatus [66]; therefore BKPyV should follow gangliosides and traffic to the Golgi apparatus. Fifth, inhibitor time courses show that BKPyV trafficking is far

from synchronized [63]. After leaving the endosome, there is a more than 4-hour difference between the fastest traveling viral particles and the slowest particles, which supports the idea that the virus may take several pathways to reach the same destination. Lastly, our primary screen result showed that RAB5A, RAB7, RAB9A, RAB11B, and SEC61A are important for BKPyV infection, which strongly supports the idea that BKPyV traffics along with gangliosides to the Golgi apparatus [66].

If BKPyV traffics to the Golgi apparatus, then the next question would be whether or not trafficking to the Golgi apparatus is required for BKPyV infection. Although BKPyV likely travels to the Golgi apparatus, I think that this route is probably not required for infection. EHNA, a dynein inhibitor, disrupts normal Golgi apparatus structure but does not affect BKPyV infection. Moreover, although cholera toxin traffics to the Golgi apparatus, trafficking to the Golgi apparatus is not required for cholera toxin to transport to the ER, and only the trans-Golgi network is required [76,78]. Finally, a direct retrograde traffic pathway between the endosome and the ER may exist [65,66,79]; therefore, even if BKPyV traffics to the Golgi apparatus, this process is more likely to be dispensable for BKPyV infection. However, I speculate that trafficking efficiency may be compromised without the Golgi apparatus route, because the Golgi apparatus route appears to be the dominant route during ganglioside retrograde trafficking.

One remaining question is what machinery is used by BKPyV to penetrate the ER membrane and enter the ER lumen. A study from Nelson et al. shows that the capsid conformational change and minor protein exposure are not required for BKPyV infection [70]. This is consistent with my speculation that BKPyV is encapsulated in sorting vesicles and associated with gangliosides on its way to the ER. After further validation of our siRNA screen hits, RAB18 and STX18 were identified as two essential host factors for BKPyV infection. Subsequent

100

experiments showed that knocking down ZW10 and RINT1 also inhibited viral infection, which indicates that RAB18, STX18, and the NRZ complex may play an important role in BKPyV infection.

Rab18 protein interacts with multiple proteins in cells, including RINT1, ZW-10, Zwilch, STX18, and ROD [80], which have been found to assist Golgi to ER trafficking [81]. The NRZ complex structure has also been partially solved (Figure 3.7) [81-83]. In brief, the N terminals of RINT1 and ZW10 mediate protein-protein interaction, and RINT1 further interacts indirectly with proteins on the ER membrane including STX18. The ZW10 interaction with RAB18 is GTP-dependent, and RAB18 is thought to assist the tethering of COPI vesicle to NRZ complex on the ER membrane [80]. The protein-protein interaction studies indicate that ZW10, RINT1, and STX18 together form a linear structure, and this complex is predicted to form a protrusion about 20 nm in length from the ER membrane [84]. This, in turn, is expected to interact with Rab18 on the vesicle surface and mediate vesicle fusion (Figure 3.9). ZW10 also has additional functions besides being part of the NRZ. It also forms a RZZ complex [81], which regulates mitosis and chromatin separation. However, because BKPyV induces G2/M arrest, ZW10 is not likely to affect BKPyV infection when it is part of the kinetochores.

Other viruses and toxins

Gangliosides play important roles in both endocytosis and retrograde trafficking. Polyomaviruses and several toxins are proposed to take advantage of lipid-mediated endocytosis, which has been reviewed by Ewers and Helenius [85].

Beside polyomaviruses, some non-enveloped viruses infect cells in a similar manner; therefore, they may also take advantage of this lipid-mediated retrograde trafficking pathway to

establish an infection [86]. By silencing critical ganglioside synthesis enzymes, gangliosides have been demonstrated to be important for rotavirus infection [87]. After binding to gangliosides, rotavirus also traffics to and gets sorted in the endosome[88]. Norovirus also binds to gangliosides [89,90], and forms a deep invagination on GUVs [91]. Norovirus may also get internalized and traffic to the endosome in the same way as polyomavirus. Some adeno-associated viruses (AAV) use gangliosides as receptors, and AAV may also traffic to the Golgi apparatus and the ER before entering the cytosol [92]. Gangliosides therefore may guide AAV through the sorting process. Lastly, HPV infection is also independent of clathrin, caveolin, cholesterol, and dynamin, and the retrograde paths of both HPV and BKPyV can be blocked with retrograde traffic inhibitors retro-1, retro-2, and BFA. This suggests that HPV and BKPyV share the same pathway during intracellular trafficking: therefore, HPV may also enter this lipid mediated retrograde trafficking pathway.

Considering that ganglioside to ER trafficking is intrinsic [66], I speculate that viruses or toxins that bind to gangliosides may hitch onto gangliosides and traffic along with them to the endosome, Golgi apparatus, or ER. Some transmembrane proteins may affect the intrinsic ganglioside recycling; therefore, extra care is necessary when interpreting results from the co-receptor experiments.

Conclusions

In this dissertation, details about the process of BKPyV attachment and intracellular entry have been discussed. Based on these results, I propose the following model. At the beginning of the BKPyV life cycle, the cholesterol in the plasma membrane regulates the position and confirmation of gangliosides so that the oligosaccharide is pointing at the proper angle for initial

viral attachment (Figure 4.1). After the virus attaches to the gangliosides, the rest of the available VP1 capsid proteins will bind to adjacent gangliosides. As more and more gangliosides are recruited to the site of attachment, invaginations gradually occur based on the binding force between gangliosides and VP1. Because each BKPyV particle is capable of interacting with 360 ganglioside molecules from any direction, the interaction between gangliosides and VP1 may be sufficient for vesicle fission without the help of other host proteins; however, it is still possible that host proteins assist the fission step (Figure 4.2A). At this stage of infection, because both caveolin and gangliosides are enriched in the cholesterol-rich domain of the plasma membrane, BKPyV is expected to colocalize with caveolin, although caveolin is not required for invagination formation. After endocytosis (Figure 4.2B), the virus enters the endosome, still binds to gangliosides. Late endosome acidification activates sorting machinery mediated by Rab proteins that sort gangliosides into COPI-coated secondary vesicles based on the ceramide structures of the gangliosides. When gangliosides are sorted in to secondary vesicles, the BKPyV particles that bind those gangliosides are also sorted into the secondary vesicles along with the gangliosides. After this sorting step, a few BKPyV particles traffics along microtubules towards the ER (Figure 4.2E). A majority of the secondary vesicles traffic to the Golgi apparatus before trafficking to the ER (Figure 4.2C), and arrive at the ER (Figure 4.2D) about 4-8 hours later than vesicles directly trafficking to the ER. When vesicles containing viral particles reach the adjacent area of the ER, Rab18 on the surface of the vesicle interact with STX18/NRZ complex, which mediates fusion of the virus-containing vesicles to the the ER membrane (Figure 4.2F); thus BKPyV reaches the ER lumen (Figure 3.9).

This dissertation provided new details regarding polyomavirus endocytosis and intracellular trafficking. Polyomaviruses had been thought to bind to different gangliosides and
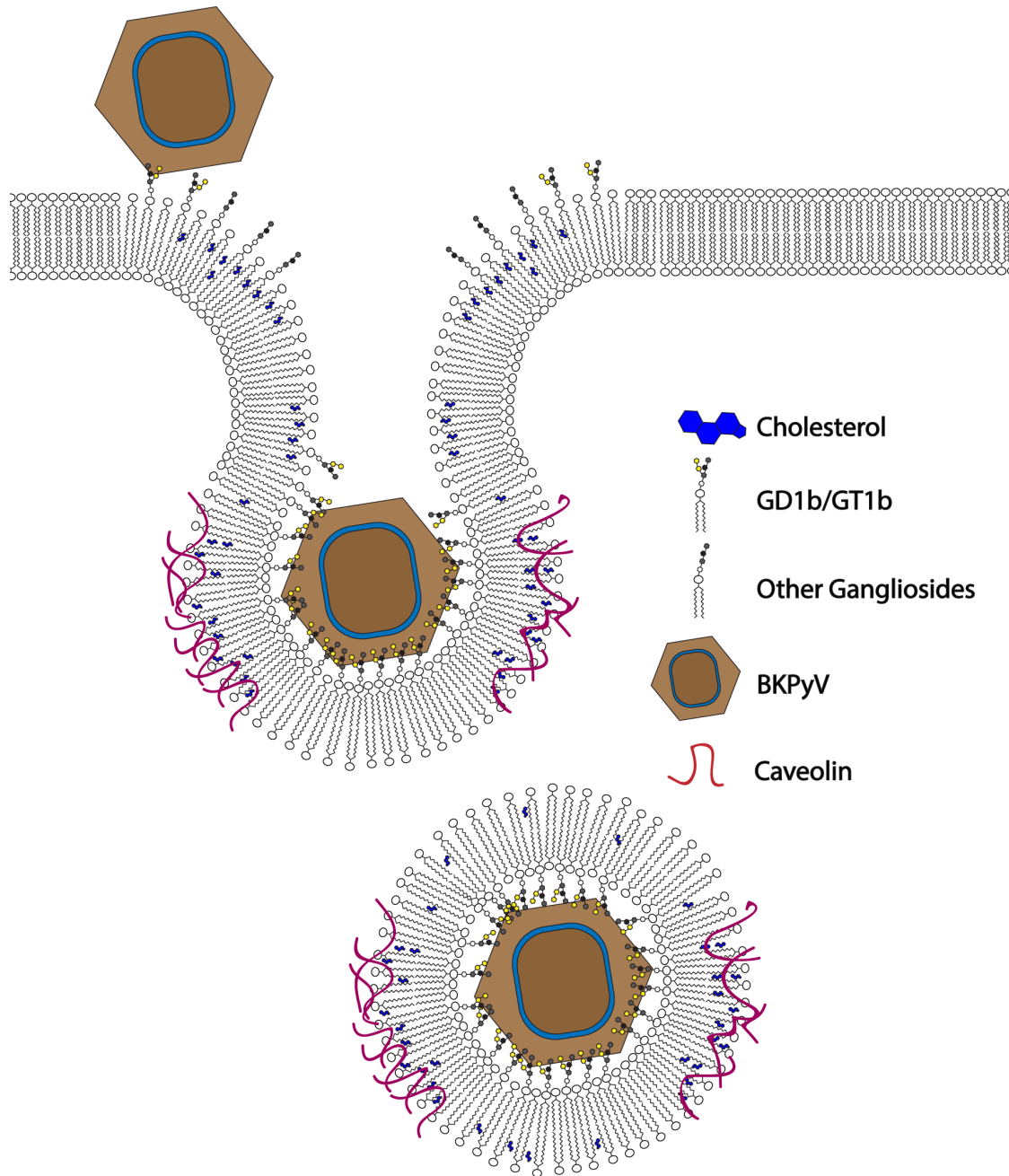
Figure 4.1: Model of BKPyV attachment and endocytosis.
Cholesterol regulates the position of gangliosides in the membrane. BKPyV particles first bind to gangliosides GD1b or GT1b on the cell surface. The BKPyV particle recruits more ganglioside GD1b or GT1b to the attachment site and eventually gets encapsulated into an endocytic vesicle.
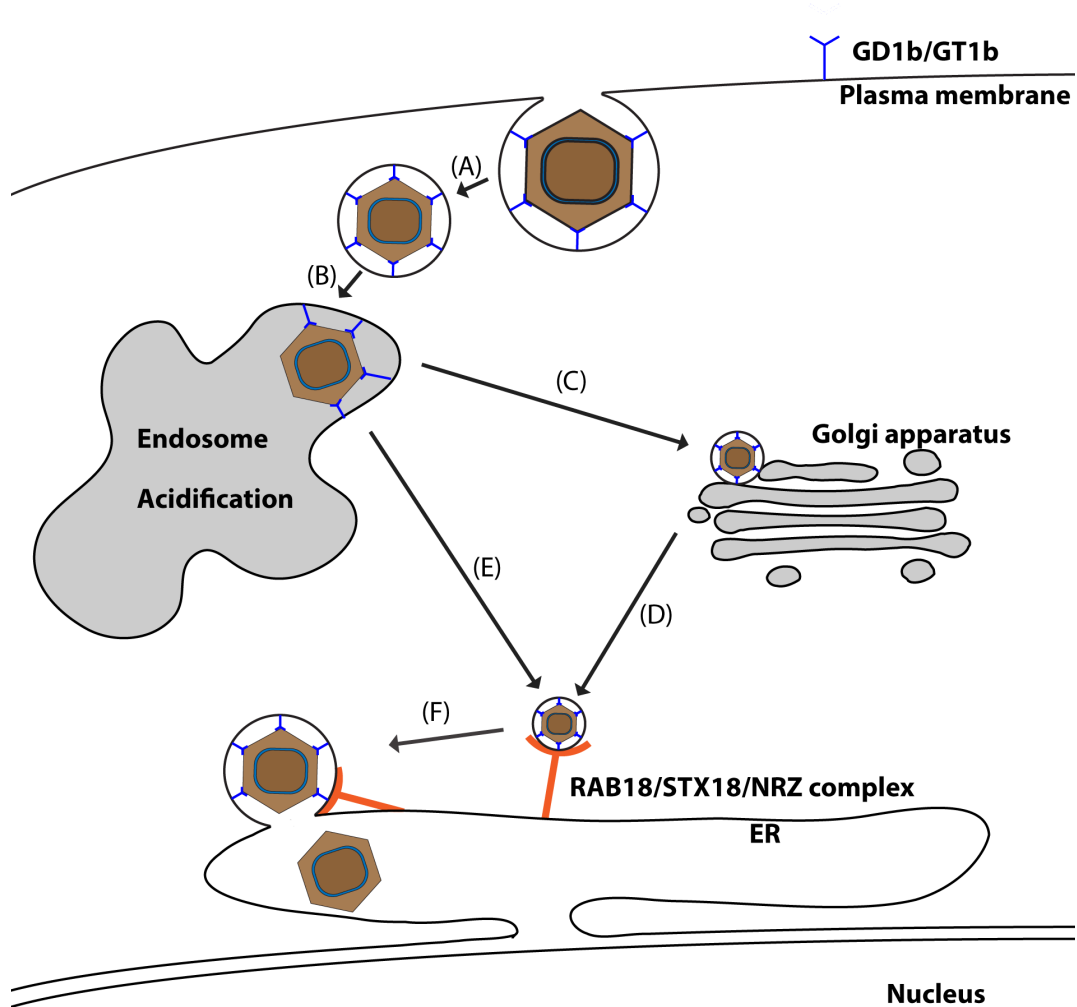
Figure 4.2: BKPyV intracellular traffic.
(A) Vesicle fission. (B) Encapsulated virus. Virus is still binding to gangliosides. (C)(D)(E) Virus sorted based on the ceramide structure of ganglioside. After acidification, viral particles are encapsulated in secondary vesicle. The secondary vesicles then traffic to ER directly or via the Golgi apparatus as determined by ganglioside structure. (F) Secondary vesicles with Rab18 are captured by the STX18/NRZ complex, and fuse to the ER.

become internalized via different pathways: the caveolin mediated pathway, the clathrin mediated pathway, and the caveolin- and clathrin-independent pathway. However, my experiments along with those of others demonstrate that caveolin is dispensable for MPyV, SV40, and BKPyV infection. This suggests that polyomaviruses use similar pathways to enter host cells. Based on this finding, a new model of viral entry and intracellular trafficking is proposed. Many other viruses have similar trafficking patterns compared to polyomavirus, such as HPV, norovirus, and rotavirus. These viruses could also take advantage of some parts of this pathway to establish infection.

In the future, several topics regarding viral entry and intracellular trafficking are worth further investigation. First, the fission step of BKPyV endocytosis is still unknown. The function of the dynamin protein in viral endocytosis could not be determined, either with Dynasore treatment, or with the siRNA screen. Dynamin has multiple roles in various cell compartments [62], therefore more careful studies are necessary to reveal its role in BKPyV infection. Next, the viral disassembly process is far from fully understood. As previously discussed, BKPyV remains intact before fusing to the ER, and it has been shown that ER proteins are important for capsid disassembly. However, how VP1 is cleaved, and whether this cleavage process is necessary for BKPyV infection is still a mystery. Third, more evidence is required to fully understand the role of the RAB18/STX18/NRZ protein complex. Further study of this complex will also help answer the question of the importance of the Golgi apparatus in BKPyV entry. The fourth unsolved question is the role of Rab proteins during ganglioside retrograde trafficking. Applying retrograde trafficking inhibitors, retro-1 and retro-2, blocked the trafficking of cholera toxin, shiga toxin, polyomavirus, and HPV, which suggests that the Rab-dependent ganglioside retrograde pathway could be a common pathway shared by several pathogens and toxins.

106

Understanding this pathway will be rewarding, and will also help answer many unsolved

questions. This may eventually benefit clinical applications, suggesting ways of preventing virus

spread to other cells after reactivation.

References

1.   Zhao L, Marciano AT, Rivet CR, Imperiale MJ. Caveolin- and clathrin-independent entry of BKPyV into primary human proximal tubule epithelial cells. *Virology*. 2016;492:66-72. doi:10.1016/j.virol.2016.02.007.

2.   Damm E-M, Pelkmans L, Kartenbeck J, Mezzacasa A, Kurzchalia T, Helenius A. Clathrin- and caveolin-1-independent endocytosis: entry of simian virus 40 into cells devoid of caveolae. *J Cell Biol*. 2005;168(3):477-488. doi:10.1083/jcb.200407113.

3.   Gilbert JM, Goldberg IG, Benjamin TL. Cell penetration and trafficking of polyomavirus. *J Virol*. 2003;77(4):2615-2622. doi:10.1128/JVI.77.4.2615-2622.2003.

4.   Liebl D, Difato F, Horníková L, Mannová P, Štokrová J, Forstová J. Mouse polyomavirus enters early endosomes, requires their acidic pH for productive infection, and meets transferrin cargo in Rab11-positive endosomes. *J Virol*. 2006;80(9):4610-4622. doi:10.1128/JVI.80.9.4610-4622.2006.

5.   Shogomori H, Futerman AH. Cholera toxin is found in detergent-insoluble rafts/domains at the cell surface of hippocampal neurons but is internalized via a raft-independent mechanism. *J Biol Chem*. 2001;276(12):9182-9188. doi:10.1074/jbc.M009414200.

6.   Torgersen ML, Skretting G, van Deurs B, Sandvig K. Internalization of cholera toxin by different endocytic mechanisms. *J Cell Sci*. 2001;114(Pt 20):3737-3747.

7.   Brass AL, Dykxhoorn DM, Benita Y, et al. Identification of host proteins required for HIV infection through a functional genomic screen. *Science*. 2008;319(5865):921-926. doi:10.1126/science.1152725.

8.   Zhou H, Xu M, Huang Q, et al. Genome-scale RNAi screen for host factors required for HIV replication. *Cell Host Microbe*. 2008;4(5):495-504. doi:10.1016/j.chom.2008.10.004.

9.   König R, Zhou Y, Elleder D, et al. Global analysis of host-pathogen interactions that regulate early-stage HIV-1 replication. *Cell*. 2008;135(1):49-60. doi:10.1016/j.cell.2008.07.032.

10.   Reiss S, Rebhan I, Backes P, et al. Recruitment and activation of a lipid kinase by hepatitis C virus NS5A is essential for integrity of the membranous replication compartment. *Cell Host Microbe*. 2011;9(1):32-45. doi:10.1016/j.chom.2010.12.002.

11.   Karlas A, Machuy N, Shin Y, et al. Genome-wide RNAi screen identifies human host factors crucial for influenza virus replication. *Nature*. 2010;463(7):818-822. doi:10.1038/nature08760.

12.   König R, Stertz S, Zhou Y, et al. Human host factors required for influenza virus replication. *Nature*. 2010;463(7282):813-817. doi:10.1038/nature08699.

13.   Krishnan MN, Ng A, Sukumaran B, et al. RNA interference screen for human genes associated with West Nile virus infection. *Nature*. 2008;455(7210):242-245. doi:10.1038/nature07207.

14.   Lipovsky A, Popa A, Pimienta G, et al. Genome-wide siRNA screen identifies the retromer as a cellular entry factor for human papillomavirus. *Proc Natl Acad Sci USA*. 2013;110(18):7452-7457. doi:10.1073/pnas.1302164110.

15.   Popa A, Zhang W, Harrison MS, et al. Direct binding of retromer to human papillomavirus type 16 minor capsid protein L2 mediates endosome exit during viral infection. McBride AA, ed. *PLoS Pathog*. 2015;11(2):e1004699. doi:10.1371/journal.ppat.1004699.

16.   Goodwin EC, Lipovsky A, Inoue T, et al. BiP and multiple DNAJ molecular chaperones in the endoplasmic reticulum are required for efficient simian virus 40 infection. *MBio*. 2011;2(3):e00101-e00111. doi:10.1128/mBio.00101-11.

17.   Bagchi P, Walczak CP, Tsai B. The endoplasmic reticulum membrane j protein C18 executes a distinct role in promoting simian virus 40 membrane penetration. Dermody TS, ed. *J Virol*. 2015;89(8):4058-4068. doi:10.1128/JVI.03574-14.

18.   Fire A, Xu S, Montgomery MK, Kostas SA, Driver SE, Mello CC. Potent and specific genetic interference by double-stranded RNA in Caenorhabditis elegans. *Nature*. 1998;391(6):806-811. doi:10.1038/35888.

19.   Shea PR, Shianna KV, Carrington M, Goldstein DB. Host genetics of HIV acquisition and viral control. *Annu Rev Med*. 2013;64:203-217. doi:10.1146/annurev-med-052511-135400.

20.   Goff SP. Knockdown screens to knockout HIV-1. *Cell*. 2008;135(3):417-420. doi:10.1016/j.cell.2008.10.007.

21.   Bushman FD, Malani N, Fernandes J, et al. Host cell factors in HIV replication: meta-analysis of genome-wide studies. *PLoS Pathog*. 2009;5(5):e1000437. doi:10.1371/journal.ppat.1000437.

22.   Jackson AL, Bartz SR, Schelter J, et al. Expression profiling reveals off-target gene regulation by RNAi. *Nat Biotechnol*. 2003;21(6):635-637. doi:10.1038/nbt831.

23.   Jackson AL, Burchard J, Schelter J, et al. Widespread siRNA "off-target" transcript

silencing mediated by seed region sequence complementarity. *RNA*. 2006;12(7):1179-1187. doi:10.1261/rna.25706.

24.   Birmingham A, Anderson EM, Reynolds A, et al. 3' UTR seed matches, but not overall identity, are associated with RNAi off-targets. *Nat Meth*. 2006;3(3):199-204. doi:10.1038/nmeth854.

25.   Tschuch C, Schulz A, Pscherer A, et al. Off-target effects of siRNA specific for GFP. *BMC Mol Biol*. 2008;9(1):60. doi:10.1186/1471-2199-9-60.

26.   Mohr S, Bakal C, Perrimon N. Genomic screening with RNAi: results and challenges. *Annual review of biochemistry*. 2010;79:37-64. doi:10.1146/annurev-biochem-060408-092949.

27.   Sigoillot FD, Lyman S, Huckins JF, et al. A bioinformatics method identifies prominent off-targeted transcripts in RNAi screens. *Nat Meth*. 2012;9(4):363-366. doi:10.1038/nmeth.1898.

28.   Franceschini A, Meier R, Casanova A, et al. Specific inhibition of diverse pathogens in human cells by synthetic microRNA-like oligonucleotides inferred from RNAi screens. In: Vol 111. 2014:4548-4553. doi:10.1073/pnas.1402353111.

29.   Low JA, Magnuson B, Tsai B, Imperiale MJ. Identification of gangliosides GD1b and GT1b as receptors for BK virus. *J Virol*. 2006;80(3):1361-1366. doi:10.1128/JVI.80.3.1361-1366.2006.

30.   Nilsson J, Miyazaki N, Xing L, et al. Structure and assembly of a T=1 virus-like particle in BK polyomavirus. *J Virol*. 2005;79(9):5337-5345. doi:10.1128/JVI.79.9.5337-5345.2005.

31.   Neu U, Allen S-AA, Blaum BS, et al. A structure-guided mutation in the major capsid protein retargets BK polyomavirus. Galloway DA, ed. *PLoS Pathog*. 2013;9(10):e1003688. doi:10.1371/journal.ppat.1003688.

32.   Stehle T, Yan Y, Benjamin TL, Harrison SC. Structure of murine polyomavirus complexed with an oligosaccharide receptor fragment. *Nature*. 1994;369(6):160-163. doi:10.1038/369160a0.

33.   Stehle T, Harrison SC. High-resolution structure of a polyomavirus VP1-oligosaccharide complex: implications for assembly and receptor binding. *EMBO J*. 1997;16(16):5139-5148. doi:10.1093/emboj/16.16.5139.

34.   Neu U, Hengel H, Blaum BS, et al. Structures of Merkel cell polyomavirus VP1 complexes define a sialic acid binding site required for infection. Imperiale M, ed. *PLoS Pathog*. 2012;8(7):e1002738. doi:10.1371/journal.ppat.1002738.

35.   Ströh LJ, Neu U, Blaum BS, Buch MHC, Garcea RL, Stehle T. Structure analysis of the

major capsid proteins of human polyomaviruses 6 and 7 reveals an obstructed sialic acid binding site. *J Virol*. 2014;88(18):10831-10839. doi:10.1128/JVI.01084-14.

36.   Neu U, Maginnis MS, Palma AS, et al. Structure-function analysis of the human JC polyomavirus establishes the LSTc pentasaccharide as a functional receptor motif. *Cell Host Microbe*. 2010;8(4):309-319. doi:10.1016/j.chom.2010.09.004.

37.   Lingwood D, Simons K. Lipid rafts as a membrane-organizing principle. *Science*. 2010;327(5961):46-50. doi:10.1126/science.1174621.

38.   Lingwood CA, Manis A, Mahfoud R, Khan F, Binnington B, Mylvaganam M. New aspects of the regulation of glycosphingolipid receptor function. *Chem Phys Lipids*. 2010;163(1):27-35. doi:10.1016/j.chemphyslip.2009.09.001.

39.   Maginnis MS, Haley SA, Gee GV, Atwood WJ. Role of N-linked glycosylation of the 5-HT2A receptor in JC virus infection. *J Virol*. 2010;84(19):9677-9684. doi:10.1128/JVI.00978-10.

40.   Caruso M, Belloni L, Sthandier O, Amati P, Garcia M-I. Alpha4beta1 integrin acts as a cell receptor for murine polyomavirus at the postattachment level. *J Virol*. 2003;77(7):3913-3921. doi:10.1128/JVI.77.7.3913-3921.2003.

41.   Dugan AS, Eash S, Atwood WJ. An N-linked glycoprotein with alpha(2,3)-linked sialic acid is a receptor for BK virus. *J Virol*. 2005;79(22):14442-14445. doi:10.1128/JVI.79.22.14442-14445.2005.

42.   Qian M, Tsai B. Lipids and proteins act in opposing manners to regulate polyomavirus infection. *J Virol*. 2010;84(19):9840-9852. doi:10.1128/JVI.01093-10.

43.   You J, O'Hara SD, Velupillai P, et al. Ganglioside and non-ganglioside mediated host responses to the mouse polyomavirus. Meyers C, ed. *PLoS Pathog*. 2015;11(10):e1005175. doi:10.1371/journal.ppat.1005175.

44.   Maraldi NM, Barbanti-Brodano G, Portolani M, La Placa M. Ultrastructural aspects of BK virus uptake and replication in human fibroblasts. *J Gen Virol*. 1975;27(1):71-80. doi:10.1099/0022-1317-27-1-71.

45.   Drachenberg CB, Papadimitriou JC, Wali R, Cubitt CL, Ramos E. BK polyoma virus allograft nephropathy: ultrastructural features from viral cell entry to lysis. *Am J Transplant*. 2003;3(11):1383-1392.

46.   Eash S, Querbes W, Atwood WJ. Infection of vero cells by BK virus is dependent on caveolae. *J Virol*. 2004;78(21):11583-11590. doi:10.1128/JVI.78.21.11583-11590.2004.

47.   Moriyama T, Marquez JP, Wakatsuki T, Sorokin A. Caveolar endocytosis is critical for BK virus infection of human renal proximal tubular epithelial cells. *J Virol*. 2007;81(16):8552-8562. doi:10.1128/JVI.00924-07.

48. Banerjee S, Li Y, Wang Z, Sarkar FH. Multi-targeted therapy of cancer by genistein. *Cancer Lett*. 2008;269(2):226-242. doi:10.1016/j.canlet.2008.03.052.

49. Andres A, Donovan SM, Kuhlenschmidt MS. Soy isoflavones and virus infections. *J Nutr Biochem*. 2009;20(8):563-569. doi:10.1016/j.jnutbio.2009.04.004.

50. Ilangumaran S, Hoessli DC. Effects of cholesterol depletion by cyclodextrin on the sphingolipid microdomains of the plasma membrane. *Biochem J*. 1998;335 (Pt 2):433-440.

51. Simons K, Toomre D. Lipid rafts and signal transduction. *Nat Rev Mol Cell Biol*. 2000;1(1):31-39. doi:10.1038/35036052.

52. Sandvig K, Bergan J, Kavaliauskiene S, Skotland T. Lipid requirements for entry of protein toxins into cells. *Prog Lipid Res*. 2014;54:1-13. doi:10.1016/j.plipres.2014.01.001.

53. Rodal SK, Skretting G, Garred O, Vilhardt F, van Deurs B, Sandvig K. Extraction of cholesterol with methyl-beta-cyclodextrin perturbs formation of clathrin-coated endocytic vesicles. *Mol Biol Cell*. 1999;10(4):961-974.

54. Querbes W, O'Hara BA, Williams G, Atwood WJ. Invasion of host cells by JC virus identifies a novel role for caveolae in endosomal sorting of noncaveolar ligands. *J Virol*. 2006;80(19):9402-9413. doi:10.1128/JVI.01086-06.

55. Parton RG, Simons K. The multiple faces of caveolae. *Nat Rev Mol Cell Biol*. 2007;8(3):185-194. doi:10.1038/nrm2122.

56. Sonnino S, Mauri L, Chigorno V, Prinetti A. Gangliosides as components of lipid membrane domains. *Glycobiology*. 2007;17(1):1R–13R. doi:10.1093/glycob/cwl052.

57. Ströh LJ, Gee GV, Blaum BS, et al. Trichodysplasia spinulosa-associated polyomavirus uses a displaced binding site on VP1 to engage sialylated glycolipids. *PLoS Pathog*. 2015;11(8):e1005112. doi:10.1371/journal.ppat.1005112.

58. Mathivet L, Cribier S, Devaux PF. Shape change and physical properties of giant phospholipid vesicles prepared in the presence of an AC electric field. *Biophys J*. 1996;70(3):1112-1121. doi:10.1016/S0006-3495(96)79693-5.

59. Wesołowska O, Michalak K, Maniewska J, Hendrich AB. Giant unilamellar vesicles - a perfect tool to visualize phase separation and lipid rafts in model systems. *Acta Biochim Pol*. 2009;56(1):33-39. doi:10.1128/JVI.02180-08.

60. Bacia K, Schwille P, Kurzchalia T. Sterol structure determines the separation of phases and the curvature of the liquid-ordered phase in model membranes. *PNAS*. 2005;102(9):3272-3277. doi:10.1073/pnas.0408215102.

61. Ewers H, Römer W, Smith AE, et al. GM1 structure determines SV40-induced membrane

invagination and infection. *Nature Cell Biology*. 2010;12(1):11–8–suppp1–12. doi:10.1038/ncb1999.

62.   Ferguson SM, De Camilli P. Dynamin, a membrane-remodelling GTPase. *Nature Reviews Molecular Cell Biology*. 2012;13(2):75-88. doi:10.1038/nrm3266.

63.   Jiang M, Abend JR, Tsai B, Imperiale MJ. Early events during BK virus entry and disassembly. *J Virol*. 2009;83(3):1350-1358. doi:10.1128/JVI.02169-08.

64.   Engel S, Heger T, Mancini R, et al. Role of endosomes in simian virus 40 entry and infection. *J Virol*. 2011;85(9):4198-4211. doi:10.1128/JVI.02179-10.

65.   Qian M, Cai D, Verhey KJ, Tsai B. A lipid receptor sorts polyomavirus from the endolysosome to the endoplasmic reticulum to cause infection. Galloway D, ed. *PLoS Pathog*. 2009;5(6):e1000465. doi:10.1371/journal.ppat.1000465.

66.   Chinnapen DJ-F, Hsieh W-T, Welscher te YM, et al. Lipid sorting by ceramide structure from plasma membrane to ER for the cholera toxin receptor ganglioside GM1. *Dev Cell*. 2012;23(3):573-586. doi:10.1016/j.devcel.2012.08.002.

67.   Rainey-Barger EK, Mkrtchian S, Tsai B. Dimerization of ERp29, a PDI-like protein, is essential for its diverse functions. *Mol Biol Cell*. 2007;18(4):1253-1260. doi:10.1091/mbc.E06-11-1004.

68.   Schelhaas M, Malmström J, Pelkmans L, et al. Simian Virus 40 depends on ER protein folding and quality control factors for entry into host cells. *Cell*. 2007;131(3):516-529. doi:10.1016/j.cell.2007.09.038.

69.   Walczak CP, Tsai B. A PDI family network acts distinctly and coordinately with ERp29 to facilitate polyomavirus infection. *J Virol*. 2011;85(5):2386-2396. doi:10.1128/JVI.01855-10.

70.   Nelson CDS, Ströh LJ, Gee GV, O'Hara BA, Stehle T, Atwood WJ. Modulation of a pore in the capsid of JC polyomavirus reduces infectivity and prevents exposure of the minor capsid proteins. Imperiale MJ, ed. *J Virol*. 2015;89(7):3910-3921. doi:10.1128/JVI.00089-15.

71.   Moriyama T, Sorokin A. Intracellular trafficking pathway of BK Virus in human renal proximal tubular epithelial cells. *Virology*. 2008;371(2):336-349. doi:10.1016/j.virol.2007.09.030.

72.   Scales SJ, Gomez M, Kreis TE. Coat proteins regulating membrane traffic. *Int Rev Cytol*. 2000;195:67-144. doi:10.1016/S0074-7696(08)62704-7.

73.   Richards AA, Stang E, Pepperkok R, Parton RG. Inhibitors of COP-mediated transport and cholera toxin action inhibit simian virus 40 infection. *Mol Biol Cell*. 2002;13(5):1750-1764. doi:10.1091/mbc.01-12-0592.

74. Stechmann B, Bai S-K, Gobbo E, et al. Inhibition of retrograde transport protects mice from lethal ricin challenge. *Cell*. 2010;141(2):231-242. doi:10.1016/j.cell.2010.01.043.

75. Nelson CDS, Carney DW, Derdowski A, et al. A retrograde trafficking inhibitor of ricin and Shiga-like toxins inhibits infection of cells by human and monkey polyomaviruses. *MBio*. 2013;4(6):e00729–13. doi:10.1128/mBio.00729-13.

76. Feng Y, Jadhav AP, Rodighiero C, Fujinaga Y, Kirchhausen T, Lencer WI. Retrograde transport of cholera toxin from the plasma membrane to the endoplasmic reticulum requires the trans-Golgi network but not the Golgi apparatus in Exo2-treated cells. *EMBO Rep*. 2004;5(6):596-601. doi:10.1038/sj.embor.7400152.

77. Zhang W, Kazakov T, Popa A, DiMaio D. Vesicular trafficking of incoming human papillomavirus 16 to the Golgi apparatus and endoplasmic reticulum requires γ-secretase activity. *MBio*. 2014;5(5):e01777–14. doi:10.1128/mBio.01777-14.

78. Fujinaga Y, Wolf AA, Rodighiero C, et al. Gangliosides that associate with lipid rafts mediate transport of cholera and related toxins from the plasma membrane to endoplasmic reticulm. *Mol Biol Cell*. 2003;14(12):4783-4793. doi:10.1091/mbc.E03-06-0354.

79. Pelkmans L, Kartenbeck J, Helenius A. Caveolar endocytosis of simian virus 40 reveals a new two-step vesicular-transport pathway to the ER. *Nature Cell Biology*. 2001;3(5):473-483. doi:10.1038/35074539.

80. Gillingham AK, Sinka R, Torres IL, Lilley KS, Munro S. Toward a comprehensive map of the effectors of rab GTPases. *Dev Cell*. 2014;31(3):358-373. doi:10.1016/j.devcel.2014.10.007.

81. Tagaya M, Arasaki K, Inoue H, Kimura H. Moonlighting functions of the NRZ (mammalian Dsl1) complex. *Front Cell Dev Biol*. 2014;2(286):25. doi:10.3389/fcell.2014.00025.

82. Civril F, Wehenkel A, Giorgi FM, et al. Structural analysis of the RZZ complex reveals common ancestry with multisubunit vesicle tethering machinery. *Structure*. 2010;18(5):616-626. doi:10.1016/j.str.2010.02.014.

83. Hirose H, Arasaki K, Dohmae N, et al. Implication of ZW10 in membrane trafficking between the endoplasmic reticulum and Golgi. *EMBO J*. 2004;23(6):1267-1278. doi:10.1038/sj.emboj.7600135.

84. Ren Y, Yip CK, Tripathi A, et al. A structure-based mechanism for vesicle capture by the multisubunit tethering complex Dsl1. *Cell*. 2009;139(6):1119-1129. doi:10.1016/j.cell.2009.11.002.

85. Ewers H, Helenius A. Lipid-mediated endocytosis. *Cold Spring Harb Perspect Biol*. 2011;3(8):a004721-a004721. doi:10.1101/cshperspect.a004721.

86. Taube S, Jiang M, Wobus CE. Glycosphingolipids as receptors for non-enveloped viruses. *Viruses*. 2010;2(4):1011-1049. doi:10.3390/v2041011.

87. Martínez MA, López S, Arias CF, Isa P. Gangliosides have a functional role during rotavirus cell entry. *J Virol*. 2013;87(2):1115-1122. doi:10.1128/JVI.01964-12.

88. Arias CF, Silva-Ayala D, López S. Rotavirus entry: a deep journey into the cell with several exits. Tsai B, ed. *J Virol*. 2015;89(2):890-893. doi:10.1128/JVI.01787-14.

89. Taube S, Perry JW, Yetming K, et al. Ganglioside-linked terminal sialic acid moieties on murine macrophages function as attachment receptors for murine noroviruses. *J Virol*. 2009;83(9):4092-4101. doi:10.1128/JVI.02245-08.

90. Han L, Tan M, Xia M, Kitova EN, Jiang X, Klassen JS. Gangliosides are ligands for human noroviruses. *J Am Chem Soc*. 2014;136(36):12631-12637. doi:10.1021/ja505272n.

91. Rydell GE, Svensson L, Larson G, Johannes L, Römer W. Human GII.4 norovirus VLP induces membrane invaginations on giant unilamellar vesicles containing secretor gene dependent α1,2-fucosylated glycosphingolipids. *Biochimica et Biophysica Acta (BBA) - Biomembranes*. 2013;1828(8):1840-1845. doi:10.1016/j.bbamem.2013.03.016.

92. Nonnenmacher M, Weber T. Intracellular transport of recombinant adeno-associated virus vectors. *Gene Ther*. 2012;19(6):649-658. doi:10.1038/gt.2012.6.